PHILOSOPHICAL TRANSACTIONS OF THE ROYAL SOCIETY A MATHEMATICAL, PHYSICAL & ENGINEERING SCIENCES

Bifurcations of One- and Two-Dimensional Maps

P. Holmes and D. Whitley

Phil. Trans. R. Soc. Lond. A 1984 **311**, 43-102
doi: 10.1098/rsta.1984.0020

Phil. Trans. R. Soc. Lond. A **311**, 43–102 (1984) [43]
Printed in Great Britain

BIFURCATIONS OF ONE- AND TWO-DIMENSIONAL MAPS

BY P. HOLMES AND D. WHITLEY†

Department of Theoretical and Applied Mechanics and Center for Applied Mathematics, Cornell University, Ithaca, N.Y. 14853, U.S.A.

(*Communicated by E. C. Zeeman, F.R.S. – Received 7 July 1983*)

CONTENTS

We study the qualitative dynamics of two-parameter families of planar maps of the form

$$F_{\mu,\epsilon}(x, y) = (y, -\epsilon x + f_\mu(y)),$$

where $f_\mu: \mathbb{R} \to \mathbb{R}$ is a C^3 map with a single critical point and negative Schwarzian derivative. The prototype of such maps is the family $f_\mu(y) = \mu - y^2$ or (in different coordinates) $f_\lambda(y) = \lambda y(1-y)$, in which case $F_{\mu,\epsilon}$ is the Hénon map. The maps $F_{\mu,\epsilon}$ have constant Jacobian determinant ϵ and, as $\epsilon \to 0$, collapse to the family f_μ. The behaviour of such one-dimensional families is quite well understood, and we are able to use their bifurcation structures and information on their non-wandering sets to obtain results on both local and global bifurcations of $F_{\mu,\epsilon}$, for small ϵ. Moreover, we are able to extend these results to the area preserving family $F_{\mu,1}$, thereby obtaining (partial) bifurcation sets in the (μ, ϵ)-plane. Among our conclusions we find that the bifurcation sequence for periodic orbits, which is restricted by Sarkovskii's theorem and the kneading theory for one-dimensional maps, is quite different for two-dimensional families. In particular, certain periodic orbits that appear at the end of the one-dimensional sequence appear at the beginning of the area preserving sequence, and infinitely many families of saddle node and period doubling bifurcation curves cross each other in the (μ, ϵ)-parameter plane between $\epsilon = 0$ and $\epsilon = 1$. We obtain these results from a study of the homoclinic bifurcations (tangencies of stable and unstable manifolds) of $F_{\mu,\epsilon}$ and of the associated sequences of periodic bifurcations that accumulate on them. We illustrate our results with some numerical computations for the orientation-preserving Hénon map.

† Present address: Faculty of Mathematical Studies, University of Southampton, Southampton S09 5NH, U.K

1. Introduction

In this paper we consider the local and global bifurcations of two-parameter families of diffeomorphisms of the plane, $F_{\mu,\epsilon}$, that have constant Jacobian determinant ϵ. As $\epsilon \to 0$ the behaviour of $F_{\mu,\epsilon}$ is increasingly well approximated by a one-dimensional map f_μ. We explore the relation between the bifurcation sets and invariant sets of such one- and two-dimensional maps. Specifically, we consider the family

$$F_{\mu,\epsilon}(x, y) = (y, -\epsilon x + f_\mu(y)); \epsilon \in [0, 1], \tag{1.1}$$

where $f_\mu : \mathbb{R} \to \mathbb{R}$ is an even function with a single non-degenerate critical point (a maximum) at $x = 0$. Precise definitions are given in §2. We assume that, as μ increases, the non-wandering set Ω_μ of f_μ changes from the empty set to a Cantor set on which f_μ is conjugate to a one-sided shift on two symbols. Similarly, we assume that for each fixed $\epsilon \in (0, 1]$ there are values $-\infty < s_1(\epsilon) < \bar{h}_1(\epsilon) < \infty$ such that, for $\mu < s_1$ the non-wandering set $\Omega_{\mu,\epsilon}$ of $F_{\mu,\epsilon}$ is empty, while for $\mu > \bar{h}_1$, $F_{\mu,\epsilon}|_{\Omega_{\mu,\epsilon}}$ is conjugate to a two-sided shift on two symbols: a Smale horseshoe (Smale 1963, 1967). We are thus interested in the bifurcations in which horseshoes are created.

The main motivation for the present study comes from considering Poincaré maps $P_{\delta,\gamma}$ corresponding to linearly damped T-periodically forced oscillators of the form

$$\ddot{x} + \delta\dot{x} + g(x) = \gamma p(t); p(t) = p(t+T), \quad \delta, \gamma \geqslant 0, \tag{1.2}$$

an example of which is Duffing's equation

$$\ddot{x} + \delta\dot{x} - x + x^3 = \gamma \cos \omega t. \tag{1.3}$$

Since the flow of (1.2) contracts volumes uniformly in the three-dimensional $(x, \dot{x}, t)$ extended phase space, $P_{\delta,\gamma}$ has constant Jacobian determinant; in fact we have

$$\epsilon = \det DP_{\delta,\gamma} = \mathrm{e}^{-\delta T} \in (0, 1]. \tag{1.4}$$

In typical cases, as the force level γ is increased, $P_{\delta,\gamma}$ exhibits bifurcations to horseshoes of the type considered in this paper. For specific details regarding Duffing's equation, see Holmes & Whitley (1983*a*, *b*), and the earlier studies of Holmes (1979), Moon & Holmes (1979), Ueda (1980) and Greenspan & Holmes (1982, 1983).

A number of numerical studies of the bifurcations of one- and two-dimensional maps exist, see, for example, Gumowski & Mira (1980); El-Hamouly & Mira (1981); Arneodo *et al.* (1982); Grebogi *et al.* (1982). The studies of Hénon's map (Hénon 1976; Simo 1979) are of particular relevance to the present paper, since this map can be put into the form (1.1) with

$$f_\mu(y) = \mu - y^2, \tag{1.5}$$

although we note that for the parameter values used by Hénon, the map is orientation reversing. Throughout this paper, we shall use the orientation *preserving* Hénon map as our main example. We also refer the reader to van Strien (1982), Gambaudo & Tresser (1983) and Tresser *et al.* (1979) for related work on the creation of horseshoes. Recently Yorke & Alligood (1983) have proved that period doubling sequences occur in a rather general context during the creation of horseshoes in $\mathbb{R}^n$. Their results nicely complement our discussions in §§4 and 5.

A major question that we do not seriously address here is that of whether maps such as (1.1) can possess strange attractors for $\epsilon \neq 0$. The results of Jakobson (1981) (cf. Misiurewicz 1981*b*) establish that $F_{\mu,0}$ does have strange attractors on a μ-set of positive Lebesgue measure, since f_μ

does. Also see Collet & Eckmann (1980*a*, *b*). We hope to return to this question in subsequent work. We remark that Newhouse's results on diffeomorphisms with infinitely many sinks do not preclude the possibility that $F_{\mu,\epsilon}$ has strange attractors for a parameter set of positive measure (Newhouse 1974, 1979, 1980).

This present paper is organized as follows. In §2 we review results on the bifurcations and non-wandering sets of one-dimensional maps and sketch the structure of the bifurcation set for a 'versal' family. While this section contains little original work it does collect together the related results of several authors. In particular, we include an outline of the kneading theory of Milnor & Thurston (1977), and state a theorem that describes a natural decomposition of the non-wandering set Ω_μ. The latter is originally due to Jonker & Rand (1981), but within the class of maps with negative Schwarzian derivative, the subsequent work of Singer (1978), Misiurewicz (1981*a*), Guckenheimer (1979), and van Strien (1982) allows considerable simplification. Nitecki (1981) provides an extensive review of one dimensional dynamics from a rather different viewpoint.

In §3 we state and prove theorems extending the bifurcation results to two-dimensional families of the form (1.1). In doing so we outline a two-dimensional analogue of the famous period doubling bifurcation sequence studied by Feigenbaum (1978) and construct a C^1 planar diffeomorphism having a non-wandering set corresponding to that of the one-dimensional map at the first Feigenbaum accumulation point (Whitley 1983). While the saddle–node and period doubling sequences carry over to the two-dimensional map fairly directly, we find great differences in 'later' global bifurcations in which homoclinic orbits and cycles are created in the two-dimensional map. In particular we find open sets of parameter values for which two or more stable periodic orbits coexist, in marked contrast to the one-dimensional situation, in which at most one stable periodic orbit exists for each μ-value (Singer 1978). Our results also imply the existence of wild hyperbolic sets (Newhouse 1979, 1980) and thus that there are parameter values for which countably many stable periodic orbits coexist (cf. Robinson 1983).

In §4 we discuss the homoclinic bifurcations of $F_{\mu,\epsilon}$; $\epsilon \in (0, 1]$ in more detail and show that, to each of certain bifurcation points for f_μ there corresponds a 'Cantor fan' of homoclinic bifurcation curves for $F_{\mu,\epsilon}$. We use the results of Gavrilov & Silnikov (1972, 1973) to show that each of these curves is the limit of a sequence of saddle node and period doubling bifurcation curves for periodic orbits. In §5 we use these results to show that infinitely many families of bifurcation curves must cross each other in the (μ, ϵ)-plane. We conclude that the sequence of bifurcations to periodic orbits observed as one moves through a family such as $F_{\mu,\epsilon}$ for fixed ϵ can differ dramatically from that of the one-dimensional map, and we are able to trace the structures of certain such bifurcation sequences. This leads us to question the current vogue for viewing the physical world as a one-dimensional universal map.

In the final section we summarize our results in a model for the creation of horseshoes. We illustrate with numerical results for the Hénon map.

The space available here prevents us from giving a full background to the differentiable dynamical and global analytical methods used in this paper. For general background we recommend the books by Chillingworth (1976), the notes of Newhouse (1980) and Bowen (1978) and the recent text by Guckenheimer & Holmes (1983). In particular, some familiarity with the horseshoe construction due to Smale (1963, 1967) (cf. Moser 1973; Newhouse 1980) will be assumed in this paper. A nice elementary discussion of the horseshoe can be found in

Chillingworth (1976). We feel that a proper understanding of this example is an essential prerequisite in attempts to understand chaos and strange attractors in dynamical systems of dimension greater than one.

2. Bifurcations of one-dimensional maps

In this section we review some of the results on one-dimensional maps. We work with the class $\mathscr{C}$ of C^3 even functions $f: I \to I$ whose domains $I = [-a, a] \subset \mathbb{R}$ are closed intervals containing the origin and which satisfy the following properties:

(1) $f(-a) = f(a) = -a$;
(2) f has a single critical point (a maximum) at $x = 0$, and $f''(0) < 0$;
(3) the Schwarzian derivative

$$sf(x) = f'''(x)/f'(x) - \tfrac{3}{2}(f''(x)/f'(x))^2$$

is negative on $I\backslash\{0\}$.

Many of the results we describe hold for a wider class of maps with a single extremum. In particular, f need not be even and one may work with maps which are simply continuous rather than C^3. We include condition (3) since for maps f with negative Schwarzian derivative a result of Singer (1978) (see also Misiurewicz 1981*a*) implies that if p is a stable periodic point of f, then there is either a critical point of f or an endpoint of I whose ω-limit set is the orbit of p. Thus we replace (1) by

$$(1')\ f(-a) = f(a) = -a \quad \text{is an unstable fixed point, i.e.} \quad |f'(-a)| > 1,$$

so that our maps have at most one stable periodic orbit.

Here our main concern is to outline some of the properties of one-parameter families of maps in $\mathscr{C}$. We consider families $f_\mu: \mathbb{R} \to \mathbb{R}$, depending continuously on a real parameter μ, which are *full* in the sense that there are parameter values $s_1 < h_1$ so that:

(*a*) the *non-wandering set* Ω_μ of f_μ is empty for $\mu < s_1$;
(*b*) $f_\mu \in \mathscr{C}$ for $\mu \in (s_1, h_1]$;
(*c*) $f_\mu(0) > a$ if $\mu > h_1$.

In figure 1 we sketch graphs of f_μ for various values of μ. In general the interval I will vary with the parameter as in the archetypal example,

$$x \to \mu - x^2,$$

where $I = [-\frac{1}{2} - (\frac{1}{4}+\mu)^{\frac{1}{2}}, \frac{1}{2} + (\frac{1}{4}+\mu)^{\frac{1}{2}}]$ varies from $[-\frac{1}{2}, \frac{1}{2}]$ to $[-2, 2]$ as μ increases from $s_1 = -\frac{1}{4}$ to $h_1 = 2$.

2.1. *The invariant Cantor set for large μ*

For $\mu > h_1$, when f_μ no longer maps I into itself, almost all points eventually escape from I, Ω_μ is a Cantor set and $f_\mu | \Omega_\mu$ is conjugate to a full (one-sided) shift on two symbols. To see this, let $I_1 = [-a, b_1]$ and $I_2 = [b_2, a]$ where $b_1 < b_2$ are the pre-images of a (see figure 1*e*). Denote by Σ^+ the set of semi-infinite sequences $\epsilon = \{\epsilon_n\}_{n=0}^{\infty}$ of the symbols $+1$ and -1, and let $\sigma: \Sigma^+ \to \Sigma^+$ be the shift map:

$$(\sigma(\epsilon))_n = \epsilon_{n+1}.$$

To each point $x \in \Omega_\mu$ we assign a sequence $\varepsilon(x) \in \Sigma^+$ according to the rule:

$$\epsilon_n(x) = \begin{cases} +1 & \text{if } f^n(x) \in I_1, \\ -1 & \text{if } f^n(x) \in I_2. \end{cases}$$

The map $\varepsilon : \Omega_\mu \to \Sigma^+$ is surjective since $f(I_j) \supset I_1 \cup I_2$ for $j = 1, 2$; i.e. we have a 'full' transition matrix

$$A = (a_{ij}) = \begin{bmatrix} 1 & 1 \\ 1 & 1 \end{bmatrix},$$

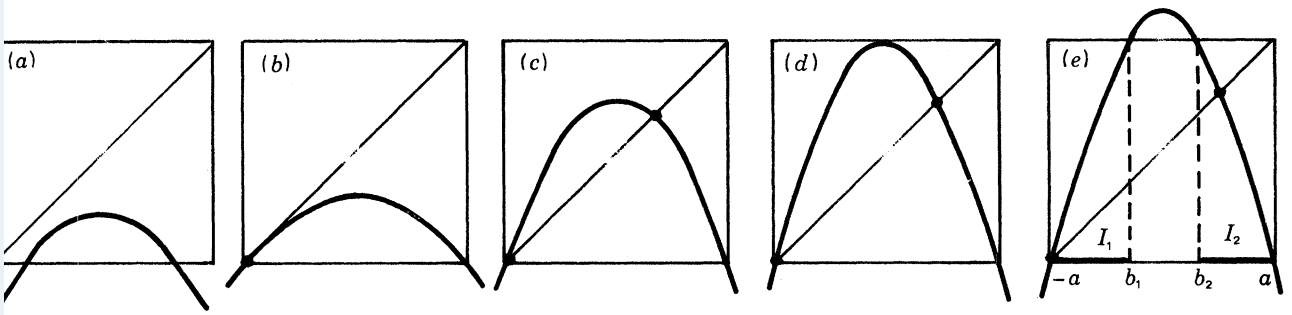

FIGURE 1. Five graphs of f_μ. (a) $\mu < s_1$. (b) $\mu = s_1$. (c) $\mu \in (s_1, h_1)$. (d) $\mu = h_1$. (e) $\mu > h_1$.

where $a_{ij} = 1$ if $f(I_i) \supset I_j$ and $a_{ij} = 0$ otherwise; ε is also injective. This is clear if the gradient of $f_\mu | I_1 \cup I_2$ is uniformly greater than one in magnitude, as is the case for $f_\mu(x) = \mu - x^2$ when $\mu > \frac{1}{4}(5 + 2\sqrt{5}) \approx 2.368$, for example. (The proof for a general map $f_\mu \in \mathscr{C}$ with $\mu > h_1$ relies on the assumption of negative Schwarzian derivative; see van Strien 1982.) Since, by definition $(\varepsilon(x))_{k+1} = (\varepsilon(f(x)))_k$, we have that $\sigma\varepsilon(x) = \varepsilon(f(x))$. Also, if Σ^+ is given the topology induced by the metric

$$d(\varepsilon, \delta) = \sum_{n=0}^{\infty} \frac{|\epsilon_n - \delta_n|}{2^n}, \tag{2.1}$$

ε is easily seen to be a homeomorphism, so that $f_\mu | \Omega_\mu$ is topologically conjugate to $\sigma | \Sigma^+$. The pair $\{I_1 \cap \Omega_\mu, I_2 \cap \Omega_\mu\}$ forms a Markov partition for Ω_μ (Bowen 1978).

The dynamics of $f_\mu | \Omega_\mu$ are now easily read from the model provided by the shift. There are countably many periodic sequences in Σ^+ (2^n for each period n) which correspond to periodic points of f_μ, as well as a countably infinite number of eventually periodic sequences, representing non-wandering points in I that are pre-images of periodic points, and an uncountable number of aperiodic sequences, corresponding to non-periodic non-wandering points of f_μ. Since the periodic points of $\sigma | \Sigma^+$ (the periodic sequences) are dense in Σ^+, the periodic points of f_μ are dense in Ω_μ. One can also show that $f_\mu | \Omega_\mu$ has a dense orbit by considering a symbol sequence that contains all finite strings of length $1, 2, 3, \ldots$.

Thus we have a complete description of the dynamics of $f_\mu \in \mathscr{C}$ for $\mu > h_1$, and we see that, as μ varies from s_1 to h_1, infinitely many periodic and non-periodic non-wandering points are created. The rest of this section is concerned with describing the major features of the bifurcation set in which these non-wandering points emerge for a full family f_μ in the range $s_1 \leqslant \mu \leqslant h_1$.

2.2. *Local bifurcations of f_μ*

There are two well known local bifurcations of periodic points that serve as building blocks for the bifurcation set: the fold, saddle-node or tangent bifurcation, and the flip or period-doubling bifurcation (cf. Guckenheimer 1977). These describe the least degenerate ways in

which the local behaviour of the map changes with the parameter, near a parameter value for which the map has a non-hyberbolic periodic point, i.e. a periodic point with eigenvalue ± 1. We state the results below for fixed points of the map, periodic points are easily accommodated by considering the relevant iterate of the map, and we suppose that the map has a non-hyperbolic fixed point at the origin when $\mu = 0$, which can always be arranged by translating coordinates. We assume that the map is C^1 with respect to the parameter.

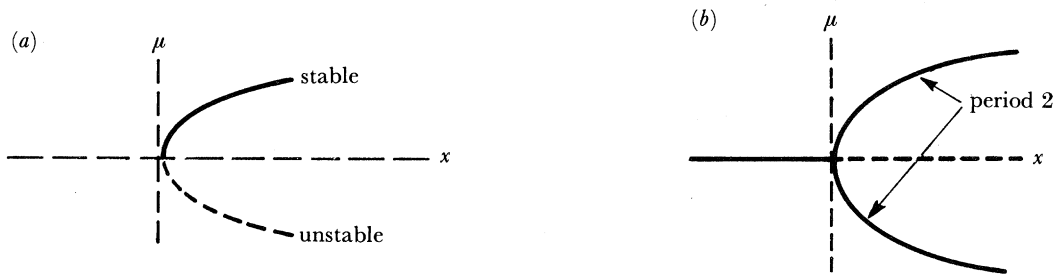

FIGURE 2. Local bifurcations. (*a*) Fold. (*b*) Flip.

PROPOSITION 2.1. (Fold bifurcation). *Let* $f: \mathbb{R} \times \mathbb{R} \to \mathbb{R}$, $(x, \mu) \to f_\mu(x)$ *be a one-parameter family of* C^2 *maps satisfying:*

$$f(0, 0) = 0, \tag{2.2}$$

$$[\partial f/\partial x]\ (0, 0) = 1, \tag{2.3}$$

$$[\partial f/\partial \mu]\ (0, 0) > 0, \tag{2.4}$$

$$[\partial^2 f/\partial x^2]\ (0, 0) < 0. \tag{2.5}$$

Then there are intervals $(\mu_1, 0)$ *and* $(0, \mu_2)$ *and* $\epsilon > 0$ *so that*

(i) *if* $\mu \in (\mu_1, 0)$ *then* f_μ *has no fixed points in* $(-\epsilon, \epsilon)$;

(ii) *if* $\mu \in (0, \mu_2)$ *then* f_μ *has two hyperbolic fixed points in* $(-\epsilon, \epsilon)$. *One is stable and the other unstable.*

Remark. Reversing one of the inequalities (2.4) or (2.5) reverses the roles of the intervals $(\mu_1, 0)$ and $(0, \mu_2)$.

PROPOSITION 2.2 (Flip bifurcation). *Let* $f: \mathbb{R} \times \mathbb{R} \to \mathbb{R}$ *be a one-parameter family of* C^3 *maps satisfying:*

$$f(0, 0) = 0, \tag{2.6}$$

and

$$[\partial f/\partial x]\ (0, 0) = -1. \tag{2.7}$$

Then there is a unique branch of fixed points $x(\mu)$ *for* μ *near* 0 *with* $x(0) = 0$. *If the eigenvalue* $\lambda(\mu) = [\partial f/\partial x]\ (x(\mu), \mu)$ *satisfies*

$$[d\lambda/d\mu]\ (0) < 0, \tag{2.8}$$

and also

$$[\partial^3 f^2/\partial x^3]\ (0, 0) < 0, \tag{2.9}$$

then there are intervals $(\mu_1, 0)$ *and* $(0, \mu_2)$ *and* $\epsilon > 0$ *so that*

(i) *if* $\mu \in (\mu_1, 0)$ *then* f_μ^2 *has a single fixed point in* $(-\epsilon, \epsilon)$ *which is a stable fixed point of* f_μ;

(ii) *if* $\mu \in (0, \mu_2)$ *then* f_μ *has one unstable fixed point and one stable orbit of period two in* $(-\epsilon, \epsilon)$.

Remark. Changing either of the inequalities (2.8) or (2.9) reverses the interval in which the period two points exist. Changing (2.8) reverses the stability of the fixed point, while changing

(2.9) reverses the stability of the period two points, although for maps with negative Schwarzian derivative a simple calculation shows that $[\partial^3 f^2/\partial x^3]\,(0, 0)$ is always negative (cf. Allwright 1978), so that a flip bifurcation for a family of maps in $\mathscr{C}$ always involves a *stable* orbit of period two.

These two bifurcations are illustrated in figure 2.

The periodic points in the shift $\sigma|\Sigma^+$ which exists for $\mu > h_1$ are created by these two types of bifurcation, a typical sequence of bifurcations being the birth of a pair of orbits of some 'basic' period k in a fold bifurcation, followed by a sequence of flip bifurcations in which stable orbits of period $2^l k$ become unstable and give rise to stable orbits of period $2^{l+1}k$, $l = 0, 1, 2, \ldots$. However, the one-dimensional nature of the map imposes strong restrictions on the order in which the basic periods may appear as the parameter varies; the presence of an orbit of a certain period necessarily implies the existence of orbits of various other periods. More precisely, we have the following results of Sarkovskii (1964) (Stefan 1977 provides an account of Sarkovskii's proof in English).

THEOREM 2.3 (Sarkovskii's theorem). *Order the natural numbers* $\mathbb{N}$ *as follows:*

$$3 \lhd 5 \lhd 7 \lhd \ldots \lhd 2\times 3 \lhd 2\times 5 \lhd 2\times 7 \lhd \ldots \lhd 2^l 3 \lhd 2^l 5 \lhd 2^l 7 \lhd \ldots \lhd 2^l \lhd \ldots$$
$$\lhd 2^3 \lhd 2^2 \lhd 2 \lhd 1.$$

If $f: \mathbb{R}\to\mathbb{R}$ *is a continuous map which has an orbit of period* n*, then* f *has an orbit of period* m *for each* $m \in \mathbb{N}$ *with* $n \lhd m$.

Note that this result applies to all continuous maps of $\mathbb{R}$, not just to maps in $\mathscr{C}$. For functions with a single extremum, proofs of Sarkovkii's theorem have subsequently been given by several authors, including Guckenheimer (1977), Jonker (1979), and Block *et al.* (1980). Li & Yorke's (1975) famous *Period three-implies chaos* includes the statement that period three starts the list.

2.3. *Kneading theory*

Sarkovskii's theorem tells us only the order of 'first' appearance of a particular period in a parameterized family, while for most periods the shift $\sigma|\Sigma^+$ contains many orbits of that period (there are, for example, 52377 orbits of period 20!; see table 2 at the end of §2). However, for families $f_\mu \in \mathscr{C}$ the *kneading theory* of Milnor & Thurston (1977), which we now outline, provides a complete description of the order of appearance of all the non-wandering points, both periodic and non-periodic, in $\sigma|\Sigma^+$. In outlining the relevant parts of the kneading theory we essentially follow the exposition of Jonker (1979). Guckenheimer (1979, 1980) provides a different, but for our purposes equivalent, formulation (cf. Guckenheimer & Holmes 1983).

For a map $f\in\mathscr{C}$ and a point $x\in I$ we define the *itinerary* of x to be the semi-infinite sequence $\boldsymbol{\varepsilon}(x) = \{\epsilon_n(x)\}_{n=0}^{\infty}$, where

$$\epsilon_n(x) = \begin{cases} +1 & \text{if } f^n(x) \in [-a, 0), \\ 0 & \text{if } f^n(x) = 0, \\ -1 & \text{if } f^n(x) \in (0, a]. \end{cases}$$

The mapping $x \mapsto \boldsymbol{\varepsilon}(x)$ has the property that $\boldsymbol{\varepsilon}(f(x)) = \sigma(\boldsymbol{\varepsilon}(x))$, but it does not reflect the ordering of the interval, given the natural lexicographic ordering for the sequences, because f

reverses orientation on $(0, a]$. To take account of this, we define the *invariant coordinate* of x, $\boldsymbol{\theta}(x) = \{\theta_n(x)\}_{n=0}^{\infty}$, by $\theta_n(x) = \prod_{i=0}^{n} \epsilon_i(x)$, or equivalently,

$$\theta_n(x) = \begin{cases} +1 & \text{if } f^{n+1} \text{ is orientation preserving near } x, \\ 0 & \text{if } f^m(x) = 0 \text{ for some } m \text{ with } 0 \leqslant m \leqslant n, \\ -1 & \text{if } f^{n+1} \text{ is orientation reversing near } x. \end{cases}$$

The basis for the kneading theory is the fact that, if the sequences are ordered lexicographically, then the mapping $x \to \boldsymbol{\theta}(x)$ is monotone decreasing (cf. Milnor & Thurston 1977; Guckenheimer & Holmes 1983).

For $f \in \mathscr{C}$ we define the *kneading invariant* of f, $\boldsymbol{\nu}(f)$, by

$$\boldsymbol{\nu}(f) = \lim_{x \uparrow 0} \boldsymbol{\theta}(x).$$

This limit exists (in the topology given by the metric (2.1)), and if we write $\boldsymbol{\nu}(f) = \{\nu_n\}_{n=0}^{\infty}$ then, since the set $\{f^{-n}(0)\}$ is finite for each n, each of the numbers ν_n is non-zero. Thus $\boldsymbol{\nu}(f) \in \Sigma^+$, and clearly $\nu_0 = +1$. We note that $\boldsymbol{\nu}(f) = -\lim_{x \downarrow 0} \boldsymbol{\theta}(x)$ (Jonker 1979).

The monotonicity of the invariant coordinate $\boldsymbol{\theta}$ implies that for each $x \in I$ either $\theta_n(x) = 0$ for all $n \geqslant 0$, $\boldsymbol{\theta}(x) \geqslant \boldsymbol{\nu}(f)$ or $\boldsymbol{\theta}(x) \leqslant -\boldsymbol{\nu}(f)$. Similarly, considering $f^n(x)$ and using the fact that $\sigma(\boldsymbol{\theta}(x)) = \theta_0(x)\,\boldsymbol{\theta}(f(x))$, we find that for any $n \geqslant 0$ either $\theta_k(x) = 0$ for all $k \geqslant n$, or $|\sigma^n(\boldsymbol{\theta}(x))| \geqslant \boldsymbol{\nu}(f)$, where $|(\theta_n)_{n=0}^{\infty}| = \{\theta_0 \times \theta_n\}_{n=0}^{\infty}$. We say that a sequence $\boldsymbol{\theta}$ of the symbols $+1$, 0 and -1 is $\boldsymbol{\nu}(f)$-*admissible* if for all $n \geqslant 0$:

$$\left.\begin{aligned} &\text{either} \quad \theta_k(x) = 0 \quad \text{for all} \quad k \geqslant n, \\ &\text{or} \qquad\qquad |\sigma^n(\boldsymbol{\theta})| \geqslant \boldsymbol{\nu}(f). \end{aligned}\right\} \tag{2.10}$$

Then by construction $\boldsymbol{\theta}(x)$ is $\boldsymbol{\nu}(f)$-admissible for each $x \in I$, and so are $\boldsymbol{\theta}(x^+) = \lim_{y \downarrow x} \boldsymbol{\theta}(y)$ and $\boldsymbol{\theta}(x^-) = \lim_{y \uparrow x} \boldsymbol{\theta}(y)$. Conversely, if $\boldsymbol{\theta}$ is a $\boldsymbol{\nu}(f)$-admissible sequence then one can show (Milnor 1977; cf. Guckenheimer 1979, 1980) that there is a point $x \in I$ such that $\boldsymbol{\theta}$ is either $\boldsymbol{\theta}(x)$, $\boldsymbol{\theta}(x^+)$ or $\boldsymbol{\theta}(x^-)$. In fact, $x = \inf\{y \in I \,|\, \boldsymbol{\theta}(y) \leqslant \boldsymbol{\theta}\}$, and if $|\sigma^n(\boldsymbol{\theta})| \geqslant \boldsymbol{\nu}(f)$ for all n, then $\boldsymbol{\theta} = \boldsymbol{\theta}(x)$.

Now $\boldsymbol{\nu} = \boldsymbol{\nu}(f) = \boldsymbol{\theta}(0^-)$ is also $\boldsymbol{\nu}(f)$-admissible, and since $\boldsymbol{\nu} \in \Sigma^+$, we have for all $n \geqslant 0$,

$$|\sigma^n(\boldsymbol{\nu})| \geqslant \boldsymbol{\nu}. \tag{2.11}$$

Any sequence $\boldsymbol{\nu} \in \Sigma^+$ that satisfies (2.11) is called an *admissible kneading invariant*. If $\boldsymbol{\nu}$ is an admissible kneading invariant then there is a map $f \in \mathscr{C}$ for which $\boldsymbol{\nu} = \boldsymbol{\nu}(f)$ (Milnor 1977; cf. Guckenheimer 1979, 1980).

The kneading invariant tells us a great deal about the map and its dynamics. In particular, the kneading invariant, together with a little information about the stable periodic orbit of f, should it have one, completely determines the topological equivalence class of f (Guckenheimer 1979). The structure of the non-wandering set $\Omega(f)$ can also be deduced from $\boldsymbol{\nu}(f)$ (Jonker & Rand 1981; see also van Strien 1982). In fact $\boldsymbol{\nu}(f)$ may be 'factorized' in a certain way so that each factor corresponds to an invariant basic subset of $\Omega(f)$, leading to a 'spectral' decomposition of $\Omega(f)$ analogous to that for an Axiom A (see Smale 1967) diffeomorphism.

Before giving a precise description of this decomposition we need several definitions. Let $\Lambda \subseteq I$ be a closed f-invariant set, i.e. $f(\Lambda) = \Lambda$. We say that Λ is *hyperbolic* if there are constants $c > 0$ and $\tau > 1$ so that for each $x \in \Lambda$ either $|(f^k)'(x)| > c\tau^k$ or $|(f^k)'(x)| < c\tau^{-k}$ for all $k \geqslant 1$. In the former case we say that Λ is hyperbolically repelling and in the latter, hyper-

bolically attracting. The *basin of attraction* of Λ is the set $B(\Lambda) = \{x \in I \mid \omega(x) \subseteq \Lambda\}$. Here $\omega(x)$ denotes the *ω-limit set* of x: $\omega(x) = \bigcap_{N\geqslant 0} \overline{\bigcup_{n\geqslant N} f^n(x)}$. We say that Λ is an *attracting set* if $\Lambda \subsetneq B(\Lambda)$. An *attractor* of f is an attracting set which contains a dense orbit.

The basic sets Ω_j in the decomposition fall into four types. The simplest possibility is that Ω_j is a periodic orbit. A second possibility is modelled by a generalization of the shift automorphism $\sigma \mid \Sigma^+$ defined above. A subset $\Sigma_s^+ \subseteq \Sigma^+$ is said to be of *finite type* if there is a finite set of blocks $B_1, \ldots, B_n$ of the symbols ± 1 so that a sequence $\boldsymbol{a}$ belongs to Σ_s^+ if and only if it does not contain any of these blocks. If Σ_s^+ is a non-empty subshift of finite type it is either a single periodic sequence or is homeomorphic to a Cantor set, and $\sigma \mid \Sigma_s^+$ is called a *subshift of finite type*. As in the case of the full shift, the periodic orbits of a subshift of finite type are dense in Σ_s^+. $\sigma \mid \Sigma_s^+$ is *transitive* if there is a sequence $\boldsymbol{a} \in \Sigma_s^+$, whose orbit $\{\sigma^n(\boldsymbol{a})\}_{n=0}^{\infty}$ under the shift is dense in Σ_s^+.

A further possibility is that Ω_j is contained in a subinterval of I on which some iterate of f is conjugate to one of the piecewise linear maps

$$g_s(x) = s - 1 - s|x|, \quad s \in (\sqrt{2}, 2]. \tag{2.12}$$

The non-wandering set of $g_s|_{[-1,1]}$ can be described exactly (cf. Jonker & Rand 1981). If $m = 2^n$ and $\sqrt{2} < s^m \leqslant 2$, $\Omega(g_s)$ consists of m disjoint closed intervals $J_1, \ldots, J_m$, together with a finite number of unstable periodic points. g_s maps J_i linearly onto J_{i+1} for $i = 1, \ldots, m-1$, and maps J_m onto J_1 with a single fold at the origin.

Finally, in certain cases the decomposition of $\Omega(f)$ has infinitely many basic sets, and f then has an attractor on which the dynamics have a symbolic model of the following type. For a sequence of positive integers k_n, $n = 1, 2, \ldots$, let $X_n = \{0, 1, \ldots, k_n\}$ and $X = \prod_{n=1}^{\infty} X_n$. The associated *adding machine* transformation $\phi: X \to X$ is defined by

$$\phi(k_1, k_2, \ldots, k_n, \ldots) = (0, 0, \ldots, 0, \ldots)$$

and

$$\phi(x_1, x_2, \ldots, x_n, \ldots) = \begin{cases} (x_1 + 1, x_2, \ldots, x_n, \ldots) & \text{if} \quad x_1 < k_1, \\ (0, 0, \ldots, x_n + 1, x_{n+1}, \ldots) & \text{if} \quad x_1 = k_1, \ldots, x_{n-1} = k_{n-1} \\ & \text{and} \quad x_n < k_n. \end{cases}$$

Thus ϕ simply performs addition of 1 with 'carry-over', but with a varying number base in each column (see Brown 1976). The set X is a minimal set for ϕ: the ϕ-orbit of every point $x \in X$ is dense in X (in the appropriate topology).

Let per (f) denote the set of periodic points of f. We can now state the major result of this section.

THEOREM 2.4 (Decomposition of $\Omega(f)$). *If $f \in \mathscr{C}$ there is a decomposition of $\Omega(f)$ into a finite or countably infinite number of closed invariant sets Ω_j, $j = 0, 1, \ldots$, including a set Ω_∞ if the number of sets is infinite. The decomposition has the following properties*:

(1) $\Omega_0 = \{-a\}$;

(2) *if the decomposition is finite, $\Omega(f) = \Omega_0 \cup \Omega_1 \cup \ldots \cup \Omega_p$, then $\Omega_i \cap \Omega_j = \varnothing$ for $0 \leqslant i < j < p$, and $\Omega_{p-1} \cap \Omega_p$ contains at most a single periodic orbit*;

(3) *if the decomposition is infinite, $\Omega(f) = \Omega_0 \cup \ldots \cup \Omega_\infty$, then the Ω_j are disjoint for all j*;

(4) *if $\Omega(f) = \Omega_0 \cup \ldots \cup \Omega_p$, $p \in \mathbb{N} \cup \{\infty\}$, then for $0 \leqslant j < p$, Ω_j is hyperbolically repelling, and either Ω_j is a periodic orbit, or $\Omega_j = \text{per}_j \cup \mathrm{C}_j$ where per_j is a finite subset of* per (f), *C_j is a Cantor set and $f: \mathrm{C}_j \to \mathrm{C}_j$ is conjugate to a transitive subshift of finite type*;

PHILOSOPHICAL TRANSACTIONS OF THE ROYAL SOCIETY A MATHEMATICAL, PHYSICAL & ENGINEERING SCIENCES

(5) *f has a unique attractor $A \subseteq \Omega_p$. The basin of attraction of A, $B(A)$, is open and dense in I if p is finite and a residual subset of I if $p = \infty$; $B(A)$ has full Lebesgue measure in I;*

(6) *if $p < \infty$ there are three possibilities for Ω_p:*

(i) *Ω_p is a periodic orbit $\{z, f(z), \ldots, f^{n-1}(z)\}$ which is either hyperbolically stable, i.e. $|(f^n)'(z)| < 1$, or is non-hyperbolic with $(f^n)'(z) = -1$, in which case $(f^{2n})''(z) = 0$ and $(f^{2n})'''(z) < 0$ so that Ω_p still attracts locally from both sides;*

(ii) *$\Omega_p = \mathrm{per}_p \cup \mathrm{C}_p$ as in (4), except C_p is not hyperbolic. The attractor is a periodic orbit $\{z, f(z), \ldots, f^{n-1}(z)\}$ contained in C_p; this orbit is not hyperbolic: $(f^n)'(z) = 1$, but $(f^n)''(z) \neq 0$ so that it still attracts locally from one side;*

(iii) *$\Omega_p = \mathrm{per}_p \cup I_p$ where per_p is a finite subset of $\mathrm{per}(f)$ which is isolated in $\Omega(f)$, and the attractor I_p is a finite union of intervals. Ω_p is the disjoint union of N closed sets Ω_p^j, $j = 1, \ldots, N$, so that for $j = 1, \ldots, N-1$, $f|\Omega_p^j$ is a homeomorphism onto Ω_p^{j+1} and $f^N|\Omega_p^N : \Omega_p^N \to \Omega_p^N$ is conjugate either to the piecewise linear map (2.12) $g_s|(-1, 1)$, for some $s \in (\sqrt{2}, 2)$, restricted to its non-wandering set, or to $g_2|[-1, 1]$ restricted to its non-wandering set;*

(7) *if the decomposition has infinitely many sets then the attractor Ω_∞ is a Cantor set and $f : \Omega_\infty \to \Omega_\infty$ is conjugate to an adding machine transformation. Ω_∞ is the closure of the orbit of the critical point of f.*

The main parts of this theorem were proved by Jonker & Rand (1981), who worked with continuous maps with a single extremum. Within the class $\mathscr{C}$ the work of Guckenheimer (1979), Misiurewicz (1981*a*), and van Strien (1982) allows considerable simplification and strengthening of their results. We shall not describe the proof of the theorem here, but we give various examples of the decomposition later.

An important property of maps of the interval is that the iterates of nearby points may not remain close to one another. Guckenheimer (1979) adopts the following definition for this phenomenon: $f \in \mathscr{C}$ has *sensitive dependence on initial conditions* if there is a set $X \subset I$ of positive Lebesgue measure and an $\epsilon > 0$ so that for each $x \in X$ and any neighbourhood U of x there is a point $y \in U$ and an integer $n > 0$ with $d(f^n(x), f^n(y)) > \epsilon$. Guckenheimer shows that $f \in \mathscr{C}$ has sensitive dependence on initial conditions if and only if an iterate of f on a subinterval of I is conjugate to a piecewise linear map g_s, $s \in (\sqrt{2}, 2]$. These are precisely the maps whose non-wandering sets have a finite decomposition in which the last set falls into case 6(iii) of theorem 2.4. We shall say that such a map has a *strange attractor*.

A related question is that of the existence of an absolutely continuous, ergodic invariant measure for f. Misiurewicz (1981*b*) shows that such a measure exists for maps which have no stable periodic orbits and for which the critical point $0 \notin \overline{\{f^n(0) \,|\, n > 0\}}$. These maps form a subset of those in case 6(iii) of the theorem. One might ask whether all maps in case 6(iii) have invariant measures; i.e. is sensitive dependence equivalent to the existence of an absolutely continuous invariant measure? (Cf. Jakobson 1978, 1981.) This is still an open question.

2.4. *The bifurcation set*

Returning to the question of the bifurcations of a full family in $\mathscr{C}$, let κ denote the set of admissible kneading invariants. We say $\boldsymbol{\nu}$ is *periodic*, with period n, if $\nu_{n+i} = \nu_i$ for all $i \geqslant 0$, and *antiperiodic*, with period n, if $\nu_{n+i} = -\nu_i$ for all $i \geqslant 0$. If $\boldsymbol{\nu}$ is periodic, the *minimal period* of $\boldsymbol{\nu}$ is the least integer n so that $\boldsymbol{\nu}$ is periodic or antiperiodic with period n. Let per be the set of periodic admissible kneading invariants, and Π be the set of admissible kneading invariants which are periodic but not antiperiodic.

For a full family $f_\mu \in \mathscr{C}$ let $k_f : [s_1, h_1] \to \kappa$ denote the map $\mu \to \nu(f_n)$. The full family $f_\mu \in \mathscr{C}$ is *versal* if

(i) k_f is monotone decreasing;
(ii) $k_f^{-1}(\nu)$ is a closed interval if $\nu \in \Pi$;
(iii) $k_f^{-1}(\nu)$ is an interval of the form $(a, b]$ if $\nu \in \mathrm{per} \backslash \Pi$;
(iv) $k_f^{-1}(\nu)$ is a singleton if $\nu \notin \mathrm{per}$.

Jonker & Rand (1981) show that any family f_μ can be factored through a versal one; i.e. there is a versal family g_μ and a continuous re-parametrization ϕ so that $k_g \circ \phi = k_f$. Therefore we shall restrict attention to a versal family f_μ, for which the problem of describing the bifurcation sequence reduces to understanding the order of κ and the relation between the kneading invariant $\nu(f)$ and the non-wandering set $\Omega(f)$, since $\nu(f)$ restricts the itineraries which can occur. The precise way in which this works is perhaps best understood by reference to the examples given below. Also see Guckenheimer (1979) and Guckenheimer & Holmes (1983).

We shall also assume that the family f_μ is *regular* in the sense that the only bifurcations of periodic points of f_μ are the fold and flip bifurcations described in propositions 2.1 and 2.2. As we remarked earlier, condition (2.9) of proposition 2.2 is automatically satisfied for maps with negative Schwarzian derivative, and it follows from the proof of Singer's theorem (see Misiurewicz 1981*a*) that the same is true of condition (2.5) of proposition 2.1. Thus we are assuming that if $p(\mu)$ is a periodic point of f_μ of (minimal) period n, the following conditions hold: if

$$(f^n_{\mu_*})'(p(\mu_*)) = 1, \quad \text{then} \quad ([\partial^2/\partial x^2] f^n_\mu(x))\,([\partial/\partial\mu] f^n_\mu(x))|_{\mu=\mu_*, x=p(\mu_*)} < 0, \tag{2.13}$$

and if

$$(f^n_{\mu_*})'(p(\mu_*)) = -1 \quad \text{then} \quad [\partial/\partial\mu]\,(f^n_\mu)'(p(\mu))|_{\mu=\mu_*} < 0. \tag{2.14}$$

Our assumption implies that the number of periodic orbits is a monotone increasing function of μ.

To describe something of the structure of κ we shall use the following notation. If β is a finite block of ± 1 then β' will denote the sequence obtained by iterating β indefinitely, and if β is either a finite or an infinite sequence of ± 1 then $\bar{\beta}$ will denote the sequence obtained by changing all the signs of β. For a sequence $\boldsymbol{\beta}$ of ± 1 we shall omit the numbers 1 and write $\boldsymbol{\beta}$ as a sequence of $+$ or $-$ signs.

The justification of the following description of κ may be found in Jonker & Rand (1981), remembering that their results can be simplified within the class $\mathscr{C}$.

A map $f \in \mathscr{C}$ has an attracting periodic orbit if and only if $\nu(f) \in \mathrm{per}$. In fact, if $\nu(f) \in \Pi$ has period n then f has a periodic orbit $O(x)$ of period n, with $0 \leqslant (f^n)'(x) \leqslant 1$, while if $\nu(f)$ is anti-periodic, i.e. $\nu(f) \in \mathrm{per} \backslash \Pi$, then f has a periodic orbit $O(x)$ and either $O(x)$ has period n and $-1 \leqslant (f^n)'(x) < 0$, or $O(x)$ has period $2n$ and $0 \leqslant (f^{2n})'(x) \leqslant 1$. For example, in the versal family f_μ, the largest admissible kneading invariant is $\nu(f_{s_1}) = ++++\ldots = (+)'$. At $\mu = s_1$, f_μ undergoes a fold bifurcation and $-a$ is a fixed point with $f'_{s_1}(-a) = 1$. The kneading invariant $\nu(f_\mu)$ remains constant until the stable fixed point which is created in the fold bifurcation crosses the critical point $x = 0$, when $\nu(f_\mu)$ changes to $(+-)'$. As μ increases the fixed point becomes unstable and creates a stable orbit of period two through a flip bifurcation, but the kneading invariant remains $(+-)'$ until one of the period two points crosses the critical point, when $\nu(f_\mu)$ becomes $(+--+)'$.

The first elements of κ, in decreasing order, form a sequence $(+)'$, $(+-)'$, $(+--+)'$,

$(+--+-++-)', \ldots$, i.e. if $(\beta)'$ is a member of this sequence the next smaller element of κ is $(\beta\bar{\beta})'$. This sequence in κ corresponds to the initial period-doubling sequence for the family f_μ. The parameter value at which a stable orbit of period 2^{l-1} has a flip bifurcation and produces a stable orbit of period 2^l will be labelled f_{2^l}.

For a periodic sequence $\nu = \{\nu_n\}_{n=0}^{\infty} \in \kappa$ of period m and an admissible $\alpha = \{\alpha_n\}_{n=0}^{\infty} \in \kappa$ we define $\nu * \alpha = \{\tau_n\}_{n=0}^{\infty}$ by $\tau_{qn+i} = \alpha_q \nu_i$, $0 \leqslant i < m$. The $*$-factors of $\nu(f)$ are related to the decomposition of $\Omega(f)$ of theorem 2.4. For example, the 'period doubling' sequence of elements of κ above may be written

$$(+)', (+)' * (+-)', (+)' * (+-)' * (+-)', (+)' * (+-)' * (+-)' * (+-)', \ldots,$$

where in the kneading invariant $(+)' * (+-)' * (+-)' * \ldots * (+-)'$, with n factors $(+-)'$ say, the first factor $(+)'$ corresponds to the fixed point in the boundary of I: $\Omega_0 = \{-a\}$, while the jth of the factors $(+-)'$ corresponds to an unstable orbit with period 2^{j-1}, except the last, which corresponds either to a stable orbit of period 2^{k-1} or to an unstable orbit of period 2^{k-1} and a stable orbit of period 2^k (case 2.6(i) of the theorem).

This initial sequence of kneading invariants has a limit which is an aperiodic sequence, called the Morse sequence, defined iteratively by $\beta_1 = +$ and $\beta_{2n} = \beta_n \bar{\beta}_n$, $n > 1$, where β_n is the block consisting of the first n terms of the sequence. In the versal family f_μ the parameter value for which $\nu(f_\mu)$ is the Morse sequence will be called F_1. The corresponding map lies in the boundary of the set of maps with zero topological entropy. The maps with this kneading invariant were studied by Misiurewicz (1981*a*), who showed that any two such maps are topologically equivalent. They have non-wandering sets which can be decomposed into an infinite number of basic sets: the unstable fixed point $-a$, an unstable periodic orbit of period 2^n for each $n = 0, 1, 2, \ldots$, and a Cantor set Ω_∞ on which the map is conjugate to the adding machine transformation where each base $k_n = 2$ (cf. Collet *et al.* 1980). This is an example of cases 3 and 7 of theorem 2.4. The corresponding factorization of the kneading invariant is

$$\nu(f_{F_1}) = (+)' * (+-)' * (+-)' * \ldots * (+-)' * \ldots.$$

Of the maps in $\mathscr{C}$ without stable periodic orbits whose non-wandering sets have finite decompositions (and hence have strange attractors), perhaps the easiest to understand are those whose kneading invariants are eventually periodic, i.e. $\sigma^n(\nu)$ is periodic for some $n > 0$, but ν is not periodic. For these maps, some iterate of the critical point is an unstable periodic point. For instance, the smallest element of κ, $\nu(f_{h_1}) = +(-)'$, is not periodic but has eventual period one, and $f_{h_1}^2(0) = -a$, the fixed point in the boundary of I (see figure 1). In the versal family f_μ there is actually a decreasing sequence of parameter values h_{2^l}, $l = 0, ., \ldots$, accumulating on F_1 from above, for which $f^{2^{l+1}}(0)$ lies in the unstable orbit of period 2^{l-1} created in the initial period-doubling sequence. The proof of the decomposition theorem shows that $f_{h_{2^l}}$ is conjugate to the piecewise linear map $g_s(x) = s - 1 - s|x|$, where $s = 2^{1/2^l}$. (It has been known for some time that this is true for the map $x \to \mu - x^2$, when $\mu = h_1 = 2$, where the conjugacy may be written down explicitly (Ulam & Von Neumann 1947; also see Ruelle 1977).)

Many other examples may be given of kneading invariants which are eventually periodic but not periodic. For instance, there is a sequence of elements of κ of the form

$$+--\ldots-(+-)',$$

with $(n-1)$ minuses, the first of which is $\nu(f_{h_2})$, corresponding to the nth iterate of the critical

point falling on the unstable fixed point in the interior of I. The associated parameter values accumulate on h_1.

Examples of the uncountable number of kneading invariants which are not eventually periodic, but which have finite decompositions and hence correspond to maps with strange attractors, are also easily constructed. These are associated with parameter values for which the orbit of the critical point falls on an unstable Cantor set created in earlier bifurcations.

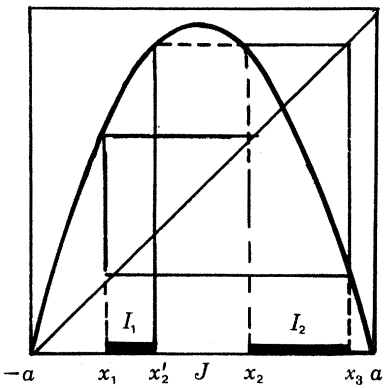

FIGURE 3. A subshift of finite type for f_{s_3}.

Embedded in the large *bifurcation box* $[s_1, h_1]$ (Gumowski & Mira 1980) there are other boxes in which the behaviour of some iterate of the map on a sub-interval of I mimics that of f_μ on I for $\mu \in [s_1, h_1]$. To illustrate this consider the next simplest 'basic' period, period 3: κ contains only one element of period 3, $(+--)'$, and if $s_3 = \inf\{\mu \mid \nu(f_\mu) = (+--)'\}$ then f_{s_3} has an orbit of period 3, $\{x_1, x_2, x_3\}$, with eigenvalue $(f_{s_3}^3)'(x_i) = 1$. Two orbits of period three are born at s_3 in a fold bifurcation. (In the family $\mu \to \mu - x^2$, $s_3 = 1.75$.) To describe $\Omega(f_{s_3})$, let x_2' be the unique point $x_2' \neq x_2$ with $f(x_2') = f(x_2)$, and let $I_1 = [x_1, x_2']$, $J = (x_2', x_2)$, and $I_2 = [x_2, x_3]$ (see figure 3). The non-wandering set of f_{s_3} consists of the fixed point $-a$, and a Cantor set $C = (I_1 \cup I_2) \backslash \bigcup_{n \geqslant 0} f^{-n}(J)$ on which f is conjugate to the subshift of finite type Σ_8^+ where the only excluded block is $++$. Alternatively, this subshift may be described by the transition matrix

$$A = \begin{array}{c} \\ I_1 \\ I_2 \end{array} \begin{array}{c} \begin{array}{cc} I_1 & I_2 \end{array} \\ \begin{bmatrix} 0 & 1 \\ 1 & 1 \end{bmatrix} \end{array} \qquad (2.15)$$

where $a_{ij} = 1$ if $f(I_j) \supset I_i$ and $a_{ij} = 0$ otherwise. (See also Smale & Williams 1976; Guckenheimer *et al.* 1977.) Note that the non-hyperbolic orbit of period three lies in C, so that C is not hyperbolic.

Immediately after the fold bifurcation at $\mu = s_3$ the map has a (hyperbolic) stable orbit of period three together with a Cantor set constructed in a similar way, but now containing the unstable hyperbolic period three orbit created in the fold bifurcation, so that the Cantor set is now hyperbolic. The kneading invariant remains $(+--)'$ until the central point in the stable orbit of period three crosses the critical point. The next elements of κ, in decreasing order, are $(+---++)'$, $(+---++-+++--)'$, ..., or, in terms of the $*$-factorization, we have a sequence

$$(+)' * (+--)', (+)' * (+--)' * (+-)', (+)' * (+--)' * (+-)' * (+-)', \ldots,$$

which corresponds to a period-doubling sequence based on the initially stable period three orbit. This is exactly analogous to the original period-doubling sequence based on the stable fixed point, and this sequence of kneading invariants has the limit

$$+--+++-+++--+++--+---++\ldots,$$

or

$$(+)'*(+--)'*(+-)'*(+-)'*\ldots*(+-)'*\ldots,$$

which is constructed in the same manner as the Morse sequence, but is based on the block $+--$. The map f_μ with this kneading invariant has a non-wandering set which consists of the fixed point $-a$, the subshift Σ_s^+ described above, one unstable orbit of period 2^n3 for each $n = 0, 1, \ldots$, and a Cantor set Ω_∞ on which f_μ is conjugate to the adding machine whose first base $k_1 = 3$ and whose other bases $k_n = 2$, $n \geqslant 2$.

The end of the period three 'box' is the parameter value $\mu = h_3$ at which an iterate of the critical point falls on the unstable orbit of period three created in the fold bifurcation at s_3. We have $\nu(f_{h_3}) = +--(-++)'$. In $[s_3, h_3]$ one can find sequences of parameter values for which iterates of the critical point fall on unstable periodic orbits born in the period-doubling sequence following the fold bifurcation at s_3, etc.: the behaviour of f_μ^3 being exactly similar to that of f_μ in $[s_1, h_1]$.

As a final example of the decomposition theorem, note that the admissible kneading invariant

$$(+)'*(+--)'*(+--)'*\ldots*(+--)'*\ldots,$$

lies between $(+--)'$ and $+--(-++)'$, so the associated parameter value F_3 lies in $[s_3, h_3]$. The non-wandering set of the map with this kneading invariant has an infinite decomposition: the fixed point $-a$, a sequence of Cantor sets Ω_n, $n = 0, 1, 2, \ldots$, on (each of) which f is conjugate to a subshift of finite type, and a Cantor set Ω_∞ on which f is conjugate to the adding machine where each base $k_n = 3$. Each Cantor set Ω_n, $n < \infty$, is contained in 3^n2 disjoint sub-intervals, and if the two closest to the critical point are labelled I_1, I_2, then $f^{3^n} | C_n \cap (I_1 \cup I_2)$ is conjugate to the subshift of finite type described by the transition matrix (2.15).

Similar bifurcation structures occur within each of the countably many bifurcation boxes $[s_k^j, h_k^j]$. Here our subscript k denotes the period of the basic orbits on which the bifurcating components of Ω are built, as in $[s_1, h_1]$, $[s_3, h_3]$, and the superscript j is used to denote the order of appearance of the period-k boxes with increasing μ. We note that, while boxes of period k contain boxes of all periods mk, $m = 3, 4, \ldots$, the boxes are either pairwise disjoint or one is completely contained within another. In tables 1 and 2 at the end of this section we give some examples.

In summary, a map whose kneading invariant is periodic has an attracting periodic orbit, and this orbit attracts a set of points in I which is open and dense, and has full Lebesgue measure. If the kneading invariant is not periodic but has a finite number of $*$-factors then the associated map has a strange attractor which is a union of intervals. If $\nu(f)$ is aperiodic but has an infinite decomposition then the attractor is a Cantor set which attracts points in a residual subset of I, also of full measure, but these maps do not have sensitive dependence on initial conditions, and so do not have strange attractors. Some of the admissible kneading invariants are listed in table 1 and the structure of the bifurcation set of a versal family is indicated in figure 4.

PHILOSOPHICAL TRANSACTIONS OF THE ROYAL SOCIETY A MATHEMATICAL, PHYSICAL & ENGINEERING SCIENCES

The question of the relative size of the set of parameter values for which the map has a stable periodic orbit and the set of those for which it has a strange attractor remains open. The results of Douady & Hubbard (1982) on two-to-one analytic maps of the complex plane show that for the quadratic family $x \to \mu - x^2$, the kneading invariant is a monotone function

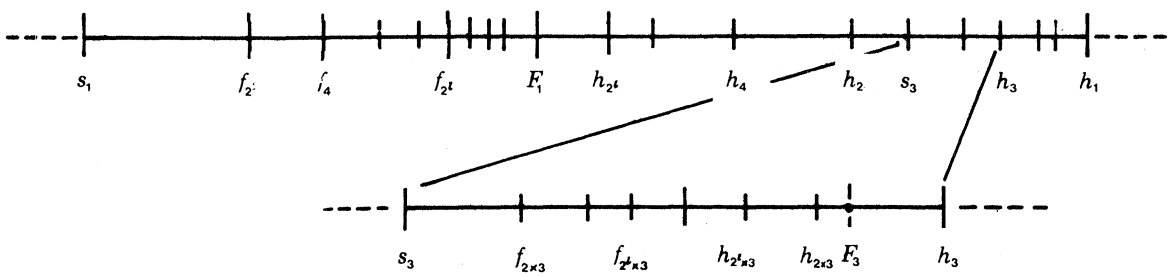

FIGURE 4. The bifurcation set for a versal family.

of μ. To establish the versality of this particular family it remains to show that the set of parameter values for which the map has a stable periodic orbit is dense in $[-\frac{1}{4}, 2]$. Douady & Hubbard's work shows that this problem can be reduced to showing that the Mandelbrot set M of the family $f_c(z) = c - z^2$, c, $z \in \mathbb{C}$,

$$M = \{c \in \mathbb{C} \mid f_c^n(0) \not\to \infty\},$$

is locally connected (Douady 1982). So far this has not been proved.

In contrast, according to Jakobson (1981), for this family there is a set of parameter values of positive Lebesgue measure for which the map has an absolutely continuous, ergodic invariant measure. These maps have strange attractors.

One further, quite remarkable feature of families of one-dimensional maps that deserves mention is the universality discovered by Feigenbaum (1978), although we do not use it subsequently in this paper. It has been verified by Lanford (1982) (cf. Collet *et al.* 1980) that for a class of maps including the quadratic family $x \to \mu - x^2$, the lengths $d_l = h_{2^l} - f_{2^l}$ converge to zero, independently of the particular family, at Feigenbaum's universal rate

$$\lim_{n\to\infty} [d_n/d_{n+1}] = 4.669\ldots.$$

Now the numbers h_{2^l} and f_{2^l} accumulate, from above and below respectively, on the Feigenbaum point F_1 where the non-wandering set of the map has a decomposition into an infinite number of basic sets, and there is similar universal behaviour near any map f_μ with an infinite decomposition for $\Omega(f_\mu)$. For example, consider the map f_{F_3} with kneading invariant $(+--)' * (+--)' * (+--)' * \ldots$. Here, as we saw above, $\Omega(f_{F_3})$ consists of the fixed point $-a$, an infinite sequence of Cantor sets Ω_n on which the map is a subshift of finite type, and a Cantor set Ω_∞ on which the map is the base three adding machine.

To understand the universality at the first Feigenbaum point F_1, the map f_{F_1} is thought of as lying in the stable manifold of a fixed point of a 'doubling' operator $\mathcal{T}_2$ acting on a function space (see Collet *et al.* 1980). The fixed point of $\mathcal{T}_2$ has a single eigenvalue of modulus greater than one, and this is the universal constant $\delta_2 = 4.669\ldots$. A similar argument may be advanced, at least heuristically, to see that there is universal behaviour associated with other maps for which Ω has an infinite decomposition, such as f_{F_3}. For example, we can introduce a 'tripling' operator $\mathcal{T}_3$, where, in the notation of figure 3, $\mathcal{T}_3 f$ is defined to be a suitably

rescaled version of $f^3|_{[x_1', x_2]}$. Thus, whereas $\mathscr{T}_2$ removes a periodic orbit from the non-wandering set, $\mathscr{T}_3$ removes a Cantor set. We then conjecture that $\mathscr{T}_3$ has a unique fixed point (in an appropriate function space) with a single eigenvalue δ_3 lying outside the unit circle. The universal constant δ_3 then controls the asymptotic rate of various bifurcation sequences which accumulate on F_3.

For example, in any full family there is a sequence of fold bifurcations of period 3^n, $n \geqslant 1$, at parameter values s_{3^n}, starting with s_3 where the orbit of period three is born, which accumulates on F_3 from below, and

$$\lim_{n\to\infty} [(s_{3^n} - s_{3^{n+1}})/(s_{3^{n+1}} - s_{3^{n+2}})] = \delta_3,$$

independently of the family chosen. Derrida *et al.* (1979) have calculated $\delta_3^{-1} \sim 0.0181$. See Cvitanović & Myrheim (1983) for related ideas in a complex context.

In a similar manner we can introduce quadrupling, quintupling, ..., operators $\mathscr{T}_4$, $\mathscr{T}_5$, ..., etc., and we can also consider compositions of these operators. The map with kneading invariant

$$(+)' * (+--)' * (+---)' * (+--)' * (+---)' * \ldots$$

for instance, should lie in the stable manifold of a fixed point of $\mathscr{T}_4 \circ \mathscr{T}_3$.

Obviously a great deal of work must be done to justify rigorously these assertions, which in any case are somewhat aside from the interests of the present paper.

We conclude this section with two tables that exemplify the theory presented above. In the first we show some admissible kneading invariants in the period one and period three bifurcation boxes $[s_1, h_1]$ and $[s_3, h_3]$. In the second table we show the numbers and genealogies of all periodic orbits of periods $2^l k \leqslant 24$. To compute the figures in this table we select periods m starting at 1 and use the fact that, for $\mu > h_1$, the map f_μ^m has 2^m fixed points. From 2^m we subtract n = the sum of all the periodic points whose periods divide m, giving $N(m) = (2^m - n)/m$ orbits of period m. If m is even, we look back at the number $N(\frac{1}{2}m)$ of periodic orbits of period $\frac{1}{2}m$ and compute how many of these start their lives as stable orbits. As the theory of this section shows, of the $2S(\frac{1}{2}m)$ such orbits created in saddle-nodes S are initially stable, while (if $\frac{1}{2}m$ is even) all of the remaining $F(\frac{1}{2}m) = N(\frac{1}{2}m) - 2S(\frac{1}{2}m)$ born in flips of $\frac{1}{4}m$ period orbits are stable initially. Each of these stable orbits subsequently undergoes a flip bifurcation, yielding a period m orbit: thus $F(m) = N(\frac{1}{2}m) - 2S(\frac{1}{2}m) + S(\frac{1}{2}m) = N(\frac{1}{2}m) - S(\frac{1}{2}m)$ of the period m orbits are born in flips and the remaining ones arise in $S(m) - \frac{1}{2}(N(m) - F(m))$ saddle–nodes which open the bifurcation boxes $[s_m^j, h_m^j]$, $1 \leqslant j \leqslant S(m)$.

For example, take $m = 20$. There are 99 orbits of period 10, 6 of period 5, 3 of period 4, 1 of period 2 and the two fixed points. Thus $N(m) = (2^{20} - (99 \times 10 + 6 \times 5 + 3 \times 4 + 1 \times 2 + 2 \times 1))/20 = (1048576 - 1036)/20 = 52377$. Of the 99 orbits of period $\frac{1}{2}m = 10$, $F(\frac{1}{2}m) = F(10) = S(5) = 3$ are born in flips of period $\frac{1}{4}m = 5$ orbits, while 96 arise in $S(10) = 48$ saddle nodes. Thus $F(m) = 99 - 48 = 51$ and $S(m) = (52377 - 51)/2 = 26163$. We note that $N(m) \sim 2^m/m$, $S(m) \sim 2^{m-1}/m$ and $F(m) \sim 2^{m/2}/m$ (m even).

3. Continuation of bifurcations to the planar case

We now turn to the two-parameter family of maps of the plane

$$F_{\mu,\epsilon}(x, y) = (y, -\epsilon x + f_\mu(y)), \tag{3.1}$$

where f_μ is a family of one-dimensional maps of the type considered in the previous section.

TABLE 1. SOME ADMISSIBLE KNEADING INVARIANTS AND ITINERARIES OF THE ASSOCIATED PERIODIC ORBITS, IN THE ORDER OF APPEARANCE WITH INCREASING μ

(The itinerary is that of the superstable periodic orbit with the 0 corresponding to the critical point replaced by a +. The kneading in variant is obtained directly from this itinerary according to the prescription on pages 49–50.)

period, $2^l k$	order of appearance, j	bifurcation point	itinerary	kneading invariant	remarks
1	(1)	s_1	$(+)'$	$(+)'$	first period doubling sequence
$2^1 \times 1$	(1)	f_2	$(+-)'$	$(+-)'$	
$2^2 \times 1$	(1)	f_4	$(+-+-)'$	$(+--+)' = (+-)' * (+-)'$	
$2^\infty \times 1$	(1)	F_1		$(+-)' * (+-)' * \ldots$	Morse sequence: first Feigenbaum point
6	1	s_6^1	$(+-+---)'$	$(+--+-+)'$	first period 6
—	—	h_2	$+-+(-)'$	$+--(+-)'$	$f^3(0) = b$
7	1	s_7^1	$(+-+-----)'$	$(+--+-+-)'$	first period 7
5	1	s_5^1	$(+-+--)'$	$(+--+-)'$	first period 5
7	2	s_7^2	$(+-+--+-)'$	$(+--+--+)'$	
3	(1)	s_3	$(+-+)'$	$(+--)'$	beginning of 3 box
$2^1 \times 3$	(1)	$f_{3\times 2}$	$(+-+-+-+)'$	$(+---++)'$	period 3 doubles
—	—	h_3	$+-+(+-+)'$	$+--(--+)'$	end of 3 box
7	3	s_7^3	$(+-+-+-+)'$	$(+---++-)'$	
5	2	s_5^2	$(+-+-+)'$	$(+---+)'$	
7	4	s_7^4	$(+-+-+---)'$	$(+---+-+)'$	
—	—	—	$+-++(-)'$	$+---(+-)'$	$f^4(0) = b$
6	2	s_6^2	$(+-+-+-)'$	$(+---+-)'$	
7	5	s_7^5	$(+-+-+--+)'$	$(+---+--)'$	
4	(1)	s_4	$(+-++)'$	$(+---)'$	last period 4
7	6	s_7^6	$(+-+++-+)'$	$(+----++)'$	
6	3	s_6^3	$(+-+++-)'$	$(+----+)'$	
—	—	—	$+-+++(-)'$	$+----(+-)'$	$f^5(0) = b$
7	7	s_7^7	$(+-+++--)'$	$(+----+-)'$	
5	3	s_5^3	$(+-+++)'$	$(+---+)'$	last period 5
7	8	s_7^8	$(+-++++-)'$	$(+------+)'$	
—	—	—	$+-++++(-)'$	$+-----(+-)'$	$f^6(0) = b$
6	4	s_6^4	$(+-++++)'$	$(+-----)'$	last period 6
7	9	s_7^9	$(+-++++++)'$	$(+-------)'$	last period 7
—	—	h_1	$+-(+)'$	$+(-)'$	fin de la partie
				within the 3 box	
3	(1)	s_3	$(+-+)'$	$(+--)'$	period 3 doubling sequence
$2^1 \times 3$	(1)	$f_{2\times 3}$	$(+-+)'$	$(+--)' * (+-)'$	
$2^2 \times 3$	(1)	$f_{2^2\times 3}$	$(+-+)'$	$(+--)' * (+-)' * (+-)'$	
$2^\infty \times 3$	(1)	F_3		$(+--)' * (+-)' * (+-)' * \ldots$ (Morse 3 sequence)	Feigenbaum 3 point
3×3	?	$s_9^?$	$(+-++-+--+)'$	$(+--)' * (+--)'$	period $3 \times 3 = 9$
				$(+--)' * (+--)' * (+--)' * \ldots$	base 3 adding machine
—	—	h_3	$+-+(+-+)'$	$+--(-++)'$	$f(0)$ = point of period 3

Note that when $\epsilon = 0$, (3.1) is a singular map which collapses the plane into the curve $y = f_\mu(x)$, on which the dynamics are governed by f_μ; thus the results of §2 give a complete description of the bifurcation set of (3.1) when $\epsilon = 0$. We now wish to describe how the bifurcation set extends to the (μ, ϵ)-plane when ϵ is non-zero. We shall restrict attention to $\epsilon \in (0, 1]$,

in which case $F_{\mu,\epsilon}$ is an orientation-preserving diffeomorphism, although many of our results are valid for arbitrary ϵ.

We shall assume that f_μ is a regular, versal family, and for simplicity we suppose that f_μ is

TABLE 2. SADDLE NODES AND FLIPS FOR ORBITS OF PERIOD $2^l k \geqslant 24$

period, m	number of orbits, $N(m)$	number of saddle–nodes, $S(m)$ (= number of boxes, $1 \leqslant j \leqslant S(m)$)	number of flips, $F(m)$
1	2	1	0
2	1	0	1
3	2	1	0
4	3	1	1
5	6	3	0
6	9	4	1
7	18	9	0
8	30	14	2
9	56	28	0
10	99	48	3
11	186	93	0
12	335	165	5
13	630	315	0
14	1161	576	9
15	2182	1091	0
16	4080	2032	16
17	7710	3855	0
18	14560	7266	28
19	27594	13797	0
20	52377	26163	51
21	99858	49929	0
22	190557	95232	93
23	364722	182361	0
24	698870	349350	170
	ca. $2^m/m$	*ca.* $2^{m-1}/m$	*ca.* $2^{\frac{1}{2}m}/m$, m even

C^∞. Furthermore, since we are primarily interested in the creation of horseshoes, we henceforth assume:

$$\left.\begin{aligned}&\text{for any } \epsilon \in [0,1] \text{ there are parameter values}\\&\qquad -\infty < s_1(\epsilon) < \bar{h}_1(\epsilon) < \infty,\\&\text{so that for } \mu < s_1(\epsilon) \text{ the non-wandering set } \Omega_{\mu,\epsilon} \text{ of } F_{\mu,\epsilon} \text{ is empty, while for}\\&\mu > \bar{h}_1(\epsilon),\ F_{\mu,\epsilon}|\Omega_{\mu,\epsilon} \text{ is conjugate to the full shift on two symbols, (the two-}\\&\text{sided shift if } \epsilon > 0;\ \text{the one-sided shift if } \epsilon = 0).\end{aligned}\right\} \tag{3.2}$$

We remark that (3.2) holds for the Hénon map, where $f_\mu(y) = \mu - y^2$. There we may take $s_1(\epsilon) = -\frac{1}{4}(1+\epsilon)^2$, where the fixed points of the map are created, and we also have $\bar{h}_1(\epsilon) \leqslant \frac{1}{4}(5+2\sqrt{5})\,(1+|\epsilon|)^2$, (see Devaney & Nitecki 1979, and §4.3).

We begin by showing that the bifurcation points s_k^j and $f_{2^l k}^j$ on the μ-axis, where f_μ has fold and flip bifurcations, extend to bifurcation curves in the (μ, ϵ)-plane along which the two-dimensional family (3.1) has bifurcations of the same type. The period-doubling sequences associated with f_μ thus carry over to $F_{\mu,\epsilon}$. Unlike f_μ however, $F_{\mu,\epsilon}$ is not restricted to having a single attractor, and we indicate why it is rather unnatural, and perhaps even impossible, for a period-doubling sequence in the two-dimensional map to be completed before other bifurcations occur and multiple attractors are created.

The bifurcations that intrude into the period-doubling sequences include global, homoclinic

bifurcations, which are associated with the points in the bifurcation set of f_μ for which some iterate of the critical point of f_μ falls on an unstable periodic orbit. In the second half of this section we prove that through each point $(h^j_{2^l k}, 0)$ there passes a curve along which $F_{\mu,\epsilon}$, $\epsilon \neq 0$ has a quadratic homoclinic tangency. Here $h^j_{2^l k}$ is the first parameter value in the jth box of period $2^l k$ for f_μ for which an iterate of the critical point falls on the unstable orbit of period $2^{l-1}k$.

For a residual set of families of the form (3.1), all these bifurcation curves extend to the line $\epsilon = 1$, when the map is area preserving. It is not known if the Hénon map lies in this set.

3.1. *Bifurcations of periodic orbits*

We first consider the points $(s_k, 0)$ and $(f_{2^l k}, 0)$ in the bifurcation set of $F_{\mu,0}$ and show that they lie on bifurcation curves of $F_{\mu,\epsilon}$ in the (μ, ϵ)-plane. To begin with, we describe the case of a fold bifurcation of fixed points; similar arguments apply to flip bifurcations and bifurcations of periodic orbits.

We consider our two-parameter family $F_{\mu,\epsilon}$ as an element of $C^\infty(\mathbb{R}^2 \times \mathbb{R}^2)$, the set of smooth maps

$$F: \mathbb{R}^2 \times \mathbb{R}^2 \to \mathbb{R}^2 \times \mathbb{R}^2,$$
$$(\mu, \epsilon, x, y) \to (\mu, \epsilon, F_{\mu,\epsilon}(x, y)).$$

For some fixed large $k < \infty$, let $j^k F(\mu, \epsilon, x, y)$ denote the k-jet of F at (μ, ϵ, x, y) and let J^k be the set of all such k-jets. Define Σ to be the subset of J^k consisting of those k-jets that have a fixed point, i.e. a point (μ, ϵ, x, y) with $F_{\mu,\epsilon}(x, y) = (x, y)$, such that the Jacobian $DF_{\mu,\epsilon}(x, y)$ has an eigenvalue equal to one. Then Σ is a closed stratified subset of J^k of codimension 3 (Takens 1973). It follows from the jet transversality theorem (Hirsch 1976) that $C^\infty(\mathbb{R}^2 \times \mathbb{R}^2)$ contains an open dense subset of maps F for which the k-jet extension

$$j^k F: \mathbb{R}^2 \times \mathbb{R}^2 \to J^k,$$
$$(\mu, \epsilon, x, y) \to j^k F(\mu, \epsilon, x, y)$$

is transverse to Σ. For such an F the image of $j^k F$ intersects Σ in a one-dimensional stratified set $\tilde{\Sigma}$, and the projection of the pre-image of $\tilde{\Sigma}$ onto the (μ, ϵ)-plane is the relevant subset of the bifurcation set of $F_{\mu,\epsilon}$. The bifurcation set is therefore also a one dimensional stratified set.

Similar arguments apply to the case where the critical eigenvalue is -1, and give a bifurcation set for the fixed points of $F_{\mu,\epsilon}$ that consists of a one-dimensional stratified subset of the parameter plane. The one-dimensional strata are curves of fold or flip bifurcations, depending on whether the critical eigenvalue is $+1$ or -1. The zero-dimensional strata are either co-dimension two bifurcation points, or points where the projection of $\tilde{\Sigma}$ is not one-to-one. In the region $0 \leqslant \epsilon < 1$, the map can have fixed points with at most one eigenvalue of unit modulus, since we are assuming $\det(DF_{\mu,\epsilon}) = \epsilon$. Thus, in this region, any co-dimension two bifurcations occur at parameter values where the map has a fixed point with one critical eigenvalue at which the map restricted to the one-dimensional centre manifold (Carr 1981; Guckenheimer & Holmes 1983) has a co-dimension two bifurcation. Now there are only two co-dimension two bifurcations of one-dimensional maps (see Takens 1973). One is the cusp bifurcation, with local model $x \to x \pm x^3 + ax + b$, familiar from catastrophe theory (Zeeman 1977). The other, which we shall refer to as a codimension two flip bifurcation, is perhaps less well known. It has the local model $x \to -x \pm x^5 + ax^3 + bx$, and involves a flip bifurcation along

the a-axis which changes from a supercritical to a subcritical one at $a = 0$. (i.e. the sign of $(f^2)'''$ in proposition 2.2 changes at $a = 0$). This happens by means of a fold bifurcation of a period two orbit occurring along a curve that has a quadratic contact with the a-axis at the origin. The associated bifurcation diagrams and bifurcation sets are shown in figure 5 (in each case we assume the + sign in the local model; the − sign changes all the stability types).

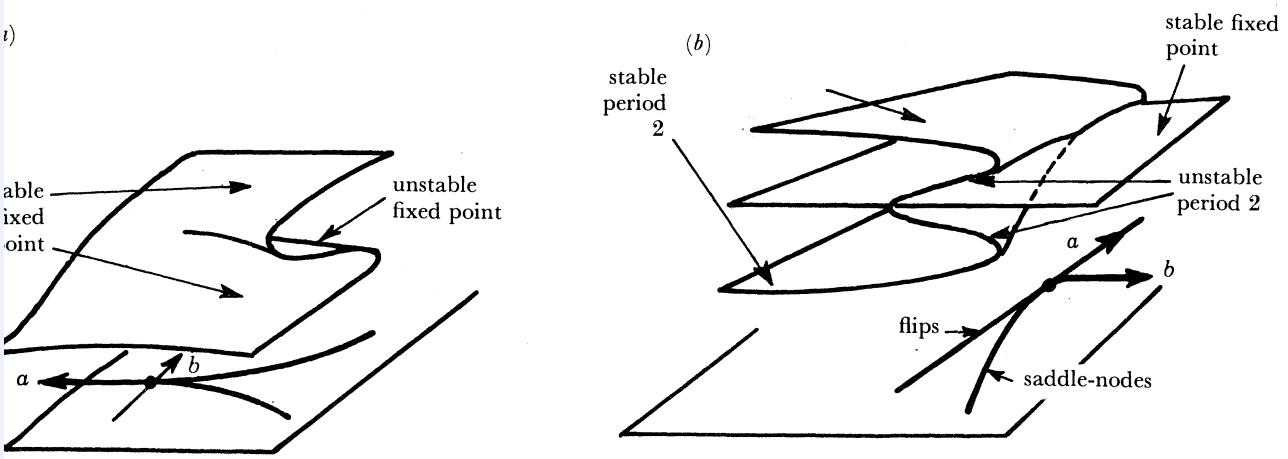

FIGURE 5. Co-dimension two bifurcations. (a) Cusp. (b) Flip.

At parameter values where the projection of $\tilde{\Sigma}$ is not one-to-one, we have two distinct bifurcations occurring simultaneously in different places in the phase space, and there is the possibility that the bifurcation curves form loops in the parameter plane. It is easy to see that this cannot happen for a curve of fold bifurcations, but it may occur for curves of flip bifurcations (and in fact this does happen in the Hénon map for $\epsilon < 0$: see the numerical studies of El Hamouly & Mira 1981).

Now, since we have assumed that for μ sufficiently small the non-wandering set of $F_{\mu,\epsilon}$ is empty, while for large μ it is the full two-shift, all bifurcation curves are trapped in a finite μ-range. Thus for a generic family the bifurcation point $(s_1, 0)$, where the fixed points in the one-dimensional family are born, extends to a bifurcation curve in the (μ, ϵ)-plane which cannot escape to ∞ in the μ-direction. Also, the bifurcation curve cannot stop at any point in the range $0 < \epsilon < 1$, since the only possible way it could end would be at a codimension two flip bifurcation, but the fold bifurcations involved in a codimension two flip are for orbits of period two. Thus $(s_1, 0)$ lies on a bifurcation curve which extends to the line $\epsilon = 1$, possibly passing through cusp points on the way. (In fact for the Hénon family this bifurcation curve is easily found explicitly, and is given by $\mu = -\frac{1}{4}(1+\epsilon)^2$.)

Similarly one sees that the flip bifurcation point $(f_2, 0)$ extends to a curve joining $\epsilon = 0$ to $\epsilon = 1$, possibly passing through codimension two flip points on the way, and possibly containing loops. (Again, for the Hénon map this curve is known to be $\mu = \frac{3}{4}(1+\epsilon)^2$.) The other bifurcations are dealt with in a similar manner. For each bifurcation point on the μ-axis there is an open dense set $\mathscr{F}$ of families for which the bifurcation point extends to a curve in the (μ, ϵ)-plane. The only way in which a bifurcation curve can avoid reaching the line $\epsilon = 1$, is for it to be a fold bifurcation curve which ends in a codimension two flip bifurcation. However, by considering the different configurations for the codimension two flip, one can show that this possibility is inconsistent with our assumptions about the regularity of the one-

dimensional family. For $\epsilon = 0$, all folds and flips occur 'to the right' (with increasing μ) and the flips are supercritical. In particular, if a curve of folds of period $2k$ originating on $\epsilon = 0$ ends in a codimension two flip of a period k orbit, then the associated curve of flips cannot itself originate on $\epsilon = 0$, since this would violate the regularity assumption outlined above. Other possibilities involving combinations of codimension two bifurcations, such as that of a curve of folds meeting a curve of flips which does not originate on $\epsilon = 0$, can similarly be shown to be inconsistent with our regularity assumptions for f_μ and with the existence of a full 2-shift for μ large.

By considering the intersection of the sets $\mathscr{F}$ for all bifurcations in the one-dimensional family, we arrive at a residual subset of regular families in which all the bifurcation points on the μ-axis extend to curves which reach $\epsilon = 1$.

We summarize the arguments above in the following:

PROPOSITION 3.1. *Suppose that $F_{\mu,\epsilon}$ is a regular family which satisfies* (3.2).

(*a*) *If f_μ has a fold bifurcation for an orbit of period k at μ_0, then there is a bifurcation curve $\mathscr{P}$ in the (μ, ϵ)-plane joining $(\mu_0, 0)$ to the line $\epsilon = 1$ so that, except possibly at isolated points of $\mathscr{P}$ where $F_{\mu,\epsilon}$ has a cusp bifurcation, $F_{\mu,\epsilon}$ has a fold bifurcation along any path transverse to $\mathscr{P}$. $\mathscr{P}$ is a smooth one-manifold except at the isolated points where it is a cusp.*

(*b*) *If f_μ has a flip bifurcation at μ_0 then there is a bifurcation curve $\mathscr{P}$ joining $(\mu_0, 0)$ to the line $\epsilon = 1$ so that, except possibly at isolated points of $\mathscr{P}$ where $F_{\mu,\epsilon}$ has a flip bifurcation of codimension two, $F_{\mu,\epsilon}$ has a flip bifurcation along any path transverse to $\mathscr{P}$. Apart from self intersections, $\mathscr{P}$ is a smooth one-manifold.*

As we shall see later, the different bifurcation curves cross each other in a very complicated way as they pass from $\epsilon = 0$ to $\epsilon = 1$. The points where two bifurcation curves intersect are, of course, parameter values where two distinct bifurcations occur simultaneously, in different parts of the phase plane. However, there are certain bifurcation curves that cannot intersect. Recall from the previous section that each fold bifurcation of f_μ is followed by an infinite sequence of flips; clearly the associated bifurcation curves do not intersect, and the two-dimensional map thus has sequences of period doubling bifurcations (infinite sequences if we assume the bifurcation curves extend uniformly to a finite value of ϵ without encountering any codimension two points).

In fact, from our transversality assumptions for $F_{\mu,\epsilon}$ it is clear that between any two consecutive flip bifurcations which arise from the initial period doubling sequence for f_μ, the non-wandering sets of $F_{\mu,0}$ and $F_{\mu,\epsilon}$ are identical for ϵ sufficiently small. Thus, for any finite N we can find an $\epsilon_0 > 0$ so that for any fixed $\epsilon \in (0, \epsilon_0)$ the one-parameter family $F_{\mu,\epsilon}$ has N successive flip bifurcations as μ increases from $s_1(\epsilon)$, in the same manner as $F_{\mu,0}$, before any bifurcations of a different type occur. We now consider in detail this initial bifurcation sequence and construct a two dimensional analogue of f_{F_1}, the one-dimensional map at the first (Feigenbaum) accumulation point.

The first bifurcation to occur, which we assume to be at $s_1(\epsilon)$, is obviously a fold bifurcation, creating a saddle q and a sink p. This is followed by a flip bifurcation at $f_2(\epsilon)$ in which the sink changes to a saddle and throws off a sink of period two. In order for this to happen, the eigenvalues of p have to pass (continuously) from $+1$ and ϵ at $s_1(\epsilon)$ to -1 and $-\epsilon$ at $f_2(\epsilon)$. They do this by first moving towards each other along the real axis, then coalescing at $\sqrt{\epsilon}$ and splitting into a complex conjugate pair which moves around the circle of radius $\sqrt{\epsilon}$ in the complex

plane. They meet again at $-\sqrt{\epsilon}$,and then split along the real axis with one moving outwards towards -1 and the other inwards toward $-\epsilon$. (Of course the motion of the eigenvalues need not be 'monotonic in μ', as we have assumed in this sketch.)

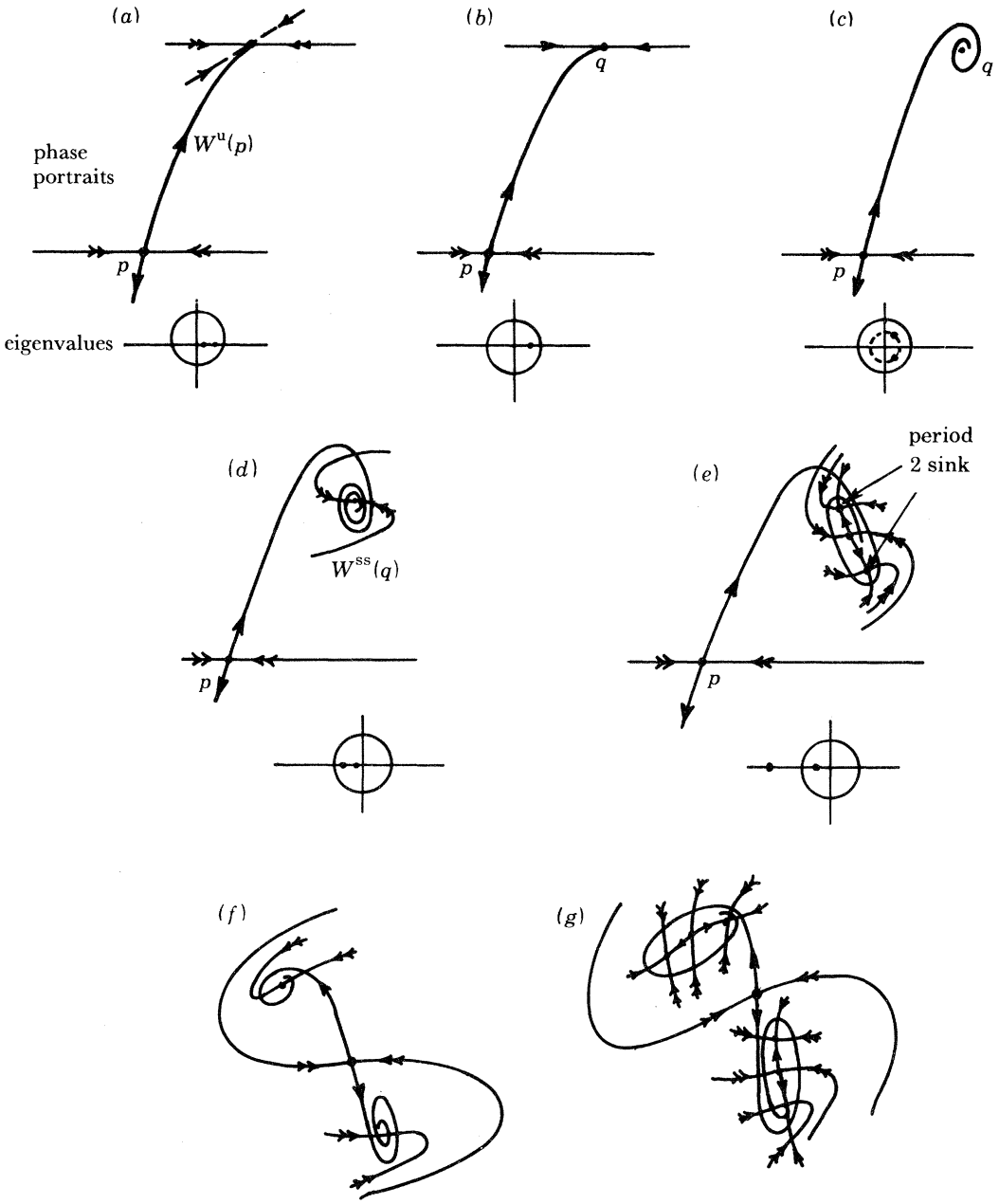

FIGURE 6. Period doubling in the plane.

The corresponding phase portraits are shown in figure 6. Immediately after the fold bifurcation one branch of the unstable manifold of the saddle $W^u(p)$, ends at the sink q and is tangent there to the eigenvector of the larger eigenvalue. As μ increases, the order of contact of $W^u(p)$ with this eigenspace gradually falls until, when the eigenvalues of q coincide, q becomes an improper node with a single real eigenvector, and $W^u(p)$ has only quadratic

contact with this eigenvector. As the eigenvalues move out into the complex plane q becomes a spiral sink and $W^u(p)$ spirals into q. Next, when the eigenvalues become real and negative, q once more has two eigenvectors and the strong stable manifold $W^{ss}(q)$, which is tangent to the eigenvector corresponding to the smaller eigenvalue, has to intersect $W^u(p)$ as shown in figure 6*d*. Finally, the flip bifurcation occurs and we have the situation of figure 6*e*.

FIGURE 7. The construction of G. (*a*) The disc D and the flow ϕ_0. (*b*) The discs D_1^1, D_1^2.

As μ crosses the next bifurcation curve, where the sink of period two has a flip bifurcation, this sequence of events is repeated. The eigenvalues of the period 2 sink follow a path similar to that for the eigenvalues of q, except that their product is ϵ^2 rather than ϵ, and the unstable manifold of q begins to spiral around the period two points (see figure 6*f*) before they become unstable (figure 6*g*).

Clearly this process can be repeated any finite number of times, and we now show how to construct a sequence of maps G_n of the unit disc $D \subset \mathbb{R}^2$ which have the same structure as $F_{\mu,\epsilon}$ after the nth flip bifurcation. The sequence G_n converges to a C^1 diffeomorphism of the disc whose non-wandering set is analogous to that of f_μ at the first Feigenbaum point.

PROPOSITION 3.2. *There is a sequence of* C^∞ *maps* $G_n : D \to D$, *with each* G_n *a diffeomorphism onto its image, so that* (1) *the periodic points of* G_n *consist of one hyperbolic saddle of period* 2^k *for each* $k = 0, 1, \ldots, n$, *plus a hyperbolic sink of period* 2^{n+1}; *and* (2) *if* p_k *is a saddle of period* 2^k *then for each* $j = k+1, \ldots, n$ *the intersection of the unstable manifold* $W^u(p_k)$ *with the stable manifold* $W^s(p_j)$ *is non-empty and transverse. All other intersection of stable and unstable manifolds of the saddles are empty.*

The sequence $\{G_n\}$ *converges in the* C^1 *topology to a diffeomorphism* G *whose non-wandering set consists of a hyperbolic saddle of period* 2^k *for each* $k = 0, 1, \ldots$, *and a Cantor set* K *on which* G *is conjugate to the base two adding machine.*

Proof. We give only a sketch of the construction, which is similar to that of Bowen & Franks (1976) (see also Narasimhan 1979). A detailed proof of the properties of the sequence G_n and its convergence may be found in Whitley (1983).

To construct G_0, we first take a smooth flow ϕ_0 on D with a phase portrait like figure 7*a*. The flow is chosen to be invariant under rotations by π about the origin, and to have three fixed points: a saddle at the origin and two sinks at $(0, \pm\frac{1}{2})$.

Now choose a time T_0 and let g_0 be the time T_0 map of ϕ_0. If we compose g_0 with a rotation through π about the origin, R_π, we then have a map $G_0 = R_\pi \circ g_0$ with a fixed saddle and a sink of period two, which looks similar to $F_{\mu,\epsilon}$ after the first flip bifurcation. However, before the sink of period two undergoes its flip bifurcation, the unstable manifold of the saddle should begin to spiral into the sink. We accomplish this for our map G_0 as follows.

Take two discs D_1^1 and D_1^2 of radius $\frac{1}{4}$, and in each of them define a flow ϕ_1 whose phase

portrait is a scaled down version of ϕ_0 (see figure 7). Let g_1 be the time T_1 map of ϕ_1. Place the discs D_1^i in D, centred at the points $(0, \pm\frac{1}{2})$, so that the 'axis' of D_1^i, i.e. the line containing the fixed points of ϕ_1, makes an angle of $\frac{1}{2}i\pi$ with the positive y-axis (cf. figure 7*b*).

Next take two smaller discs $\tilde{D}_1^i$, $i = 1, 2$, of radius $\frac{1}{8}$, inside the D_1^i, with the same centres, and let A_1^i denote the closed annulus $A_1^i = D_1^i - \mathrm{Int}\,(\tilde{D}_1^i)$. Choose a C^∞ bump function

$$\Psi(x) = \begin{cases} 1 & \text{if} \quad x \in \tilde{D}_1^1 \cup \tilde{D}_1^2, \\ 0 & \text{if} \quad x \notin D_1^1 \cup D_1^2, \end{cases}$$

where, in polar coordinates (r, θ) at the centre of D_1^i, Ψ depends only on r throughout the annulus A_1^i. Then, in a neighbourhood of D_1^i, we may put $\Psi(r, \theta) = (\Phi(r), \theta)$, where

$$\Phi(r) = \begin{cases} 1 & \text{if} \quad |r| \leqslant \frac{1}{8}, \\ 0 & \text{if} \quad |r| \geqslant \frac{1}{4}. \end{cases}$$

We now define

$$G_1 = (1 - \Psi)\, G_0 + \Psi R_{\frac{1}{2}\pi} \circ R_\pi \circ g_1,$$

where $R_{\frac{1}{2}\pi}: D_1^1 \cup D_1^2 \to D_1^1 \cup D_1^2$ denotes rotation through $\frac{1}{2}\pi$ about the centre of D_1^i, $i = 1, 2$.

The map G has a fixed saddle at the origin, a saddle of period two at $(0, \pm\frac{1}{4})$ and a sink of period four inside $\tilde{D}_1^1 \cup \tilde{D}_1^2$. The times T_0 and T_1 may be chosen so that the unstable manifold of the fixed saddle spirals around the periodic points in precisely the same manner as in $F_{\mu,\epsilon}$ after the second flip bifurcation (cf. figure 6), and also so that it intersects the stable manifold of the period two saddle transversely.

Iterating this construction, one produces a sequence of maps G_n with the same features as in the period-doubling sequence for $F_{\mu,\epsilon}$, and it is possible to arrange that the sequence G_n converges to a C^1 diffeomorphism G with the desired non-wandering set.

We note that this example is only a C^1 diffeomorphism (Whitley 1983): it is not C^2, and we suspect that there is *no* smoother map with an equivalent non-wandering set. This is because, in order not to intersect their own stable manifolds, the unstable manifolds of the saddles of period 2^k have to wrap increasingly tightly around the saddles of period 2^{k+1}. In a family such as $F_{\mu,\epsilon}$ it is clear that such homoclinic intersections could be formed at *any* stage after the orbit of period 2^k has undergone its flip bifurcation. As an (apparently) extreme example, one could imagine homoclinic intersections between the stable and unstable manifolds of the original saddle point p being created at any stage in the period-doubling sequence. In fact, we show in §4 that in the family $F_{\mu,\epsilon}$ with ϵ sufficiently close to $\epsilon = 1$, these particular intersections are actually formed before the *first* flip bifurcation occurs at the sink q.

3.2. *Homoclinic bifurcations*

We now show that the homoclinic bifurcations which create the homoclinic orbits to the saddles of period 2^{l-1} in the previous discussion occur along curves which intersect the μ-axis at the points h_{2^l} at which, in the one-dimensional map f_μ, iterate number $(2^l + 1)$ of the critical points falls on the orbit of period 2^{l-1}. In fact, we show that a homoclinic bifurcation curve originates at each point $(h_{2^l k}^j, 0)$ (cf. Van Strien 1982). It is clear that with a more detailed argument, one could also show that a homoclinic bifurcation curve passes through each point $(h, 0)$ where some iterate of f_h maps the critical point onto an unstable periodic orbit, although we do not do this here.

PROPOSITION 3.3. *Suppose that $p(\mu)$ is the periodic point of period $2^{l-1}k$ for which $f_{h_{2^l k}^j}^n(0) = p(h_{2^l k}^j)$, for some (least) iterate n, and suppose that $(\partial/\partial\mu)\,(f_\mu^n(0) - p(\mu))\big|_{\mu = h_{2^l k}^j} \neq 0$.*

Then there is an $\epsilon_0 > 0$ so that for each $\epsilon \in (0, \epsilon_0)$: (a) for μ near $h^j_{2^l k}$, $F_{\mu,\epsilon}$ has a periodic saddle $p(\mu, \epsilon)$ of period $2^{l-1}k$ with $p(\mu,0) = p(\mu)$; and (b) there is a continuous curve $h^j_{2^l k}(\epsilon)$ with $h^j_{2^l k}(0) = h^j_{2^l k}$, so that the stable and unstable manifolds of $p(h^j_{2^l k}(\epsilon), \epsilon)$ have a tangency.

Our assumption that the image of the critical point of f_μ passes through $p(\mu)$ with non-zero speed is slightly stronger than our earlier assumption that f_μ is versal, and it seems very difficult to verify in examples, except for low period orbits. However, it does hold for a residual subset of maps and we shall henceforth assume that it holds for our family f_μ.

Proof. Conclusion (*a*) follows immediately from the Implicit Function Theorem.

For (*b*) we define $g_\epsilon : I \to \mathbb{R}^2$ by $g_\epsilon(\mu) = F^n_{(\mu,\epsilon)}(0, f_\mu(0))$ and let $M_\epsilon = \{(\mu, W^s(p(\mu, \epsilon))\} \subset \mathbb{R}^3$. The hypothesis that the nth iterate of the critical point passes transversely through the periodic point at $\mu = h^j_{2^l k}$ as μ varies implies that g_0 is transverse to M at $(h^j_{2^l k}, p(h^j_{2^l k}, 0))$. Thus for small ϵ, g_ϵ intersects M transversely at a nearby point. We now choose small balls $B_r(g_\epsilon(\mu_1))$ and $B_r(g_\epsilon(\mu_2))$, $\mu_1 < h^j_{2^l k} < \mu_2$, whose radii are independent of ϵ, and which lie on opposite sides of $W^s(p(\mu, \epsilon))$ for all sufficiently small ϵ.

Now for $\mu < h^j_{2^l k}$, Ω_μ is contained in $2^l k$ disjoint subintervals $J_i(\mu)$, $i = 1, \ldots, 2^l k$, each of which is bounded by a point in the orbit of $p(\mu)$, $\{f^i_\mu(p(\mu))\}_{i=1}^{2^l k}$, and one of the immediate preimages of these points, i.e. one of the points p_i, $i = 1, \ldots, 2^{l-1}k$, with $p_i \neq f^i_\mu(p(\mu))$ and $f_\mu(p_i) = f^{i+1}_\mu(p(\mu))$. When $\mu = h^j_{2^l k}$, each J_i is mapped into itself with a single fold by the $(2^l k)$th iterate of the map. Clearly for $\mu < h^j_{2^l k}$ and ϵ small the stable and unstable manifolds of $p(\mu, \epsilon)$ do not intersect.

Since $F^n_{h^j_{2^l k}, 0}(0, f_{h^j_{2^l k}}(0)) = p(h^j_{2^l k}, 0)$, for any $\delta > 0$ we may choose ϵ small enough so that $B_\delta(0, f_\mu(0))$ contains part of the unstable manifold $W^u(p(\mu, \epsilon))$ for $\mu \in (\mu_1, \mu_2)$. As F^{-1} is continuous, δ may be chosen so that

$$F^n(B_\delta(0, f_\mu(0))) \subset B_r(g_\epsilon(\mu)).$$

Then for $\mu \in (\mu_1, \mu_2)$, $B_r(g_\epsilon(\mu))$ contains a piece of $W^u(p(\mu, \epsilon))$. As μ varies from μ_1 to μ_2 this ball crosses $W^s(p(\mu, \epsilon))$, carrying with it part of the unstable manifold, and passing through a tangency on the way.

Remarks. (i) If the periodic saddle $p(\mu, \epsilon)$ persists for all $\epsilon \in [0, 1]$ and some $\mu > \mu_p(\epsilon)$, then we can conclude that the associated homoclinic bifurcation curve $h^j_{2^l k}(\epsilon)$ transverses the (μ, ϵ)-parameter plane up to $\epsilon = 1$, since the homoclinic orbits created on $h^j_{2^l k}(\epsilon)$ form part of the non-wandering set $\Omega_{\mu,\epsilon}$ which exists for all $\mu > \bar{h}_1(\epsilon)$. In particular, since the kneading invariant is monotonic, the bifurcation curves cannot 'double back' to rejoin $\epsilon = 0$.

(ii) Since the local unstable manifold of $p(\mu, \epsilon)$ lies ϵ-close to the graph $y = f_\mu(x)$, and f_μ has a quadratic maximum, it follows that for sufficiently small ϵ our homoclinic tangency is quadratic. We will use this fact subsequently in our development of a model for homoclinic bifurcations in §4.5.

Clearly there is more than one tangency as μ increases through $h^j_{2^l k}$, but we leave a more detailed description of the bifurcation set near $(h^j_{2^l k}, 0)$ to the following section. Here we note that the bifurcation curves through the points $h_{2^l k}$ contain the homoclinic bifurcations that interrupt the period-doubling sequence of $F_{\mu,\epsilon}$, $\epsilon \neq 0$. The period-doubling sequence for f_μ does carry over to the two-dimensional map, with the flip bifurcation curves for $F_{\mu,\epsilon}$ accumulating, at the universal rate (cf. Collet & Eckmann 1980*a*), on a curve $F_1(\epsilon)$ passing through the first Feigenbaum point $(F_1, 0)$. However, the points $(h_{2^l}, 0)$ accumulate on $(F_1, 0)$ from above,

PHILOSOPHICAL TRANSACTIONS OF THE ROYAL SOCIETY A MATHEMATICAL, PHYSICAL & ENGINEERING SCIENCES

and the homoclinic bifurcation curves emanating from them tend to stray across $F_1(\epsilon)$, introducing extra non-wandering points before the period-doubling sequence for $F_{\mu,\epsilon}$ is completed.

In the following sections we will give more information on the global structure of the bifurcation set for $\epsilon \in [0, 1]$, especially concerning the crossing of various bifurcation curves. Rather than attempt to enumerate all the possibilities we will concentrate on describing a model for the creation of a horseshoe in which only essential bifurcations occur. For example, we wish to exclude the possibility that periodic points are first created and then destroyed as μ increases with ϵ fixed. We therefore adopt the following as a working assumption.

All bifurcation curves, both of periodic and homoclinic orbits, are graphs of continuous functions $\mu(\epsilon)$, $\epsilon \in [0, 1]$. Thus we assume all the bifurcation curves extend from $\epsilon = 0$ to $\epsilon = 1$ in the most straightforward way and that codimension two flip bifurcations are excluded. However cusp (pitchfork) bifurcations can still occur; in fact in the next two sections we shall see that such bifurcations *must* occur as ϵ increases.

We shall call a family $F_{\mu,\epsilon}$ which satisfies these conditions as well as those detailed earlier in this section, a *regular, versal family*. For such a family, as μ increases for any fixed $\epsilon \in [0, 1]$ the numbers of periodic orbits, homoclinic orbits and other elements of $\Omega_{\mu,\epsilon}$ increase monotonically. More precise definitions and assumptions will be given in the following sections.

4. Homoclinic bifurcations of the planar map

In this section we show that, from each of the bifurcation points $\mu = h^j_{2^l k}$ for the map f_{μ_1} there grows a 'tangled Cantor fan' consisting of uncountably many curves which traverse the (μ, ϵ) plane between $\epsilon = 0$ and $\epsilon = 1$. On each curve a distinct homoclinic bifurcation occurs, and, while on each constant ϵ slice, one 'generically' expects all such bifurcations to involve quadratic tangencies of stable and unstable manifolds of a particular periodic orbit of $F_{\mu,\epsilon}$, we show that countably many tangencies of cubic type occur. We are able to give a partial description of the homoclinic bifurcations occurring on the curves within the fan and the genealogies of the orbits created thereby, and we discuss four distinct 'signatures' of quadratic homoclinic tangencies that occur on these curves for $\epsilon \in (0, 1)$.

4.1. *Homoclinic bifurcations for $F_{\mu,\epsilon}$, $|\epsilon|$ small*

In §3 we showed that, from each point $\mu = h^j_{2^l k}$ a bifurcation curve $\mu = h^j_{2^l k}(\epsilon)$ emerges such that the stable and unstable manifolds of a point of period $2^{l-1}k$ (or period k if $l = 0$) for $F^j_{\mu,\epsilon}$ have a tangency of quadratic type. The work outlined in §2 shows that for $\mu = h^j_{2^l k}$, the map f_μ has an attracting set consisting of $2^l k$ subintervals and that, on each such subinterval, $(f^j_\mu)^{2^l k}$ is conjugate to $f_{h_1}|_I$ (or $g_2|[-1, 1]$). Thus we can essentially reduce our study of all these bifurcation points to that of the final bifurcation point $\mu = h_1$. However, we shall see that the asymptotic forms of the bifurcation sets depend on (j, k, l) as $\epsilon \to 0$ for $\mu \sim h^j_{2^l k}$.

We first describe the situation for $\mu \sim h_1$ and $\epsilon > 0$, small. Consider the stable and unstable manifolds $W^s(p)$, $W^u(p)$ of the saddle point $p \approx (-a, -a)$. Choose $\mu = h_1(\epsilon)$ so that $W^s(p)$, $W^u(p)$ are tangent at the points $p_0 \approx (0, a)$ and $p_1 \approx (a, -a)$ (here $a = f_{h_1}(0)$), and let this tangency be the first such encountered as μ is increased with ϵ fixed; i.e. for $\mu < h_1(\epsilon)$ there are no homoclinic orbits to p while for $\mu > h_1(\epsilon)$ there are at least two. See figure 8*a*. For $F_{h_1(\epsilon),\epsilon}$, the arc $pp_{-1}p_0q_{-1}p_1$ of $W^u(p)$, which lies ϵ-close to the curve $y = f_{h_1}(x)$, is mapped into the doubled curve $pp_0p_1q_0p_2$. Here the points p_i lie on the (non-transverse) homoclinic orbit. If the area of

figure $pp_{-1}p_0q_{-1}p$ is A then that of its image $pp_0p_1q_0p_2p$ is ϵA, since $\det DF_{\mu,\epsilon} = \epsilon$. Thus the width of the folded image of A is of $O(\epsilon)$, its length being approximately $4a$. Equivalently the distance d_0 from p_0 to q_0 is of $O(\epsilon)$, since p_0 and q_0 are images of the points p_{-1} and q_{-1}, which have y-coordinates ϵ-close to zero. Hence p_0 and q_0 have x-coordinates ϵ-close to zero and the distance d_1 between their images p_1, q_1 is also of $O(\epsilon)$. For example, if $f_\mu = \mu - y^2$ then we have

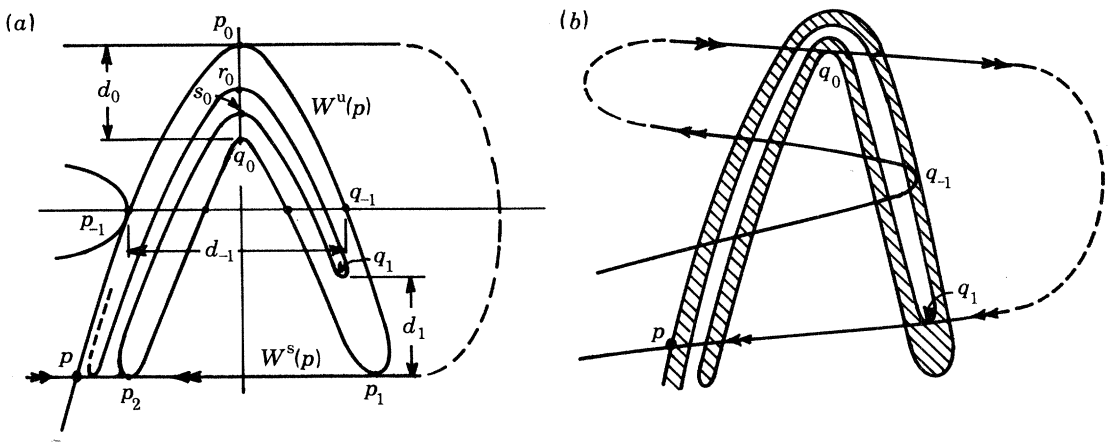

FIGURE 8. Stable and unstable manifolds of the saddle point $p = (-a, a)$ for $F_{\mu,\epsilon}$, $\epsilon > 0$, small. (a) The first tangency $\mu = h_1(\epsilon)$. (b) The last tangency, $\mu = \bar{h}_1(\epsilon)$.

$\mu = h_1 = 2$, p_{-1}, $q_{-1} \approx (\mp\sqrt{2}, 0)$, and $d_{-1} \approx 2\sqrt{2}$. Consequently we find p_0, $q_0 \approx (0, 2 \pm \sqrt{2\epsilon})$, p_1, $q_1 \approx (2 \pm \sqrt{2\epsilon}, 2 - (2 \pm \sqrt{2\epsilon})^2)$, $d_0 \approx 2\sqrt{2\epsilon}$ and $d_1 \approx 2\sqrt{34\epsilon}$.

Now the points p_i and q_i are chosen to lie on the homoclinic orbits created in the first and last tangencies respectively; figure 8b. It follows that, if p_0 and q_0 move up monotonically as μ increases for fixed ϵ, there will be a gap between the first and last bifurcation values $\mu = h_1(\epsilon)$ and $\bar{h}_1(\epsilon)$. But since p_0 and q_0 lie ϵ-close to the critical point $(0, f_\mu(0))$ of the graph $y = f_\mu(x)$, and we have already assumed that $[\partial f_\mu/\partial\mu](0) \neq 0$ for our family (cf. proposition 3.3), they do indeed move up at a finite rate. It follows immediately that the interval $\bar{h}_1(\epsilon) - h_1(\epsilon)$ between the first and last homoclinic tangencies is of length $c\epsilon + O(\epsilon^2)$, where c is an $O(1)$ constant depending on $[\partial f_\mu(0)/\partial\mu]_{\mu=h_1}$.

Moreover, even in the rough sketches of figure 8 we see that two further homoclinic tangencies must occur between $h_1(\epsilon)$ and $\bar{h}_1(\epsilon)$, as the points r_0 and s_0 pass up through the top most loop of the stable manifold near $(0, a)$. In fact for ϵ sufficiently small, depending on n, iterating the arc $pp_0p_1q_0p_2$ of the local unstable manifold produces at each step a further 2^n arcs between p_0 and q_0, of which r_0 and s_0 are but the first. If $[\partial^2 f_\mu/\partial y^2]_{y=0} \neq 0$ then all these arcs are locally like parabolas, and lead to quadratic homoclinic tangencies. Moreover, after n iterates the image of the figure $pp_{-1}p_0q_{-1}p_1p$ of area A of figure 8a is a 'rectangle' of length $2a2^n$, folded $2^n - 1$ times. (In figure 8b its second image is shaded.) Its area is $\epsilon^n A$ and thus each component of $F^n_{\mu,\epsilon}(A) \cap \{x = 0\}$ is an interval of length $O((\frac{1}{2}\epsilon)^n)$.

It is tempting to say that a Cantor set of such arcs, and their attendant homoclinic tangencies, can be constructed by taking such a process to the limit. This is unfortunately incorrect, since for $\mu \in [h_1(\epsilon), \bar{h}_1(\epsilon))$ and any $\epsilon > 0$ there is an integer N such that the Nth image of the arc containing q_0 lies above the line $y = 0$. Image number $(N+1)$ of this arc then lies to the

right of $x = 0$, thereby depriving the Cantor set construction of a middle interval for removal. However, if we pick $\mu > \bar{h}_1(\epsilon)$, then all future images of arcs between p_0 and q_0 created in previous iterations of $pp_0p_1q_0p_2$ *do* lie below $y = 0$ and we can pick a 'vertical' curve $\mathscr{V}(\mu)$ passing through p_0, r_0, s_0, q_0 such that $W^u(p) \cap \mathscr{V}(\mu)$ is a Cantor set. Each point h in this Cantor set forms the top of an arc of $W^u(p)$ which intersects the top most loop of $W^s(p)$ in two transverse homoclinic points h^+, h^-, one on each side of $\mathscr{V}(\mu)$; h^+ and h^- are uniquely defined as the two homoclinic points which bound the shortest arc of $W^u(p)$ containing h.

Let h denote an endpoint of a closed interval remaining after n steps in the construction of the Cantor set $W^u(p) \cap \mathscr{V}(\mu)$. The discussion above shows that, for ϵ sufficiently small, as μ decreases from $\bar{h}_1(\epsilon)$ the pair of points h^+, h^- and the point h coalesce into a single, non-transverse homoclinic point. Moreover, since the manifolds depend smoothly upon the parameters μ, ϵ (for $\epsilon > 0$), the curves $\mathscr{V}(\mu)$ can be fitted together and extended for $\mu < \bar{h}_1(\epsilon)$ to form a smooth 'vertical' surface $\mathscr{V}$ in (x, y, μ) space in which the 2^n such non-transverse homoclinic points lie.

That part of the top most loop of $W^s(p)$ bounded by the left- and right-most homoclinic points can be made horizontal by a local μ-dependent change of coordinates, so that each slice $\mathscr{V}(\mu)$ of $\mathscr{V}$ is strictly vertical. On $\mathscr{V}$ the points at which tangencies occur form a set whose projection onto the (x, y) plane has length $d_0 \sim c\epsilon + O(\epsilon^2)$; moreover the primary gap $(r_0 s_0)$ in this set is of width $O(\epsilon)$, since the distances $p_{-1}r_{-1}$ and $s_{-1}q_{-1}$ are of $O(\epsilon)$ (see figure 8*a*). Proceeding iteratively as above we see that the homoclinic bifurcation set is *asymptotically* as $\epsilon \to 0$ a middle$-\alpha$ Cantor set for which $\alpha = \alpha(\epsilon) = 1 - 2c\epsilon$. The support of the set is an interval of length $c\epsilon + O(\epsilon^2)$. As μ increases this set is transported vertically at finite speed $K \sim [\partial f_\mu(0)/\partial\mu]_{\mu=h_1}$, remaining rigid to first order. Thus, in (μ, ϵ) space, the homoclinic bifurcation set for the fixed point p of $F_{\mu,\epsilon}$ is asymptotic to a *Cantor fan* over the point $(h_1, 0)$: topologically the product of a unit interval and a Cantor set, pinched at one end to a point. In §§4.3 and 4.4 we shall return to the global structure of the bifurcation set for larger ϵ and show that the curves in it must intersect one another as ϵ increases, leading to our *tangled Cantor fan*.

Before formulating our first main result we briefly discuss a further set of homoclinic bifurcations: those associated with the point $\mu = h_2$. The map f_{h_2} has the property that $f^3_{h_2}(0) = b$ is an unstable fixed point. (For the map $f_\mu = \mu - y^2$ this occurs at $\mu = h_2 \approx 1.5437$.) Thus $F_{\mu,\epsilon}$ has homoclinic bifurcations for the saddle point $q \approx (b, b)$ on a curve $\mu = h_2(\epsilon)$ with $h_2(\epsilon) \to h_2$ as $\epsilon \to 0$. Let $h_2(\epsilon)$ be the curve on which the first such homoclinic orbits occur as μ increases. In figure 9 we show the local stable and unstable manifolds $W^s_{\mathrm{loc}}(q)$, $W^u_{\mathrm{loc}}(q)$ and iterates of them. The points $a_0, \ldots, h_0$ have images $a_1, \ldots, h_1$, etc. The local stable manifold $a_0, \ldots, c_0, \ldots, p, \ldots, h_0$ lies ϵ-close to the segment of the curve $y = f_{h_1}(x)$ between the points $(f^2(0), f^3(0))$ and $(f(0), f^2(0))$.

Without giving details, from the figure we can see that the lengths of the vertical intervals e_3g_3 and b_3d_3 between points at which the first and last tangencies occur are of $O(\epsilon^2)$. This follows because *two* iterates of $F_{\mu,\epsilon}$ are necessary to form the first full loop $qd_2c_2b_2a_2$ of $W^u(q)$. Then, by arguments similar to those above, we see that the homoclinic bifurcation set of $F_{\mu,\epsilon}$ for $\epsilon > 0$, small and $\mu \sim h_2$ is asymptotically a Cantor set with support an interval of length $c_2\epsilon^2 + O(\epsilon^3)$, where $c_2 = [\partial f_\mu(0)/\partial\mu]_{\mu=h_2}$. Here, however, we have a middle $1 - 2c\epsilon^2$ Cantor set. Thus we have a fan of homoclinic bifurcations in the (μ, ϵ) plane lying in a horn of width $O(\epsilon^2)$ bounded by curves $\mu = h_2(\epsilon), \bar{h}_2(\epsilon)$.

PHILOSOPHICAL TRANSACTIONS OF THE ROYAL SOCIETY A MATHEMATICAL, PHYSICAL & ENGINEERING SCIENCES

We are now in a position to state the following.

THEOREM 4.1. *From each point* $(h^j_{2^l k}, 0)$, $j, k = 1, 2, \ldots; l = 0, 1, 2, \ldots$ *in* (μ, ϵ)*-parameter space there extends a fan of curves on which homoclinic bifurcations to a hyperbolic saddle of period* $2^{l-1}k$ *occur for* $F_{\mu,\epsilon}$. *(For* $l = 0$, *read period* k*). As* $\epsilon \to 0$ *the bifurcation set is asymptotic to a middle* $1 - 2c\epsilon^{2^l k}$ *Cantor set constructed on an interval of length* $c\epsilon^{2^l k}$, *where* $c = c(h^j_{2^l k})$ *depends on* j, k, l.

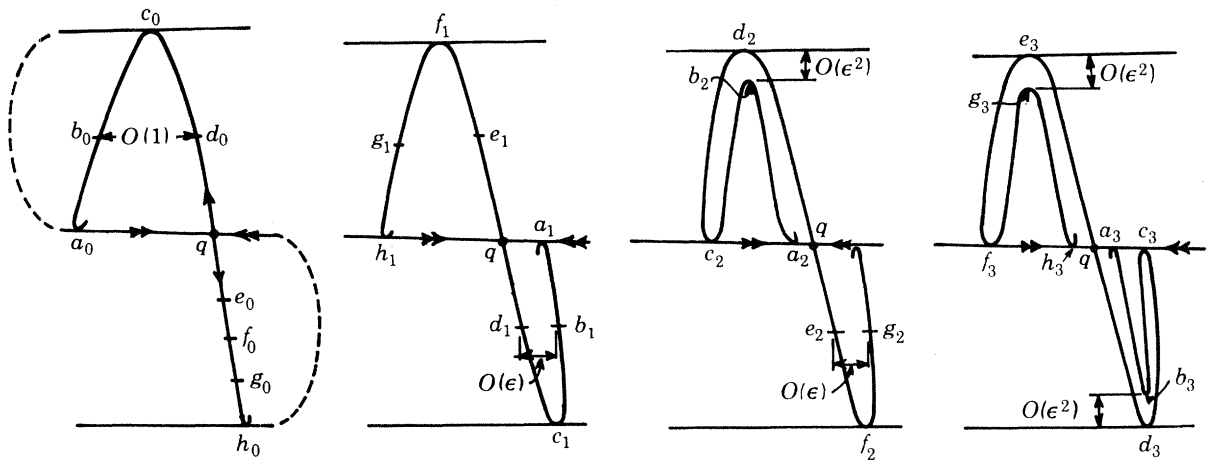

FIGURE 9. The first homoclinic bifurcation for $q \approx (b, b)$.

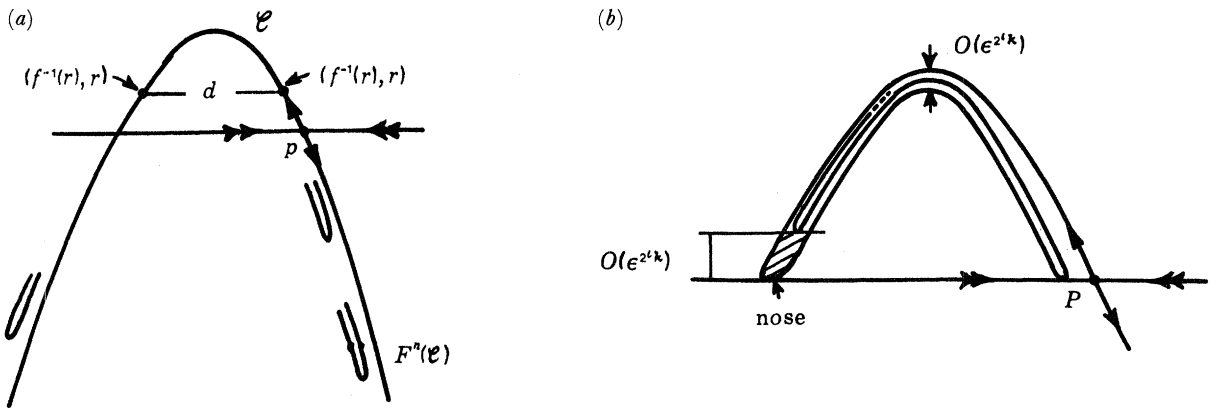

FIGURE 10. The proof of theorem 4.1.

Proof. We shall reduce the problem to the case of $F_{\mu,\epsilon}$ near $(\mu, \epsilon) = (h_1, 0)$, considered above. Fix j, k, l and consider the graph of $f^{2^l k}_{h^j_{2^l k}}$. The definition of the bifurcation point $\mu = h^j_{2^l k}$ implies that there exists an invariant subinterval $J \subset I$ containing the critical point 0 for $f^{2^l k}_\mu$; i.e. $f^{2^l k}_\mu(J) = J$; J is bounded at one end by a fixed point p for $f^{2^l k}_\mu$. If $l \geqslant 1$, p is a point of period $2^{l-1}k$ for f_μ and $Df^{2^{l-1}k}_\mu$ has a negative eigenvalue; if $l = 0$, p is a point of period k for f_μ and Df^k_μ has a positive eigenvalue. In either case, as in proposition 3.3, for ϵ sufficiently small (depending on k, l) there exists a hyperbolic fixed point P of $F^{2^l k}_{\mu,\epsilon}$ near $(f^{-1}_\mu(p), p)$ (where the appropriate pre-image is chosen), the eigenvalues of $DF^{2^l k}_\mu$ are both positive and their product is $\epsilon^{2^l k}$.

For $\epsilon = 0$, P and its local unstable manifold $W^{\mathrm{u}}_{\mathrm{loc}}(P)$ lie on the curve $y = f(x)$, while the local stable manifold $W^{\mathrm{s}}_{\mathrm{loc}}(P)$ is a horizontal line segment $y = P$. Consider the arc $\mathscr{C}$ of $W^{\mathrm{u}}(P)$

containing the critical point $(0, f_\mu(0))$ and bounded by P and $(f^{-1}(p), p)$, where the other (non-fixed) pre-image is taken. See figure 10*a*. Since $f_\mu^n(J) \cap J = \varnothing$, the images $F_{\mu,\epsilon}^n(\mathscr{C})$ lie close to $y = f_\mu(x)$ but bounded away from the critical point for $0 < n < 2^l k$. The horizontal width of such images is therefore reduced by a factor $\epsilon/|f'_\mu(f_\mu^n(r))|$ to leading order, on each application of F. (Recall that the product of the eigenvalues of $DF_{\mu,\epsilon}(f^{n-1}(r), f^n(r))$ is ϵ.) Finally, after $2^l k$ iterates, the image of $\mathscr{C}$ returns to the neighbourhood of the critical point as a doubled curve bounding a bent strip of width *ca.* $d\epsilon^{2^l k}/\prod_{n=0}^{(2^l-1)k} |f'_\mu(f_\mu^n(r))|$; figure 10*b*. Here $d = d(j, k, l)$ is the distance between the two points $(f^{-1}(r), r)$ contained in $\mathscr{C}$ such that $f_\mu^{2^l k}(r) = 0$. Iterating another $2^l k$ times produces the quadrupled curve of figure 10*b*. The vertical distance between the two bends of $F_{\mu,\epsilon}^{2^{l+1}k}$ in the region marked 'nose' is to leading order $d\epsilon^{2^l k}\prod_{n=0}^{(2^l-1)k}[f'_\mu f_\mu^{2^l k+n}(r)/f'_\mu f_\mu^n(r)] = d\epsilon^{2^l k}K_1(j, k, l)$, since vertical distances are expanded by a factor *ca.* $f'_\mu(f^n(r))$ on each application of $F_{\mu,\epsilon}$.

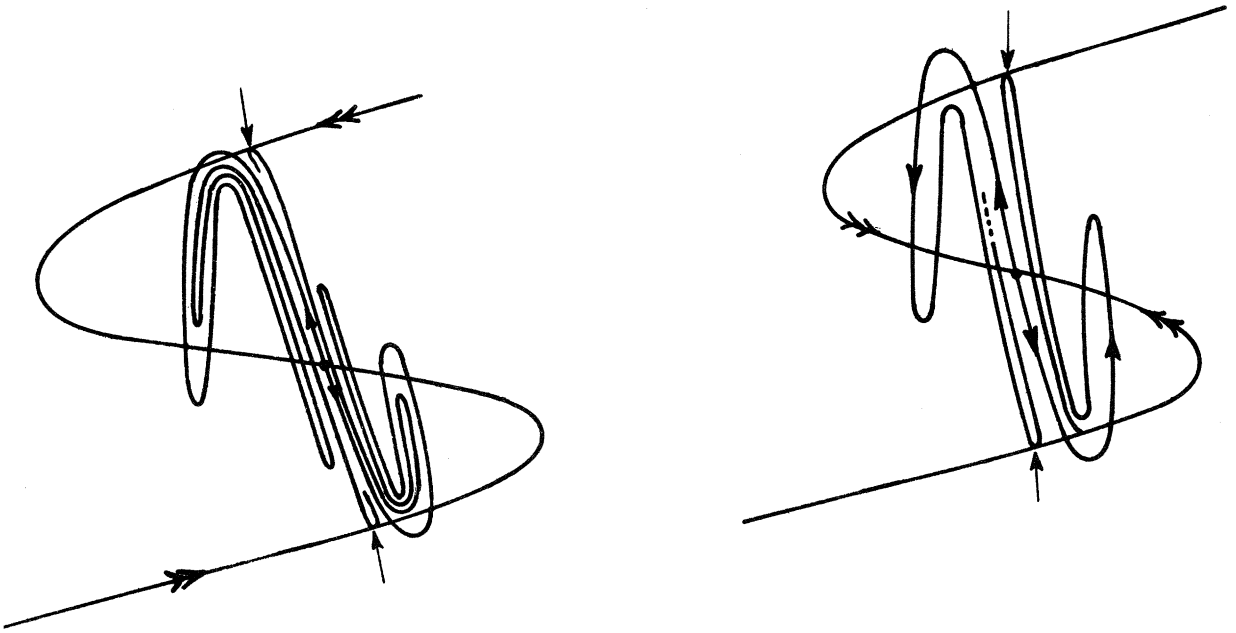

FIGURE 11. Further homoclinic bifurcations for $F_{\mu,\epsilon}$.

We next use the assumption that $K_2(j, k, l) = [\partial/\partial\mu] f^{k l_2}(0)|_{\mu=h_{2^l k}^j} \neq 0$ i.e. the images of the critical point keep moving for a versal family. Then, to first order, $\mathscr{C}$ and its image $F_{\mu,\epsilon}^{2^l k}(\mathscr{C})$ also move monotonically with speed K_2. Thus, as μ increases through $\mu = h_{2^l k}^j$ for ϵ sufficiently small, the 'nose' of the image passes through the stable manifold in a μ interval of length $d\epsilon^{2^l k}K_1/K_2$. Iterating this procedure as in the discussion above, and taking ϵ successively smaller, produces the Cantor set of bifurcations of the theorem.

Remarks. (i) As mentioned in § 2, associated with each bifurcation point of the form $\mu = h_{2^l k}^j$, $l \geqslant 1$ for f_μ, we have a countable sequence of further bifurcation points $h > h_{2^l k}^j$ for which some (higher) iterates of the critical point falls on an unstable orbit of period $2^{l-1}k$; some of these appear in table 1; $f^4(0) = b, f^5(0) = b$, etc. These will extend to fans of homoclinic bifurcations of width $c\epsilon^{2^l k}$ just as do the 'primary' ones. In figure 11 we illustrate two homoclinic bifurcations for $F_{\mu,\epsilon}$ occurring in such fans.

(ii) As shown in § 2, for any $\mu > F_1, f_\mu$ has a hyperbolic Cantor set on which the dynamics

is conjugate to a subshift of finite type. Consequently, for ϵ sufficiently small, $F_{\mu,\epsilon}$ has a hyperbolic Cantor set Λ whose local stable and unstable manifolds are, respectively, almost horizontal line segments and curves lying close to the graph $y = f_\mu(x)$. The periodic points whose homoclinic bifurcations we have just discussed lie in Λ, and the unstable manifolds of these points evidently intersect the stable manifolds of Λ transversally, so that the unstable manifolds of the periodic points accumulate on $W^u(\Lambda)$. Thus, when homoclinic bifurcations occur for the periodic point, heteroclinic bifurcations occur between the periodic point and Λ and homoclinic bifurcations occur for Λ itself. These additional bifurcation points lie within the fans of bifurcations found above.

4.2. *Periodic and homoclinic bifurcations for* $F_{\mu,\epsilon}$, $\epsilon \approx 1$

We now turn to the (almost) area preserving map

$$F_{\mu,\epsilon}(x, y) = (y, -\epsilon x + f_\mu(y)), \tag{4.1}$$

with $\epsilon \approx 1$, and consider some of the sequence of local and global bifurcations occurring as μ increases. We will assume that the sequence opens with a saddle–node bifurcation, closes with a final homoclinic bifurcation and is 'monotonic' in the sense that all saddle–node and flip bifurcations are supercritical. This has not been proved for any specific cases, but we note that Devaney & Nitecki (1979) have shown that for the Hénon map ((4.1) with $f_\mu = \mu - y^2$), there exists a curve $\mu(\epsilon) = \frac{1}{4}(5+2\sqrt{5})\,(1+|\epsilon|)^2$ such that for all $\mu > \mu(\epsilon)$ the non-wandering set of (4.1) is a hyperbolic two-shift: the map has a horseshoe. (In fact for $\mu > 2(1+|\epsilon|)^2$, F already has a topological horseshoe.) For this problem it is simple to compute the bifurcation curves $s_1(\epsilon), f_2(\epsilon), f_4(\epsilon)$ on which the first saddle–node and the first two flips occur: They are given by the expressions

$$\left.\begin{aligned} s_1(\epsilon): \mu &= -\tfrac{1}{4}(1+\epsilon)^2 \qquad (s_1(1) = -1), \\ f_2(\epsilon): \mu &= \tfrac{3}{4}(1+\epsilon)^2 \qquad (f_2(1) = 3), \\ f_4(\epsilon): \mu &= \tfrac{1}{4}(5+6\epsilon+5\epsilon^2) \quad (f_4(1) = 4). \end{aligned}\right\} \tag{4.2}$$

As μ moves along the line $\epsilon = 1$ between $s_1(1)$ and $f_2(1)$ the eigenvalues of the map

$$DF_{\mu,1} = \begin{bmatrix} 0 & 1 \\ -1 & f'_\mu(\bar{y}) \end{bmatrix} \tag{4.3}$$

linearized at the elliptic fixed point, will be assumed to move monotonically with non-zero speed around the unit circle from (1, 1) to (−1, −1). It is easy to verify that this is true for the Hénon map, since trace $(DF_{\mu,1}) = -2\bar{y}$ and the elliptic fixed point lies at

$$((1+\mu)^{\frac{1}{2}} - 1,\ (1+\mu)^{\frac{1}{2}} - 1), \tag{4.4}$$

and therefore has the eigenvalues

$$\left.\begin{aligned} \lambda_{1,2} &= \mathrm{e}^{\pm \mathrm{i}\theta(\mu)}, \\ \text{with} \qquad \theta(\mu) &= \arctan\{[2(1+\mu)^{\frac{1}{2}} - (1+\mu)]^{\frac{1}{2}}/1 - (1+\mu)^{\frac{1}{2}}\}. \end{aligned}\right\} \tag{4.5}$$

Moreover, it holds in general provided that $[\partial^2 f/\partial x\,\partial\mu]\,(b(\mu)) > 0$, where $b(\mu)$ is the fixed point of f_μ in the interior of I. We conclude that there is a dense set of μ values $\mu(p, q) \in (-1, 3)$ for which $\theta(\mu) = 2\pi p/q$ with p and q relatively prime and $p/q < \frac{1}{2}$. Thus there is a dense set of *resonant bifurcations* from the elliptic centre in which orbits of period q for $F_{\mu,1}$ appear. From (4.5) we obtain these bifurcation points for the Hénon map as

$$\mu(p, q) = (1 + T^2(p, q))^{-1} + 2(1 + T^2(p, q))^{-\frac{1}{2}}, \tag{4.6}$$

where $T(p, q) = \tan(2\pi p/q)$. We list some such bifurcation points in table 3 in their order of occurrence for increasing μ.

To describe the bifurcation sets and associated local phase portraits for the map in the neighbourhood of such points in (μ, ϵ)-space, we use the normal form theory of Takens (1973) and Arnol'd (1976, 1983), which we now briefly review. We change coordinates in both parameter and state spaces so that the bifurcation point $(\mu(p, q), 1)$ and the bifurcating elliptic fixed point each lie at the origin. Let $G_{\nu,\gamma}(u, v)$ be the map expressed in these coordinates, with $\nu = \mu - \mu(p, q)$, $\gamma = \epsilon - 1$, $u = x - ((1+\mu)^{\frac{1}{2}} - 1)$, $v = y - ((1+\mu)^{\frac{1}{2}} - 1)$†, so that $\det DG_{\nu,\gamma} = \epsilon$ and $DG_{\nu,\gamma}(0, 0)$ has eigenvalues

$$\lambda, \bar{\lambda} = (1+\gamma)^{\frac{1}{2}} \exp[\pm i(2\pi p/q + \nu)]. \tag{4.7}$$

TABLE 3. RESONANT BIFURCATIONS FOR THE HÉNON MAP

p/q	$\mu(p, q)$
$\frac{1}{1}$	-1
$\frac{1}{10}$	-0.9635
$\frac{1}{9}$	-0.9453
$\frac{1}{8}$	-0.9142
$\frac{1}{7}$	-0.8590
$\frac{1}{6}$	-0.75
$\frac{1}{5}$	-0.5225
$\frac{2}{9}$	-0.3171
$\frac{1}{4}$	0
$\frac{2}{7}$	0.4945
$\frac{3}{10}$	0.7135
$\frac{1}{3}$	1.25
$\frac{3}{8}$	1.9142
$\frac{2}{5}$	2.2725
$\frac{3}{7}$	2.6137
$\frac{4}{9}$	2.7624
$\frac{1}{2}$	3

We will assume $q \geqslant 5$, to avoid the so called *strong resonances*. The normal form for G is then, in complex form $z = u + iv$:

$$G_{\nu,\gamma}(z) = \lambda(\nu, \gamma)\, z + \sum_{k=1}^{[\frac{1}{2}(q-2)]} \alpha_{2k+1}(\nu, \gamma)\, z^{k+1}\bar{z}^k + \beta(\nu, \gamma)\, \bar{z}^{q-1} + O(|z|^q), \tag{4.8}$$

where the complex coefficients α_j and β must be computed in specific cases. Here $[c]$ denotes the integer part of c. Putting (4.8) into polar coordinates (r, ϕ) and rescaling $r \to r/\nu$ (if $b_1(0, 0) = \operatorname{Im}(\alpha_1(0, 0)) < 0$) or $r \to -r/\nu$ (if $b_1(0, 0) > 0$), we obtain

$$\begin{pmatrix} r \\ \phi \end{pmatrix} \to \begin{pmatrix} (1+\gamma)\, r + 2\nu^{\frac{1}{2}(q-2)} \operatorname{Re}\{\beta(\nu, \gamma)\, \overline{\lambda(\nu, \gamma)}\, e^{iq\phi}\} r^{\frac{1}{2}q} \\ \phi + 2\pi p/q + \nu + \sum b_k(\nu, \gamma)\, \nu^k r^k + \operatorname{Im}\{(\overline{\lambda(\nu, \gamma)}/\beta(\nu, \gamma))\, e^{iq\phi}\}\, \nu^{\frac{1}{2}(q-2)} r^{\frac{1}{2}(q-2)} \end{pmatrix} + O(|\nu|^{\frac{1}{2}(q-1)}).$$

We wish to solve this equation for points of period q for $\mu > 0$ if $b_1 < 0$ or $\mu < 0$ if $b_1 > 0$. The qth iterate takes the form

$$\begin{pmatrix} r \\ \phi \end{pmatrix} \to \begin{pmatrix} (1+\gamma)^q\, r + 2q[A(\nu, \gamma) \cos q\phi + B(\nu, \gamma) \sin q\phi]\, r^{\frac{1}{2}q} \nu^{\frac{1}{2}(q-2)} + O(|\nu|^{\frac{1}{2}(q-1)} + |\gamma|\ |\nu|^{\frac{1}{2}(q-2)}) \\ \phi + q\nu(1 + b_1(\nu, \gamma)\, r) + O(|\nu|^{\frac{3}{2}} + |\gamma|\ |\nu|) \end{pmatrix}, \tag{4.9}$$

and making the (generic) non-degeneracy assumptions that $b_1(0, 0) = \operatorname{Im}(\alpha_1(0, 0)) \neq 0$ and

† Plus an additional linear change of coordinates, see Appendix A.

$\beta(0, 0) \neq 0$, we can use the implicit function theorem to show that (4.9) will have $2q$ fixed point solutions for (r, ϕ) provided that

$$|\gamma| < 2(-q\nu/b_1)^{\frac{1}{2}(q-2)} |\beta(0, 0)|^2. \tag{4.10}$$

(Note that our assumptions on μ and b_1 guarantee that $(-q\nu/b_1) > 0$.) We therefore find two periodic orbits of period q for $F_{\mu,\epsilon}$ within an *Arnol'd horn* asymptotically close to

$$\epsilon = 1 \pm 2|\beta(0, 0)|^2 [(\mu(p, q) - \mu)\, q/b_1(0, 0)]^{\frac{1}{2}(q-2)}, \tag{4.11}$$

as $(\mu, \epsilon) \to (\mu(p, q), 1)$. One of the orbits is of saddle type and the other is a sink (respectively source) if $\epsilon < 1$ (respectively $\epsilon > 1$); for $\epsilon = 1$ it is elliptic. These orbits are born on the boundaries of the horn in saddle–node bifurcations.

In the Appendix we give the formulae needed for computation of the coefficient $b_1(0, 0)$, which determines the direction of bifurcation, and we carry out the computation for the Hénon map. In this case we find that $b_1(0, 0) < 0$ for all $\mu \in (-1, 3)$, so that all the resonant bifurcations occur to the right of the points $(\mu, \epsilon) = (\mu(p, q), 1)$. Since we are interested in describing the 'simplest' model for the creation of horseshoes, we shall henceforth assume that the same holds for our more general family $F_{\mu,\epsilon}$.

In §5 we return to these resonant bifurcations and show how the boundaries of the horns can be connected with certain saddle node bifurcations of $F_{\mu,\epsilon}$ for ϵ small and hence with the saddle–nodes $(s_k^j, 0)$ of the one-dimensional map.

We now turn to the homoclinic bifurcations of the saddle p for $\epsilon \approx 1$. It is known that the homoclinic bifurcation structures within the Arnol'd horns are extremely complicated (cf. Aronson *et al.* 1982) and we shall for the moment restrict our attention to the first or 'outer' homoclinic bifurcation. We know that the first saddle–node bifurcation occurs on the curve $s_1(\epsilon)$. Moreover, for $\epsilon \in (0, 1)$, since $\det DF_{\mu,\epsilon} = \epsilon < 1$, this bifurcation takes place in a one-dimensional centre manifold and there is a complementary one-dimensional stable manifold. Use of invariant manifold theory (Carr 1981) permits us to conclude that one branch (the right-hand one) of the unstable manifoln of the saddle created in this bifurcation limits in the sink, *for* $(\mu - s_1(\epsilon))$ *sufficiently small and* ϵ *bounded away from* 1 (cf. phase portrait B of figure 12). In contrast, for $\epsilon = 1$, it is easy to see that homoclinic orbits to the saddle must exist for all $\mu > s_1(1)$, for if they did not then the stable and unstable manifolds of the saddle would have to lie one outside the other, and the iterated map could not then preserve areas. We conclude that, for fixed $\mu > s_1(\epsilon)$, as ϵ increases towards 1, a first homoclinic bifurcation must occur in which the stable and unstable manifolds of the saddle p have the structure illustrated in phase portrait C of figure 12. Generically this will be a quadratic tangency. Note that these manifolds have the same topological structure as those of figure 8*a*. Evidently our homoclinic bifurcation near $(\mu, \epsilon) = (s_1(1), 1)$ is the same as that growing from $(\mu, \epsilon) = (h_1, 0)$ on the curve $h_1(\epsilon)$.

We can say more. Use of the normal form theory near the point $(s_1(1), 1)$ reveals that, to all algebraic orders, the Taylor series expansion of the map is conjugate to the time one flow map of the planar vector field

$$\left.\begin{aligned} \dot{u} &= v, \\ \dot{v} &= (\mu - s_1(1)) - u^2 + \gamma(\epsilon)\,(v \pm uv);\ \gamma(1) = 0, \end{aligned}\right\} \tag{4.12}$$

(Takens 1974; Bogdanov 1975; Arnol'd 1976, 1983). It follows that, as $\mu \to s_1(1)^+$ along $\epsilon = 1$,

the stable and unstable manifolds of the saddle lie closer than any power of $|\mu - s_1(1)|$ to the smooth homoclinic loop given by the level curve of the Hamiltonian of (4.12) for $\epsilon = 1$:

$$\tfrac{1}{2}v^2 - (\mu - s_1(1))\, u + \tfrac{1}{3}u^3 = \tfrac{2}{3}(\mu - s_1(1))^{\frac{3}{2}}. \tag{4.13}$$

We conclude that, while in the generic case terms ignored in the tail of the series expansion will perturb this loop into transverse homoclinic intersections, such intersections can only exist within a horn bounded by curves of the form

$$\epsilon = 1 \pm R(\mu - s_1(1)), \tag{4.14}$$

where $O(R(\alpha)) < K|\alpha|^n$ for all n. In fact recent work of Holmes & Marsden (1983), and general beliefs based on numerical and heuristic evidence, suggest that $R(\alpha)$ is of order $e^{-c/\alpha}$: an exponentially thin horn.

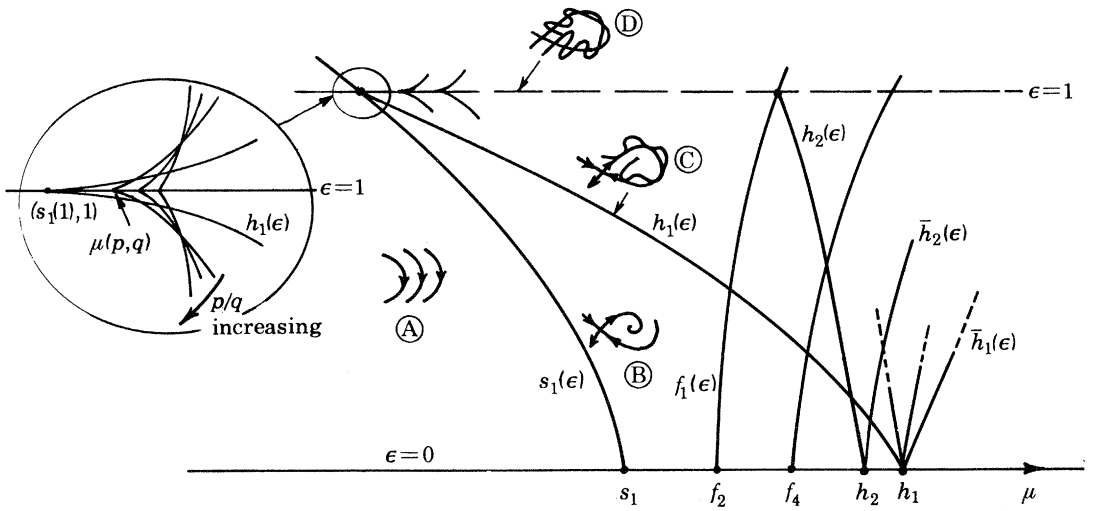

FIGURE 12. A partial bifurcation set for $F_{\mu,\epsilon}$ with some phase portraits.

We note that the work of Devaney (1982) and Devaney & Nitecki (1979) establishes that transversal homoclinic orbits do occur for the Hénon map on all but possibly a finite parameter set of the line $\epsilon = 1$, $\mu > s_1(1)$. The thesis of Gambaudo (1982) contains many examples of T-periodic perturbations of vector fields and collects results on the consequent resonant and homoclinic bifurcations in planar maps.

We now have an interesting implication: that the homoclinic bifurcation curve $h_1(\epsilon)$ based at $(h_1, 0)$ terminates at the point $(s_1(1), 1)$, where it is tangent to all orders to the line $\epsilon = 1$. Moreover, in any neighbourhood of $(s_1(1), 1)$, infinitely many resonant bifurcation curves must cross $h_1(\epsilon)$, since they are based arbitrarily close to $(s_1(1), 1)$ for large q and are tangent to $\epsilon = 1$ at *finite* orders $\frac{1}{2}(q-2)$. We conclude that, near $(s_1(1), 1)$, as ϵ increases for fixed $\mu > s_1(\epsilon)$ or μ increases for fixed $\epsilon < 1$, infinitely many saddle node bifurcations to periodic orbits occur *before* the first homoclinic bifurcation to the saddle p occurs on $h_1(\epsilon)$. In figure 12 we illustrate the partial bifurcation set and associated phase portraits. We shall return to these sequences of saddle node bifurcations in §§4.5 and 5, and show that they accumulate on the homoclinic bifurcation curves $h^j_{2^l k}(\epsilon)$ for $\epsilon \in (0, 1)$.

Similar arguments show that the homoclinic bifurcation curves $h_2(\epsilon), \ldots, h_{2^l}(\epsilon), \ldots$ based at the points $(h_2, 0), \ldots, (h_{2^l}, 0), \ldots$ terminate at the flip bifurcation points $(f_2(1), 1), \ldots,$

$(f_{2^l}(1), 1), \ldots$ at which the elliptic fixed points of period 2^{l-1}, $l \geqslant 1$ become hyperbolic and throw off elliptic fixed points of period 2^l. The curves approach each such point tangent to the $\epsilon = 1$ line at all orders, and necessarily from the right, since the fixed point in question is a saddle point only for $\mu > f_{2^l}(\epsilon)$. (Recall that we are assuming that all the flips for $F_{\mu,\epsilon}$ are supercritical.) Moreover, the elliptic periodic points created in the flip bifurcations must themselves undergo the same sequences of resonant bifurcations in each interval $\mu \in (f_{2^l}(1), f_{2^{l+1}}(1))$ as does the elliptic fixed point in $(s_1(1), f_2(1))$.

Summing up the results of this subsection, we have

PROPOSITION 4.2. *Each of the countable sequence of leftmost homoclinic bifurcation curves $h_{2^l}(\epsilon)$, $l \geqslant 0$ based at the points $(h_{2^l}, 0)$ can be extended to meet the line $\epsilon = 1$ at the saddle node and flip points $(s_1(1), 1)$ for $l = 0$, and $(f_{2^l}(1), 1)$, for $l \geqslant 1$, respectively. For $(\mu, \epsilon) = (h_{2^l}(\epsilon), \epsilon)$, $\epsilon \in (0, 1)$, the map $F_{\mu,\epsilon}$ has a homoclinic tangency of stable and unstable manifolds of a hyperbolic saddle of period 2^{l-1} (of period 1 when $l = 0$). In any neighbourhood of the points $(s_1(1), 1), \ldots, (f_{2^l}(1), 1), \ldots$ countably many resonant saddle node bifurcation curves cross $h_1(\epsilon), \ldots, h_{2^l}(\epsilon)$. If the flips $f_{2^l}(\epsilon)$ for $F_{\mu,\epsilon}$ are supercritical, then all the bifurcation horns bounded by such curves lie to the right.*

4.3. *More homoclinic bifurcations for $F_{\mu,\epsilon}$*

Since the structure of homoclinic bifurcations in the fan emerging from $(h_1, 0)$ is repeated in every other fan, we will henceforth concentrate on this *primary fan*. We have established that its left hand boundary $h_1(\epsilon)$ connects the points $(s_1(1), 1)$ and $(h_1, 0)$; it may, of course wander about and self intersect, but in accordance with our assumptions at the end of §3, let us assume that it crosses the (μ, ϵ)-plane 'smoothly' as illustrated in figure 12. This is certainly the case for the Hénon map, as El-Hamouly & Mira (1981) demonstrate numerically. Also see our figure 23 in §6. We now turn to the other homoclinic bifurcation curves based at $(h_1, 0)$. Consider the rightmost, $\bar{h}_1(\epsilon)$, first.

Our assumption that $F_{\mu,\epsilon}$ has a hyperbolic two-shift for μ sufficiently large implies that $\bar{h}_1(\epsilon)$ climbs to the line $\epsilon = 1$ and terminates there at some point $\bar{h}_1(1)$. For all $\mu > \bar{h}_1(\epsilon)$, $F_{\mu,\epsilon}$ has a topological horseshoe. From Devaney & Nitecki's (1979) results we have $\bar{h}_1(1) < 8$, although they establish hyperbolicity only for $\mu > 5 + 2\sqrt{5} \approx 9.472$. In fact El-Hamouly & Mira's (1981) results suggest $\bar{h}_1(1) \approx 5.78$ and our own computations support this (see below). We shall in fact assume henceforth that $F_{\mu,\epsilon}$ has a *hyperbolic* two shift $\Omega_{\mu,\epsilon}$ for all $\mu > \bar{h}_1(\epsilon)$.

Since between the homoclinic bifurcations on $h_1(\epsilon)$ and $\bar{h}_1(\epsilon)$ all the iterates of pieces of the unstable manifold of the saddle p in the region near $x = 0$ must pass through the top most loop of the stable manifold to ultimately generate a Cantor set of transverse homoclinic points, each member of the Cantor fan of bifurcation curves which exists near $(h_1, 0)$ must extend across the (μ, ϵ)-plane to intersect $\epsilon = 1$. One expects almost all of the homoclinic tangencies occurring on these curves to be quadratic, but it is possible to show that, for $\epsilon = 1$, a countable set of them must be of 'cubic type', i.e. bifurcations in which *three* transverse homoclinic orbits emerge from one non-transverse orbit. This fact follows from the symmetry of the area preserving map $F_{\mu,1}(x, y) = (y, -x + f_\mu(y))$, when f_μ is an even function. In that case, if $\{x_n, y_n\}$ is an orbit of $F_{\mu,1}$, then it is easy to check that $\{y_{-n}, x_{-n}\}$ is an orbit of $F_{\mu,1}^{-1}$. Thus, if $(\bar{x}, \bar{y})$ is a point on the unstable manifold $W^u(p)$ of the saddle $p(\mu) = (-1-(1+\mu)^{\frac{1}{2}}, -1-(1+\mu)^{\frac{1}{2}})$, it follows that $(\bar{y}, \bar{x})$ is a point on the stable manifold $W^s(p)$; W^s and W^u are reflections of each other about the line $x = y$.

Now let us see how homoclinic bifurcations occur for $F_{\mu,1}$ as μ increases from $s_1(1) = h_1(1)$

to $\bar{h}_1(1)$. Consider first the bifurcations corresponding to those in which the points r_0 and s_0 of figure 8*a* pass up through the uppermost segment of the stable manifold. Let $\mathscr{C}^u \subset W^u(p)$ be an arc containing the analogue of the point q_0 of figure 8*a* and $\mathscr{C}^s \subset W^s(p)$ be its reflection in $x = y$. In figure 13 we show how these arcs move respectively up and to the right as μ increases; these portraits are computer simulations of the Hénon map for $\epsilon = 1$. Let $\mathscr{C}^u_1$, $\mathscr{C}^s_1$

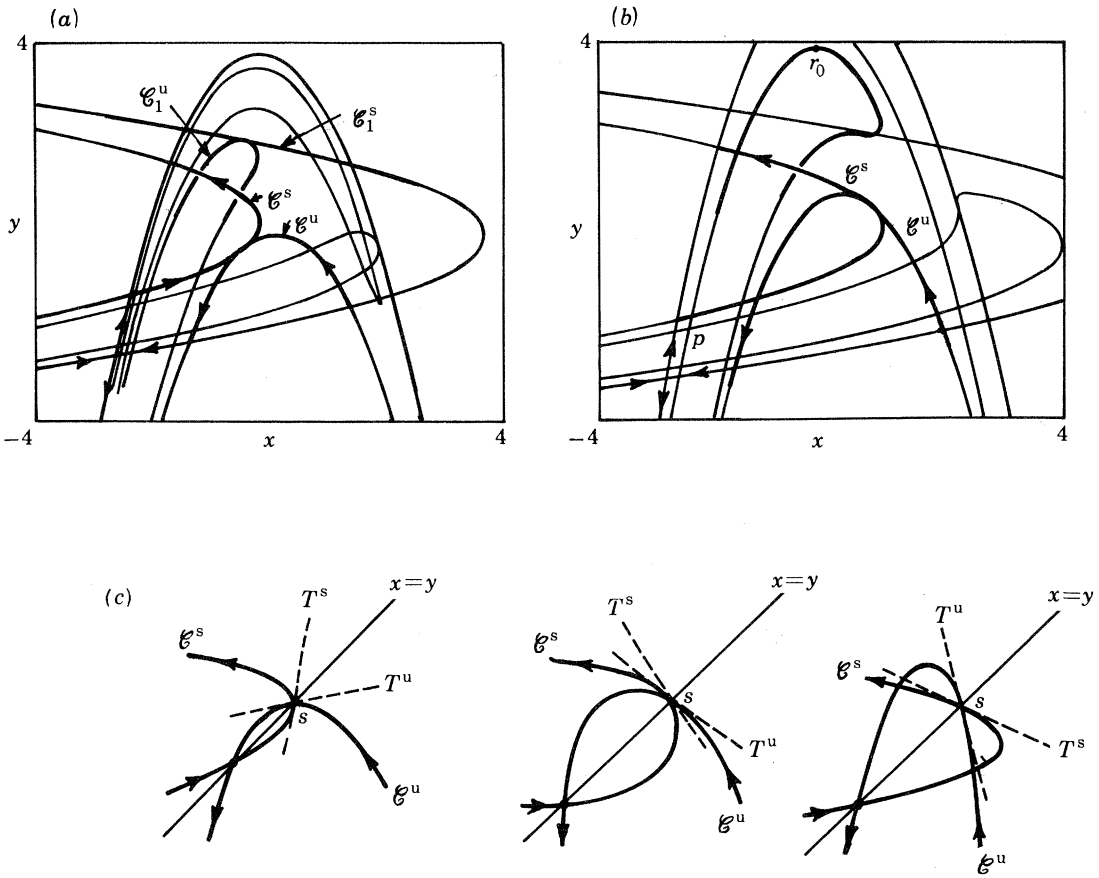

FIGURE 13. Stable and unstable manifolds of p for the area preserving map $F_{\mu,1}(x,y) = (y, -x+f_\mu(y))$. (*a*) $\mu = 1.65$ (*ca.* $h_{1,l}(1)$). (*b*) $\mu = 3.0$ (*ca.* $h_{1,r}(1)$). (*c*) How the arcs $\mathscr{C}^u$, $\mathscr{C}^s$ move as μ increases.

be the images $F_{\mu,1}(\mathscr{C}^u)$, $F_{\mu,1}(\mathscr{C}^s)$. For μ close to $h_1(1)$, $\mathscr{C}^u \cap \mathscr{C}^s = \varnothing$ and as μ increases, owing to the symmetry, the arcs first intersect on the line $x = y$ with a common tangent along that line. Their images intersect on the top most loop of $W^s(p)$ and it is not difficult to see that this defines the point $r_0 \in \mathscr{C}^u_1$, cf. figure 8*a*, although here, for $\epsilon = 1$, the distances d_0 and d_1 are both of $O(1)$ and the point q_0 is far from p_0. This tangency defines a bifurcation point $\mu = h_{1,l}(1)$, the left end point of the first interval which will be removed in constructing the Cantor set of bifurcations.

Continuing to increase μ we see that $\mathscr{C}^u$ and $\mathscr{C}^s$ now intersect in two transverse homoclinic points, let $s = s(\mu)$ be the upper (and rightmost) one. Consider the tangents T^u, T^s to $\mathscr{C}^u$, $\mathscr{C}^s$ at s. As μ increases, T^u and T^s rotate anticlockwise and clockwise respectively from 45° (at $\mu = h_{1,l}(1)$) to 135° at a point $\mu = h_{1,r}(1)$, at which $\mathscr{C}^u$ and $\mathscr{C}^s$ are once again tangent. A further increase in μ causes a bifurcation in which *three* transverse homoclinic points branch from s. Comparing figure 8 with 13 we see that s plays the same role as the point s_0 for small ϵ.

Thus $h_{1,r}(1)$ is the homoclinic bifurcation point defining the right endpoint of the interval to be removed from the Cantor set, *and it corresponds to a homoclinic tangency of cubic type.*

Similar arguments apply to every family of homoclinic orbits that contains a curve of points $t(\mu)$ (in (x, y, μ)-space) on the surface $x = y$ such that the tangent to $W^u(p)$ is normal to $x = y$ for some $t(\mu^*)$. The symmetry implies that every point contained in $W^u(p) \cap \{x = y\}$ is a homoclinic point, and is necessarily non-transverse if the tangent is normal to $x = y$. To check that there is a bifurcation from one to three (transverse) homoclinic orbits at such points we need merely check that the tangents vary continuously with μ. Devaney & Nitecki's (1979) results imply that, for μ sufficiently large, all homoclinic orbits are transverse and all bifurcations have occurred, while for μ sufficiently close to $s_1(1) = h_1(1)$ countably many of the orbits in question have not yet been created. Since the manifolds (and their tangents at points on $x = y$) vary smoothly with μ we conclude that there must be a countable set of homoclinic bifurcations of cubic type. This proves

PROPOSITION 4.3. *As μ increases from $h_1(1)$ to $\bar{h}_1(1)$ for $\epsilon = 1$ there is a countable sequence of homoclinic bifurcations of cubic type.*

Although it is implicit in our assumption that $F_{\mu,\epsilon}$ is a regular versal family, we have not been able to prove that all these cubic bifurcations are supercritical in that the number of homoclinic orbits always increases at each bifurcation point. However, we shall assume this and shall further assume that, for $\epsilon < 1$, these cubic bifurcations become quadratic. Thus we arrive at the simplest model of the primary homoclinic bifurcation set for $F_{\mu,\epsilon}$. However, before unveiling this model we show that the structure of the fan is not that of the Cantor fan to which it is asymptotic as $\epsilon \to 0$. Rather, we shall see that infinitely many of the bifurcation curves growing from $(h_1, 0)$ necessarily intersect each other as ϵ increases, even under our 'simplest case' assumptions, and that further tangencies of cubic type must occur for $\epsilon \in (0, 1)$.

4.4. *The tangled homoclinic fan for $F_{\mu,\epsilon}$*

To demonstrate why the homoclinic bifurcation curves must cross, let ϵ increase from 0 to 1, keeping the point (μ, ϵ) on a given bifurcation curve, say that connecting the points $(h_1, 0)$ and $(s_1(1), 1)$. For ϵ small, the loops of $W^u(p)$ are all ϵ-close to a segment of the curve $y = f_{h_1}(x)$; in particular, there are infinitely many arcs of $W^u(p)$ crossing a line connecting the homoclinic tangent point r_1 and the point q_1, where the last homoclinic tangency will occur at $\mu = \bar{h}_1(\epsilon)$. There are also infinitely many 'quasi-horizontal' segments of $W^s(p)$ crossing the line connecting r_1 and q_1. To see this, we observe that there is a (least) integer k such that the kth pre-image $r_{-k} = F^k(r_0)$ of r_0 lies on the rightmost segment of $W^s(p)$. (r_{-2} in figure 14). Successive pre-images of r_{-k} then accumulate on p along the leftmost segment of $W^u(p)$: as they do so, infinitely many pre-images of portions of the arcs A r_{-k} B (figure 14) of $W^s(p)$ fall across the line connecting r_1 and q_1. The y coordinates of points in these segments are independent of ϵ at leading order. In contrast, the discussion at the beginning of this section shows that, as $\epsilon \to 0$, the points q_1 and s_1 and the attendant arcs of $W^u(p)$ approach r_1 at a rate linear in ϵ. These arcs must therefore cross the segments of $W^s(p)$, leading to a countable set of 'secondary' homoclinic tangencies. This argument can be repeated on each bifurcation curve based at $(h_1, 0)$ *except* the two outer ones $h_1(\epsilon)$ and $\bar{h}_1(\epsilon)$, since in those cases all the segments of $W^s(p)$ lie outside $W^u(p)$, or all the arcs of $W^u(p)$ lie below the tangency point q_1 respectively. (These curves form the limits of the homoclinic bifurcation set.) We therefore have

PHILOSOPHICAL TRANSACTIONS OF THE ROYAL SOCIETY A MATHEMATICAL, PHYSICAL & ENGINEERING SCIENCES

PROPOSITION 4.4. *On each homoclinic bifurcation curve within the interior of the primary fan bounded by* $h_1(\epsilon)$, $\bar{h}_1(\epsilon)$ *there is a further countable set of homoclinic bifurcation points. For such parameter values, two distinct non-transverse homoclinic orbits exist simultaneously.*

However, we note that while each of these 'secondary' homoclinic bifurcation points $h_1^s \in h_{1,l}(\epsilon)$ (for example) extends to a bifurcation curve $h_1^s(\epsilon)$ that generically crosses the

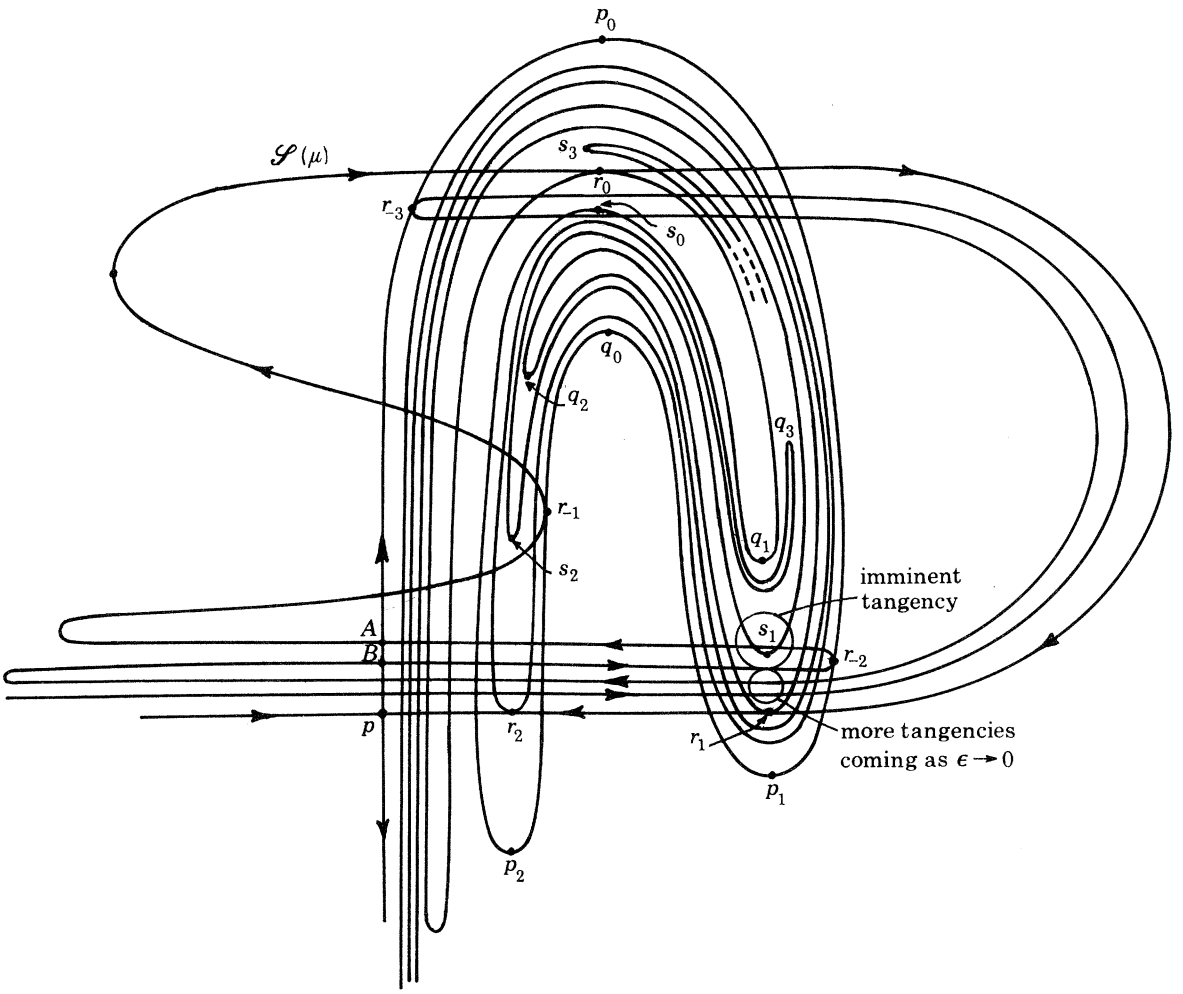

FIGURE 14. More homoclinic tangencies for $F_{\mu,\epsilon}$, the *top most branch* $\mathscr{S}(\mu) \subset W^s(p)$ is defined in the text below, and the role of the arc $Ar_{-2}B$ is explained in the text.

primary homoclinic bifurcation curve $h_{1,l}(\epsilon)$ transversely, $h_1^s(\epsilon)$ is not a 'new' bifurcation curve. In fact as $\epsilon \to 0$ $h_1^s(\epsilon)$, $h_{1,l}(\epsilon) \to h_1$: the results of §4.1 imply that the bifurcation curves 'untangle' as ϵ decreases so that the set is asymptotic to a Cantor fan. We must now address the creation of the homoclinic orbits in more detail.

First some definitions. Let $\mu \geqslant h_1(\epsilon)$ and fix $\epsilon \in (0, 1]$. Recall that $p = p(\mu)$ is the saddle point on the left. The *top most loop* $\mathscr{S}(\mu) \subset W^s(p)$ is the arc bounded by the points $a_{-1}(\mu)$, $a_0(\mu)$, where $F^2_{\mu,\epsilon}(a_{-1}) = F_{\mu,\epsilon}(a_0) = (0, y_a)$ is the lowest point on $W^s(p) \cap \{x = 0\}$. The *topmost loop* $\mathscr{U}(\mu) \subset W^u(p)$ is the arc bounded by the saddle point p and the right most homoclinic point lying on the arc $pa_0 \subset W^s(p)$. Note that $\mathscr{U}(\mu)$ intersects $\mathscr{S}(\mu)$ in two transverse homoclinic points h^+ (left) and h^- (right) for $\mu > h_1(\epsilon)$, figure 15*a*. Since the invariant manifolds depend smoothly on μ, the arcs $\mathscr{S}(\mu)$, $\mathscr{U}(\mu)$ and their images under F, F^{-1} form smooth two-manifolds

$\mathscr{S}$, $\mathscr{U}$ in (x, y, μ)-space. Of course $\mathscr{U}$ does not exist for $\mu < h_1(\epsilon)$, since the homoclinic points h^+, h^- and their images coalesce and vanish at $\mu = h_1(\epsilon)$.

Now suppose $\mu > h_1(\epsilon)$, so that $F_{\mu,\epsilon}$ has a hyperbolic two shift, and consider the set $\mathscr{C}(\mu) = \overline{(\bigcup_{n\geqslant 0} F^n(\mathscr{U}(\mu))) \cap \mathscr{S}(\mu)}$ (the overbar denotes closure).

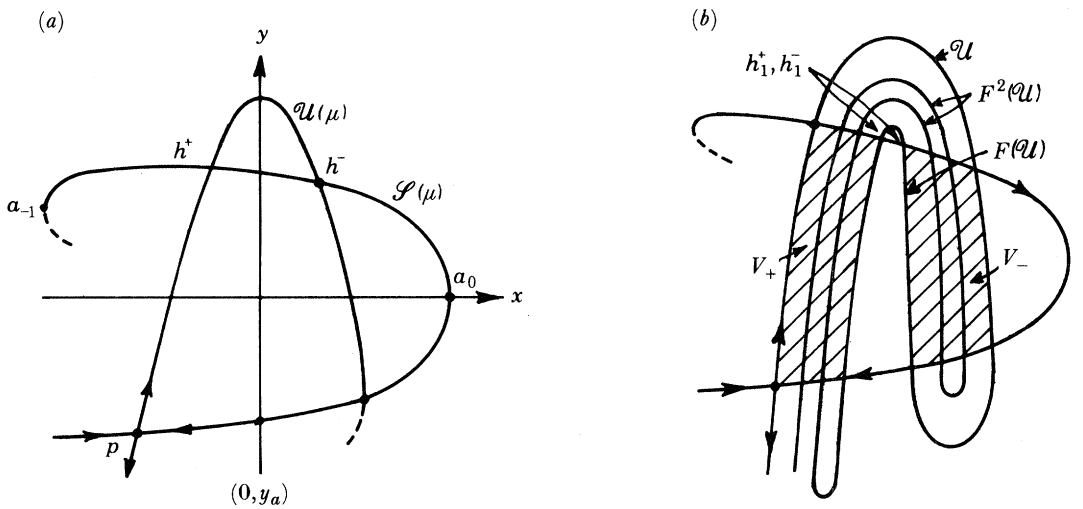

FIGURE 15. The arcs $\mathscr{U}(\mu)$, $\mathscr{S}(\mu)$ and $F^n_{\mu,\epsilon}(\mathscr{S}(\mu))$.

LEMMA 4.5. *For $\mu > h_1(\epsilon)$, $\mathscr{C}(\mu)$ is a Cantor set of transverse homoclinic points.*

Proof. The fact that $F_{\mu,\epsilon}$ has a horseshoe implies that $F(\mathscr{U}(\mu))$ intersects $\mathscr{S}(\mu)$ in four points h^+, h_1^+, h_1^-, h^- that form the upper left and right corners respectively for two closed 'vertical' strips V_+, V_- (cf. Moser 1973), figure 15*b*. Iterating further it is easy to see that $F^n(V_+ \cup V_-)$ intersects $\mathscr{S}(\mu)$ in 2^n closed intervals, the lengths of which decrease by a factor $c < 1$ at each iterate, due to the hyperbolicity. The boundaries of these intervals are the points

$$(\bigcup_{i=0}^{n} F^i(\mathscr{U}(\mu))) \cap \mathscr{S}(\mu).$$

Proceeding to the limit and taking the closure, we have the required Cantor set.

We next index the transverse homoclinic points in $\mathscr{C}(\mu)$ using the natural symbol sequences inherited from the two-sided shift on the symbols $+$, $-$. Specifically, let $\mathscr{V}(\mu)$ be a 'vertical' line which lies between the strips V_+, V_-. Next let $\boldsymbol{a}(h) = \{a_j(h)\}_{j=-\infty}^{\infty}$ be a sequence of the symbols $\pm$ corresponding to the homoclinic point $h \in \mathscr{C}(\mu)$, generated by the rule

$$a_j(h) = \begin{cases} + & \text{if } F^j(h) \text{ lies to the left of } \mathscr{V}(\mu), \\ - & \text{if } F^j(h) \text{ lies to the right of } \mathscr{V}(\mu). \end{cases}$$

In accordance with our terminology for one-dimensional maps, we shall call $\boldsymbol{a}(h)$ the *itinerary* of h, noting however that it is doubly infinite, since $F_{\mu,\epsilon}$ is invertible for $\epsilon \neq 0$. Note that the 2^n 'new' homoclinic points generated at the nth stage of our construction (those lying in $(F^n(\mathscr{U}(\mu)) - F^{n-1}(\mathscr{U}(\mu))) \cap \mathscr{S}(\mu)$) have itineraries of the form $\ldots + + a_{-n} a_{-n-1} \ldots a_{-1} a_0 - + \ldots$, containing a non-trivial 'central' blocks of length $n+2$. We call these the *nth stage homoclinic points*. We also note that a_{-n} is always the symbol $-$.

The homoclinic points $h \in \mathscr{C}(\mu)$ can be ordered from left to right on $\mathscr{S}(\mu)$ by using an

adaptation of the invariant coordinate for the one dimensional map. We define the *inverse coordinate* $\boldsymbol{\theta}^-(h)$ for a point $h \in \mathscr{C}(\mu)$ from its itinerary $a(h)$ as $\boldsymbol{\theta}^-(h) = \{\theta_j^-(h)\}_{j=0}^{\infty}$, where

$$\theta_j^-(h) = \prod_{i=0}^{j} a_{-i}(h). \tag{4.15}$$

We then have

LEMMA 4.6. *The lexicographical ordering on inverse coordinates determines the order of the homoclinic points on* $\mathscr{S}$: if $\boldsymbol{\theta}^-(h) > \boldsymbol{\theta}^-(l)$ *then* h *lies to the left of* l.

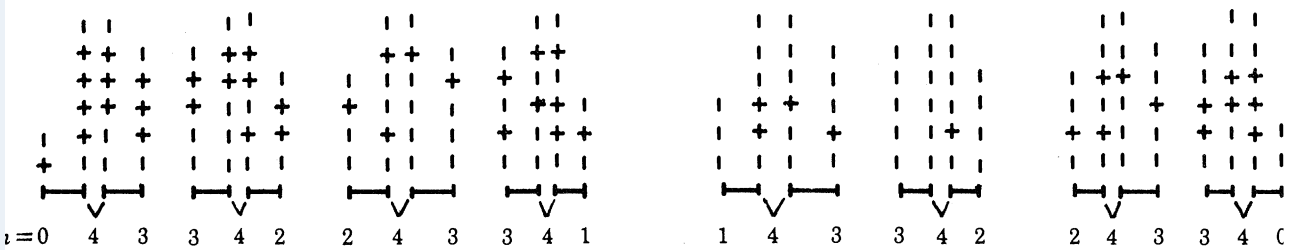

FIGURE 16. Central blocks of itineraries of homoclinic orbits.

Proof. Let two coordinates $\boldsymbol{\theta}^-(h)$, $\boldsymbol{\theta}^-(l)$ differ first at the kth symbol, suppose $\theta_k^-(h) = +$, $\theta_k^-(l) = -$. Thus each pair of points $F^{-j}(h)$, $F^{-j}(l)$ lies on the same side of $\mathscr{V}$ for $0 \leqslant j \leqslant k-1$. Suppose first that each orbit visits the right side an even number of times between $k-1$ and 0. Then each sequence has an even number of signs and the itineraries have kth symbols $a_{-k}(h) = +$, $a_{-k}(l) = -$. Thus $F^{-k}(h)$ lies to the left of $F^{-k}(l)$. But since each orbit makes an even number of visits to the right side, h also lies to the left of l. If there is an odd number of visits then $a_{-k}(h) = -$, $a_{-k}(l) = +$ and $F^{-k}(k)$ lies to the *right* of $F^{-k}(l)$; however the net effect of F^k is now to *reverse* orientation and we will have h to the left of l.

We can therefore use the inverse coordinates to attach the correct itineraries to the homoclinic points in $\mathscr{S}(\mu)$. Figure 16 shows those up to the fourth stage.

We can, of course, extend the concept of double-sided itineraries and inverse coordinates to any of the points q contained in the non-wandering set $\Omega_{\mu,\epsilon}$ of $F_{\mu,\epsilon}$ for $\mu > \bar{h}_1(\epsilon)$. In particular, we shall use those associated with periodic orbits in §5.

We next let μ decrease and consider how the homoclinic orbits coalesce and vanish. By the implicit function theorem, each of the homoclinic points $h \in \mathscr{S}(\mu)$ extends to a unique, smooth curve $h(\mu) \subset \mathscr{S}$ for $\mu > \bar{h}_1(\epsilon)$, but for $\mu \leqslant \bar{h}_1(\epsilon)$ pairs of these curves join to form loops. The points where the projections of such loops onto the μ axis are not locally 1:1 are the homoclinic bifurcation points. We call the loops *homoclinic bifurcation diagrams*. For example, the points $h_1(\epsilon)$, $h_{1,l}(\epsilon)$, $h_{1,r}(\epsilon)$, $h_1(\epsilon)$ referred to above correspond to loops connecting the points $+-$, $--$; $-++-$; $-+--$; $--+-$, $----$ and $-+-$, $---$ respectively, figure 17*a*. Note that our cubic tangency results of §4.3 implies that, for $\epsilon = 1$ these loops intersect as indicated in figure 17*b*. Here and henceforth we continue to identify the transverse homoclinic points which persist for $\mu \in (h_1(\epsilon), \bar{h}_1(\epsilon))$ by the itineraries which they have for $\mu > \bar{h}_1(\epsilon)$, although we recognize that the meaning of these sequences is unclear: there is no unique analogue for $F_{\mu,\epsilon}$ of the critical point which permits the definition of itineraries for f_μ. However, in §5 we shall extend the definition of itineraries uniquely for certain points of $\Omega_{\mu,\epsilon}$ to the range $\mu \in (h_1(\epsilon), \bar{h}_1(\epsilon))$.

Our assumption of §3 that $F_{\mu,\epsilon}$ is a regular versal family includes the assumption that the number of homoclinic points is monotone increasing with μ for each fixed $\epsilon \in (0, 1]$. This implies that for each pair of homoclinic orbits there is precisely one bifurcation point on $\mathscr{S}$, giving a Cantor set of such points. However, the projection of this set onto the μ axis is not always 1:1, since homoclinic bifurcations can coincide, by proposition 4.4. However, recalling

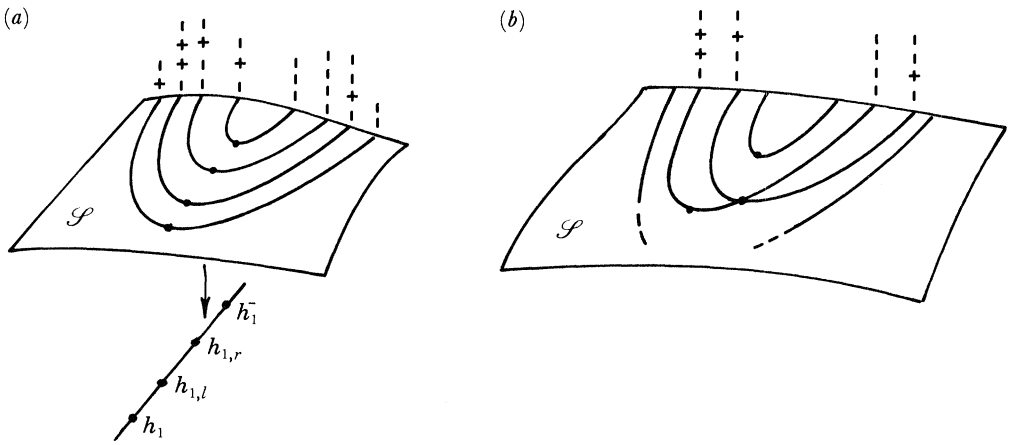

FIGURE 17. Some homoclinic bifurcation diagrams. (*a*) $\epsilon < 1$. (*b*) $\epsilon = 1$.

that we found these bifurcations by varying ϵ, keeping $\mu = h_1^*(\epsilon)$ a homoclinic bifurcation point, we see that for a versal family these coincident bifurcations occur for at most a countable set $\mathscr{E}_1 \subset (0, 1]$ of parameters ϵ for which the quasi-horizontal segments of $W^s(p)$ and certain arcs of $W^u(p)$ in the proof of proposition 4.4 are tangent. Removing this set, and the analogous sets for all other homoclinic bifurcation curves, we are left with a residual subset $\mathscr{E} \subset (0, 1]$ for which the projection is 1:1. We then have

PROPOSITION 4.7. *For each $\epsilon_0 \in \mathscr{E}$ fixed, the primary homoclinic bifurcation set intersects $\epsilon = \epsilon_0$ in a Cantor set.*

The values $\mu = h_1^*(\epsilon)$, $\epsilon \in \mathscr{E}_1$ for which this fails are evidently points at which homoclinic bifurcation curves in the fan cross. To see how the order of the homoclinic bifurcations can change as ϵ increases, we return to figure 14 and consider the positions of the loops of $W^u(p)$ containing the points $s_3, q_3 = F^3_{\mu,\epsilon}(s_0), F^3_{\mu,\epsilon}(q_0)$ relative to the top most loop $\mathscr{S}(\mu) \subset W^s(p)$. The arguments of §4.1 show that, for sufficiently small ϵ, both s_3 and q_3 must lie close to r_3 and below $\mathscr{S}(\mu)$. Now keep $\mu = h_{1,l}(\epsilon)$, so that homoclinic tangencies r_i persist, and let ϵ increase so that s_1 and q_1 rise relative to r_1. The results of §4.3 for the area preserving case show that there exist values $\epsilon \in (0, 1)$ such that q_3 and s_3 lie in $\mathscr{S}(\mu)$, first to the left of r_0, then to the right. The two loops 'unravel', leading to four bifurcation points in which eight transverse homoclinic orbits vanish.

We now examine the bifurcation diagrams corresponding to these orbits. For simplicity we take only the loop containing q_3. For small ϵ and $\mu \in h_{1,l}(\epsilon)$ there are evidently four transverse homoclinic orbits with itineraries having the central blocks $---+\,+-$, $-+-+\,+-$, $-+-+--$ and $---+--$, reading from left to right (cf. figure 18). In this case, letting μ decrease, we find the bifurcation diagram of figure 18*a* in which the two relevant bifurcation

points are labelled $h(---+\pm-)$, $h(-+-+\pm-)$, indicating the genealogy of the orbits. In contrast, for ϵ large, no such bifurcations occur for $\mu \leqslant h_{1,l}(\epsilon)$. In this case, then, let μ *increase* so that the point q_3 moves up to first cross $\mathscr{S}(\mu)$ to the right of r_0. As it does so the two orbits $-+-+--$, $---+--$ appear, followed by the two $---++-$, $-+-++-$ as q_3 next crosses $\mathscr{S}(\mu)$ to the left of r_0. We now have the bifurcation diagram of figure 18*b*.

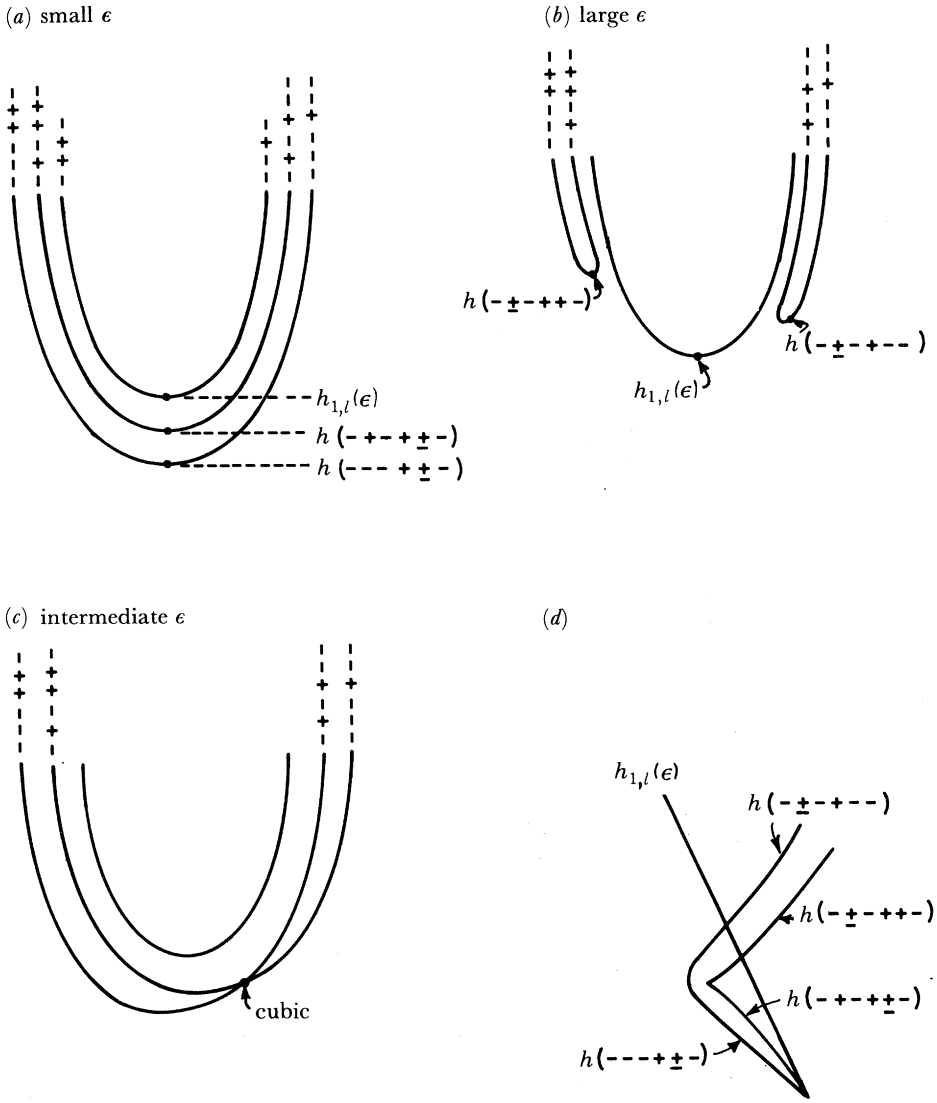

FIGURE 18. Towards the homoclinic tangle. (*a*)–(*c*) bifurcation diagrams, (*d*) the bifurcation set.

Evidently for some intermediate value of ϵ the bifurcation diagram of figure 18*c* must occur, implying the existence of a homoclinic tangency of cubic type in which the *genealogy* of the homoclinic orbits is interchanged. Once the loops connecting $---++-$, $---+--$ and $-+-++-$, $-+-+--$ are broken and replaced by loops connecting $---++-$, $-+-++-$ and $-+-+--$, $---+--$ the two bifurcation curves can swing to the right and cross $h_{1,l}(\epsilon)$, leading to the *tangled Cantor fan* of figure 18*d* (cf. figure 23).

Since locally we can change coordinates so that $W^s(p)$ is the x-axis, the homoclinic points can be represented as zeros of a function. The bifurcation sets of figures 18*a* and *b* correspond to the creation of pairs of zeros from quadratic (double) roots while that of figure 18*c* corresponds to the creation of three zeros from a triple root. Thus, using conventional arguments in singularity theory, we see that in a regular versal family, one of the pair of homoclinic bifurcation curves necessarily contains a cusp.

The discussions at the beginning of this section show that this happens infinitely many times for certain pairs of homoclinic orbits with longer and longer non-trivial central blocks. For small ϵ two such pairs bifurcate from degenerate itineraries with central blocks of the forms $--\ldots\pm-$ and $-+\ldots\pm-$ (with increasing μ), we call these *regular homoclinic bifurcations*. In contrast, for large ϵ they come from degenerate blocks of the forms $-\pm\ldots--$ and $-\pm\ldots\ldots+-$ in *irregular homoclinic bifurcations*. However, although we can appropriately pair the itineraries which the homoclinic orbits ultimately have for $\mu \geqslant \bar{h}_1(\epsilon)$ to indicate their genealogies, these itineraries do not have a straightforward interpretation for $\mu < \bar{h}_1(\epsilon)$, since the partition of the plane by $\mathscr{V}(\mu)$ into left and right can no longer be carried out unambigously. We shall return to this problem when we attempt to trace the bifurcation curves for periodic orbits in §5.

TABLE 4.

central block of itinerary	stage	θ^-	bifurcation point
$(+)\pm-(+)'$		$+++++\ldots$	$\mu_1(\epsilon)$
$(+)'-+++\pm-(+)'$	4	$+++--\ldots$	
$(+)'--++\pm-(+)'$	4	$+++-+\ldots$	
$(+)'-++\pm-(+)'$	3	$+++---\ldots$	
$(+)'--+\pm-(+)'$	3	$++-+++\ldots$	
$(+)'---+\pm-(+)'$	4	$++-+--\ldots$	
$(+)'-+-+\pm-(+)'$	4	$++--+\ldots$	
$(+)'-+\pm-(+)'$	2	$++----\ldots$	$\mu_1^l(\epsilon)$
$(+)'--\pm-(+)'$	2	$+-++++\ldots$	$\mu_1^r(\epsilon)$
$(+)'-+--\pm-(+)'$	4	$+-++--\ldots$	
$(+)'----\pm-(+)'$	4	$+-+-++\ldots$	
$(+)'---\pm-(+)'$	3	$+-+---\ldots$	
$(+)'-+-\pm-(+)'$	3	$+--+++\ldots$	
$(+)'--+-\pm-(+)'$	4	$+--+--\ldots$	
$(+)'-++-\pm-(+)'$	4	$+---+\ldots$	
$(+)'-\pm-(+)'$	1	$+-----\ldots$	$\bar{\mu}_1(\epsilon)$

We can, however, order the creation of certain homoclinic orbits uniquely, using the inverse coordinates θ^- associated with them. From lemma 4.6 we have a relation between the order of homoclinic points on $\mathscr{S}(\mu)$ and their inverse coordinates. If we consider only those orbits which undergo regular bifurcations to pairs with itineraries of the forms $..++-a_{-(n-1)}\ldots a_{-1}\pm-++\ldots$, the associated bifurcation diagrams are nested non-intersecting loops in $\mathscr{S}$. (cf. figure 18*a*). This shows that, if h^+, l^+ are the left-most homoclinic points in $\mathscr{S}(\mu)$ on two such loops, then h^+ must appear before l^+ as μ increases. The other results of this section then lead to:

THEOREM 4.8. *For any $N < \infty$ there exists $\epsilon(N) > 0$ such that for $0 < \epsilon < \epsilon(N)$ the homoclinic orbits $h^\pm$ to the saddle point p having itineraries of the form $(+)'-a_{-(n-1)}\ldots.\, a_{-1}\pm-(+)'$ with $n \leqslant N$*

are created pairwise in 2^N regular homoclinic bifurcations as μ increases. The bifurcation curves $\mu(h^{\pm}, \epsilon)$, $\mu(l^{\pm}, \epsilon)$ on which two such orbits are created are ordered as $\mu(h^{\pm}, \epsilon) < \mu(l^{\pm}, \epsilon)$ (respectively $> \mu(l^{\pm}, \epsilon)$) if $\boldsymbol{\theta}^-(h^+) > \boldsymbol{\theta}^-(l^+)$ (respectively $\boldsymbol{\theta}^-(h^+) < \boldsymbol{\theta}^-(l^+)$).

Example. The ordering for $N = 4$ is given in table 4 (cf. figure 16).

We end this section by extending our discussion of regular and irregular homoclinic bifurcations and deducing a partial bifurcation diagram and bifurcation set for the homoclinic orbits of stages $n \leqslant 4$. We refer to the area preserving case discussed in §4.3 and use the symmetry arising from the fact that f_μ is even. As μ increases for $\epsilon = 1$ we observe the phase portraits of figure 19 (also see figure 13 above). (Again we use numerical simulation of the Hénon map, but the symmetry permits us to draw more general conclusions.) We follow the relative positions of the arc $A_0 \subset W^{\mathrm{u}}(p)$ containing the point q_0, and its images $A_i = F^i(A_0)$ and the arc $B_0 \subset W^{\mathrm{s}}(p)$, its image $B_1 = \mathscr{S}(\mu)$ and pre-images $B_{-i} = F^{-i}(B_0)$. The symmetry implies that A_i and B_{-i} are reflections of each other in $x = y$.

We now construct the bifurcation diagram for $\epsilon = 1$. The first and second stage homoclinic points were dealt with earlier, they are created in four homoclinic bifurcations in the pairs $\pm -$, $- + \pm -$, $- - \pm -$ and $- \pm -$ respectively, the third being of cubic type and occurring as the arcs A_0, B_0 intersect on $x = y$ (cf. figure 13, above), of the remaining four, the second and last are regular bifurcations, apparently of quadratic type, and the first occurs simultaneously as the pair of fixed points is created in the saddle node (cf. §4.2).

Unfortunately, symmetry fails us in the four bifurcations leading to the eight third-stage homoclinic orbits, since they do not contain points on $x = y$. Thus they can be either regular or irregular, but we note that in either case, the corresponding two bifurcation curves do not intersect as ϵ varies from 0 to 1, although one of them may contain a cusp. The numerical results of figures 19*b*, *d* suggest that in each pair, the first to occur is a regular quadratic bifurcation and the second is cubic.

The first four fourth-stage orbits to appear, with central blocks $- + + + \pm -$, $- - + + \pm -$, do so in regular bifurcations as the arcs A_1 and B_{-1} first meet on $x = y$ (figure 19*a*). The next four fourth-stage orbits ($- + - - \pm -$, $- - - - \pm -$) to appear do so also in regular bifurcations as A_1 and B_{-1} next meet on $x = y$ (figure 19*c*). The symmetry implies that the last of each of these pairs is a bifurcation of cubic type. Of the remaining eight fourth stage orbits, the pairs $- - + - \pm -$, $- + + - \pm -$ appear in regular bifurcations which occur as the double loop marked $\hat{A}$ of figure 19*c* rises through $B_+ = \mathscr{S}(\mu)$. In contrast, $- \pm - + - -$ and $- \pm - + + -$ appear in *irregular* bifurcations in that order as the arc A_3 containing q_3 finally completes its winding journey. These bifurcations occur in the range $h_{1,r}(1)$, $\bar{h}_1(1)$ after the first regular fourth stage bifurcations in that range, but we cannot place them more precisely.

Thus we arrive at the partial bifurcation diagram and bifurcation set of figure 19*e*, *f*. One can iterate such a construction and hence show that for all $n \geqslant 4$, certain of the nth stage homoclinic bifurcations, which are regular and occur 'early' in the Cantor fan for ϵ sufficiently small, are necessarily irregular and occur late for ϵ sufficiently close to 1. Moreover, a similar analysis clearly extends to the fans emerging from each of the bifurcation points $(h^j_{2^l k}, 0)$.

PHILOSOPHICAL TRANSACTIONS OF THE ROYAL SOCIETY A MATHEMATICAL, PHYSICAL & ENGINEERING SCIENCES

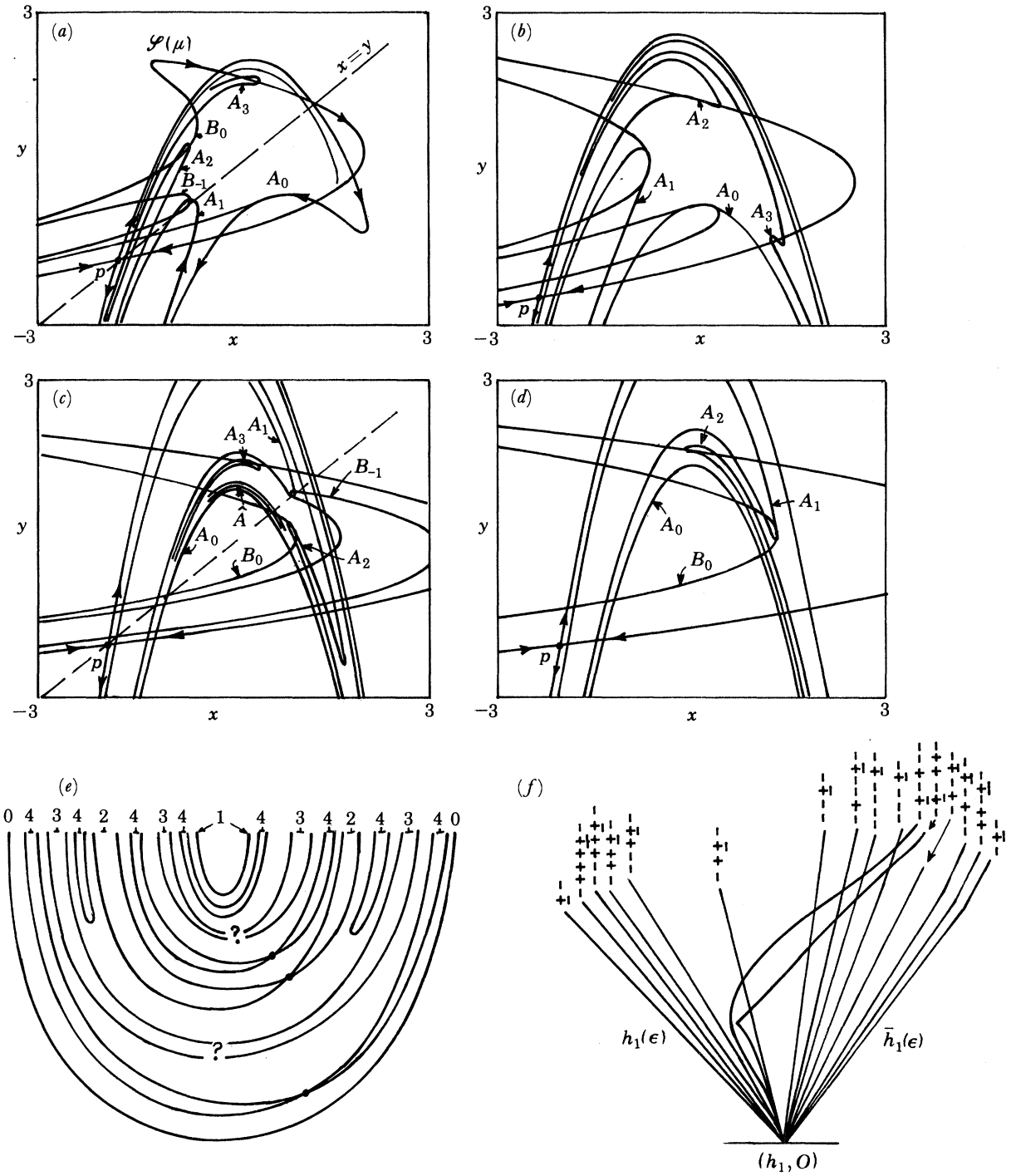

FIGURE 19. Towards the homoclinic bifurcation set for $\epsilon = 1$. (*a*) $\mu = -0.1$, first 4th-stage orbits. (*b*) $\mu = 0.80$, first 3rd-stage orbits (*c*) $\mu = 4.1$, second 4th-stage orbits. (*d*) $\mu = 4.9$, second 3rd-stage orbits. (*e*) The bifurcation diagram. (*f*) The bifurcation set: a tangled Cantor fan.

4.5. *Normal forms for the homoclinic bifurcations for* $F_{\mu,\epsilon}$, $\epsilon \in (0, 1)$

We end this section with an adaptation of the results of Gavrilov & Silnikov (1972, 1973) to the present case. They considered quadratic homoclinic tangencies and showed that such bifurcation points are the limits of sequences of saddle–node and flip bifurcations of certain periodic orbits. Their work is closely related to that of Newhouse (1974, 1979, 1980), who showed that wild hyperbolic sets, whose stable and unstable manifolds exhibit persistent tangencies, and countable sets of stable periodic orbits can exist near homoclinic tangencies.

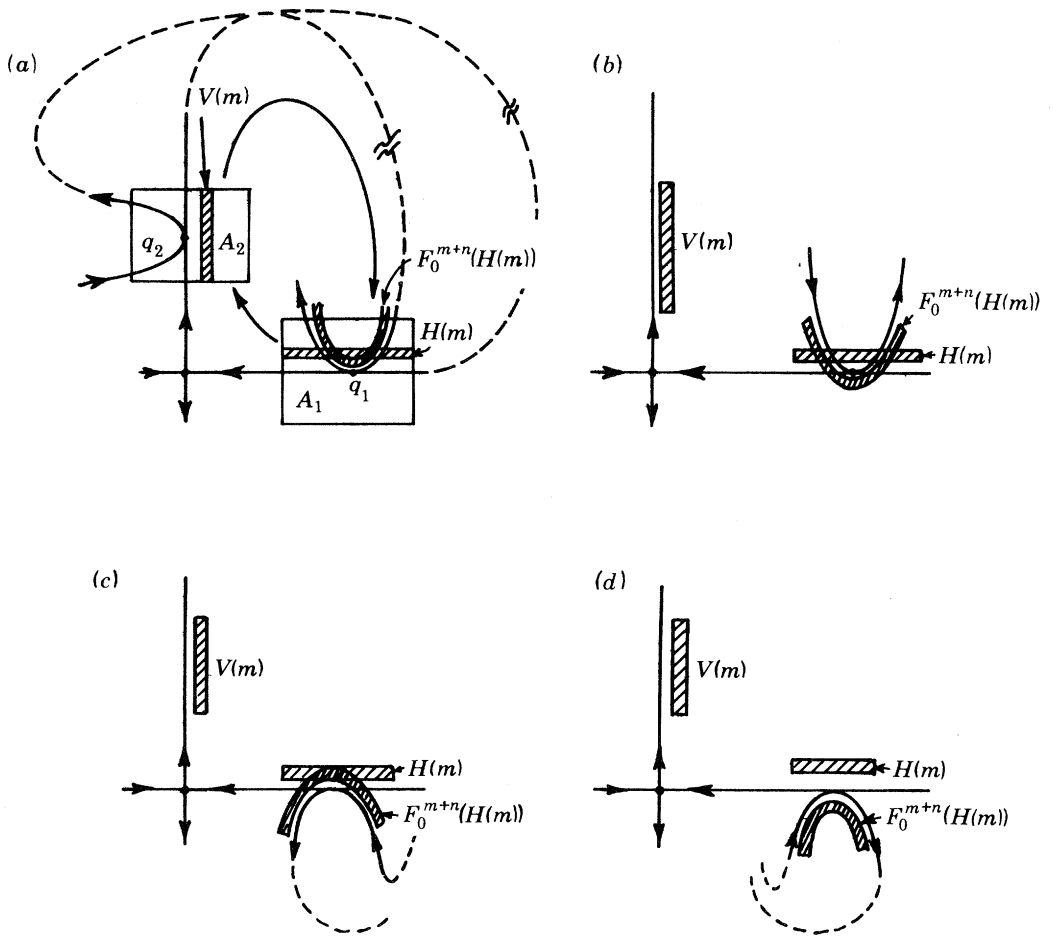

FIGURE 20. The four signatures of quadratic homoclinic tangencies.
Case (*a*) $\alpha > 0$, $\delta > 0$, (*b*) $\alpha < 0$, $\delta > 0$, (*c*) $\alpha > 0$, $\delta < 0$, (*d*) $\alpha < 0$, $\delta < 0$.

To illustrate the argument, fix $\epsilon = \epsilon_0 \in (0, 1)$ and consider a one parameter family of maps $F_\nu = F_{\mu - h_1^*(\epsilon_0), \epsilon_0}$ such that for $\nu < 0$ $W^u(p) \cap W^s(p) = \varnothing$ in some neighbourhood, while for $\nu > 0$ we have transversal intersections and at $\nu = 0$, F_0 has a quadratic tangency q in that neighbourhood. (For example, $\mu = h_1^*(\epsilon)$ is one of the bifurcation curves in the primary homoclinic fan.) We pick a coordinate system (x, y) such that, in a neigbourhood U of p, $W^s(p)$ and $W^u(p)$ are given by $y = 0$ and $x = 0$ respectively. Let $q_2 = (0, \bar{y})$ and $q_1 = (\bar{x}, 0) = F_0^n(q_2)$ for some (large) integer n be (non-transverse) homoclinic points and A_1, A_2 be neighbourhoods

of q_1, q_2 lying in U as shown in figure 20*a*. Here we show the first such tangency. Now for large m the map $F_\nu^m: A_1 \to A_2$ is well approximated by

$$DF_\nu(p))^m = \begin{bmatrix} \lambda^m & 0 \\ 0 & \gamma^m \end{bmatrix}, \tag{4.16}$$

where $0 < \lambda < 1 < \gamma$, and $\lambda\gamma = \epsilon_0 < 1$ and $m \to \infty$ as we pick domains in A_1 closer and closer to $W^s(p)$. The form of the map $F_0^n: A_2 \to A_1$ (n is fixed) may also be approximated since, by hypothesis, the vertical line $W^u(p) \cap A_2$ is mapped to the parabola $W^u(p) \cap A_1$ and the parabola $W^s(p) \cap A_2$ to the horizontal line $W^s(p) \cap A_1$. Also, as ν varies, the images undergo a vertical translation. Thus we have the 'model' map

$$F_\nu^n: A_2 \to A_1 \approx (x, y) \to (\bar{x} - \alpha(y - \bar{y}), \beta x + \delta(y - \bar{y})^2 - \delta\nu). \tag{4.17}$$

(Here we assume that, to first order, vertical lines map to parabolas and that the inverse images of horizontal lines are likewise parabolas.) For the case of figure 20*a* we have $\alpha, \beta, \delta > 0$. Composing the two maps and rescaling to remove the redundant parameter β we arrive at a quadratic approximation to the map $F_\nu^{m+n}: A_1 \to A_1$:

$$G_{\nu,m}: (x, y) \to (\bar{x} - \alpha(\gamma^m y - \bar{y}), \lambda^m \alpha x + \delta(\gamma^m y - \bar{y})^2 - \delta\nu); \alpha = \pm 1. \tag{4.18}$$

Of course, the domain of the map is not the whole of A_1, since some points never return to A_1; in particular, we require $\gamma^m y - \bar{y}$ sufficiently small. More precisely, we fix an integer m and a horizontal strip $H(m) \subset A_1$ such that $F^m(H(m)) \cap A_2$ is a vertical strip $V(m)$ and hence $F_\nu^{m+n}(H(m)) \cap A_1$ is non-empty. Equation (4.18) then permits us to compute the approximate bifurcation value $\nu_1(m)$ for which a pair of periodic orbits, a saddle and a sink, of period $m+n$ appear in a saddle node bifurcation:

$$\nu_1(m) = (1/\delta)\,(\alpha\bar{x}\lambda^m - \bar{y}\gamma^{-m}) - \tfrac{1}{4}[(\lambda^m + \gamma^{-m})/\delta]^2, \tag{4.19}$$

since for $\nu = \nu_1(m)$ (4.18) has two coincident fixed points which split apart or vanish as ν varies. For large m, since γ^{-m}, λ^m and $(\lambda\gamma)^m = \epsilon_0^m \to 0$, we have

$$\nu_1(m) \sim -\gamma^{-m}\bar{y}/\delta, \tag{4.20}$$

i.e. $\nu_1(m) \to 0^-$ for $\delta > 0$ and $\nu(m) \to 0^+$ for $\delta < 0$. Thus the homoclinic tangency at $\nu = 0$ is the limit of a countable sequence of saddle node bifurcations occurring for $\nu < 0$ in cases (*a*) and (*b*) of figure 20 and for $\nu > 0$ in cases (*c*) and (*d*). It is amusing to note that these bifurcations accumulate at the geometric rate $1/\gamma$, where γ is the largest eigenvalue of $DF_\nu(p)$ and thus is specific to the particular map and not a universal number.

Equation (4.18) can further be solved for flip bifurcation points $\nu_2(m) \in (\nu_1(m), 0)$ for the sink, to yield

$$\nu_2(m) = (1/\delta)\,(\alpha\bar{x}\lambda^m - \bar{y}\gamma^{-m}) + \tfrac{3}{4}[(\lambda^{-m} + \gamma^{-m})/\delta]^2 \sim -\gamma^{-m}\bar{y}/\delta + 3\gamma^{-2m}/4\delta^2. \tag{4.21}$$

It is, in fact, apparent from the sketches of the strips $H(m)$ and their images $F_\nu^{m+n}(H(m))$ of figure 20*a*, that, as the homoclinic tangency approaches, so full horseshoes of successively higher periods $m+n$ are created. (The Smale–Birkhoff homoclinic theorem (Smale 1963; Moser 1973; Guckenheimer & Holmes 1983) implies that hyperbolic horseshoes of *all* sufficiently large periods $m+n$ exist near the point $q_1 \in A_1$ for all $\nu > 0$.) We conclude that $\nu_2(m)$ is but the first of a countable sequence of period doubling bifurcations which must take place before $\nu = 0$, since for $\nu > 0$ (respectively $\nu < 0$) there is a full $(m+n)$-horseshoe in A_1 near q_1,

containing points of all periods for the map F^{m+n}. In fact countable sets of further bifurcations must also occur, in which points of period $2^l 3(m+n)$, $2^l 5(m+n)$; $l = 1, 2, \ldots$, etc. are created. Since such sequences occur for each sufficiently large m we have a countable sequence of countable sequences of bifurcations all accumulating on $\nu = 0$. One can thus find sinks of arbitrarily high period in any neighbourhood of a non-transverse homoclinic point q, and finite sets of these sinks persist when the homoclinic tangency is broken. Newhouse's results (1979, 1980) give more information and in particular show that the closure of the set of homoclinic points of a suitably perturbed map is contained in the closure of the set of its periodic sinks.

We note that the creation of the $(m+n)$-horseshoe contained in $H(m) \cap F_\nu^{m+n}(H(m))$ for F_ν^{m+n} between the saddle node bifurcation point $\nu_1(m)$ and $\nu = 0$ will mirror in miniature all the features of the creation of the 1-horseshoe for F_{μ,ϵ_0} itself. In the next section we shall address the task of connecting the bifurcation sets in which such $k = (m+n)$-shoes are created with the boxes $[s_k^j, h_k^j]$ for the one-dimensional map.

In establishing the convergence of saddle–node and flip bifurcations to $\nu = 0$ we have shown that the homoclinic bifurcation point is inaccessible from one side, in Gavrilov & Silnikov's term. It turns out that, in case (a) this point is inaccessible from *both* sides, since a further sequence of saddle–nodes accumulates on $\nu = 0$ from above for $\alpha, \delta > 0$. We refer the reader to Gavrilov & Silnikov (1973) for details, noting that our cases (a, b, c, d) correspond to cases 10, 4, 1 and 2 respectively in table 1 of that paper. The orbits created in this second sequence of saddle–nodes are ones containing points which remain close to the saddle p for two passes of length m_1 and m_2, with $m_2 \gg m_1$.

We shall need asymptotic estimates of the saddle node bifurcation points for these orbits in §5, so we outline their derivation briefly. Composing two maps $G_{\nu,m_2} \circ G_{\nu,m_1}$ of the form (4.18) we find that double pass periodic orbits correspond to real roots of the pair of simultaneous quadratic equations

$$\left.\begin{aligned} Y_2 &= (1+\gamma^{m_2}\lambda^{m_1})^{-1}\,(\gamma^{m_2}\lambda^{m_1}\alpha\bar{x} - \bar{y} + \gamma^{m_2}\delta Y_1^2 - \gamma^{m_2}\delta\nu), \\ Y_1 &= (1+\gamma^{m_1}\lambda^{m_2})^{-1}\,(\gamma^{m_1}\lambda^{m_2}\alpha\bar{x} - \bar{y} + \gamma^{m_1}\delta Y_2^2 - \gamma^{m_1}\delta\nu), \end{aligned}\right\} \tag{4.22}$$

when $Y_i = \gamma^{m_i} y - \bar{y}$. It is possible to check that a saddle–node bifurcation for an orbit of period $m_1 + m_2 + 2n$ occurs at a point $\nu_1(m_1, m_2)$, with

$$\nu_1(m_1, m_2) \in (0, (\lambda^{m_1}\alpha\bar{x} - \gamma^{-m_2}\bar{y})/\delta). \tag{4.23}$$

Now, for fixed λ, γ and α, $\delta > 0$ we can choose $m_2 \gg m_1 (\gg 1)$ such that $\lambda^{m_1}\alpha\bar{x} > \gamma^{-m_2}\bar{y}$ and $\nu_1(m_1, m_2) > 0$. Thus, in case (a) we can find an accumulating sequence of saddle–nodes approaching $\nu = 0$ from above, as claimed. However, a careful examination of the other three cases $\alpha > 0$, $\delta < 0$ and $\alpha < 0$, $\delta \gtrless 0$ shows that such (m_1, m_2) orbits appear on the same sides of $\nu = 0$ as do the single pass orbits found above, and bifurcations of this type therefore appear to be inaccessible only from one side. See Guckenheimer & Holmes (1983, chap. 6.6) for an alternative approach to these double pass bifurcations and the horseshoes created subsequent to them.

We remark that all four types (a)–(d) of homoclinic bifurcations occur on curves in the primary fan, as a return to our discussion in §4.4 and careful attention to figure 14 will show. We summarize:

PROPOSITION 4.9. *Choose $\epsilon_0 \in (0, 1)$. Suppose that $\mu = h_1^*(\epsilon_0)$ is a bifurcation point for F_{μ,ϵ_0} on a curve $h_1^*(\epsilon)$ in the primary homoclinic fan. Then in any neighbourhood of $(h_1^*(\epsilon_0), \epsilon_0)$ to the left of the curve $h_1^*(\epsilon)$ there is an accumulating sequence of saddle–node, flip and homoclinic bifurcations in which, fixed points and horseshoes of arbitrarily high period are created for $F_{\mu,\epsilon}$ as μ increases for fixed ϵ. Moreover*

if the homoclinic tangency is of type (a) (for example $h_1^*(\epsilon) = h_1(\epsilon)$), then accumulating bifurcation sequences can be found in any neighbourhood of $h_1^*(\epsilon_0)$ on both sides of $h_1^*(\epsilon)$.

When we trace bifurcation curves for periodic orbits in the next section we shall see how these accumulating sequences behave for $\epsilon \to 0$ and $\epsilon \to 1$. For instance, it is clear that the sequence to the left of $h_1(\epsilon)$ for $\epsilon < 1$ must somehow switch across to the right as $\epsilon \to 1$, since $\mu = h_1(1) = s_1(1)$ is the leftmost bifurcation point for $F_{\mu,1}$ and the non-wandering set is empty for $\mu < s_1(1)$ and $\epsilon = 1$.

5. Bifurcations of periodic orbits for the planar map

In §3 we showed that each of the saddle node and flip bifurcation points s_k^j, $f_{kl_2}^j$ for the one-dimensional map could be extended to a unique curve $\mu = s_k^j(\epsilon), f_{2^l k}^j(\epsilon)$ which crosses the (μ, ϵ) plane to meet the line $\epsilon = 1$. While it is clear the order of the flips $f_{2^l k}^j(\epsilon)$ within a sequence (j, k fixed, l increasing) must remain as in the one-dimensional map – an orbit cannot flip before it exists! – we shall see that the ordering of the bifurcation boxes $[s_k^j(\epsilon)\ h_k^j(\epsilon)]$ changes dramatically, even under our assumption of the 'monotonic' creation of additional periodic and homoclinic orbits for $F_{\mu,\epsilon}$ as μ increases for fixed ϵ. We shall use the ordering established in theorem 4.8 for certain homoclinic bifurcations together with the accumulation results for periodic orbits of proposition 4.9 to link certain bifurcation sequences $[s_k^j(\epsilon), h_k^j(\epsilon)]$ to homoclinic bifurcation curves in the primary fan. In this way we shall be able to trace the order of some of the bifurcations of $F_{\mu,\epsilon}$ as ϵ increases.

5.1. *Itineraries and bifurcation sequences for periodic orbits of $F_{\mu,\epsilon}$ $\epsilon \in (0, 1)$*

The discussion in §4.4 shows that for a regular versal family $F_{\mu,\epsilon}$, pairs of homoclinic orbits are created in quadratic homoclinic tangencies as μ increases for fixed ϵ, apart from the 'transition' values of ϵ for which tangencies of cubic type occur. Moreover, for any $N < \infty$ we can pick $\epsilon(N) > 0$ such that the (regular) homoclinic bifurcation curves for the creation of pth stage orbits, $p \leqslant N$, do not intersect for $\epsilon \leqslant \epsilon(N)$. The 2^{N+1} such homoclinic orbits arise in 2^N bifurcations with associated bifurcation diagrams like those of figure 18*a*, above and are ordered according to the prescription of theorem 4.8. In this situation we *can* meaningfully extend the itineraries of §4.4 to parameter values $\mu \in [\mu_1(\epsilon), \bar{\mu}_1(\epsilon)]$. We do this as follows.

First note that for all $\mu > \bar{h}_1(\epsilon)$ and each value of $0 < \epsilon \leqslant \epsilon(N)$ the partition curves $\mathscr{V}(\mu)$ of §4.4 can be extended into a vertical surface in (x, y, μ) space in such a manner that no homoclinic point of stage less than or equal to N lies on it, and for $\mu = \bar{h}_1(\epsilon)$ the 'last' homoclinic bifurcation point is $q_0 = \mathscr{V}(\mu) \cap \mathscr{S}(\mu)$. We next connect the 2^N pth stage homoclinic bifurcation points $p \leqslant N$ on $\mathscr{S}(\mu)$ to form a curve $v(\mu)$ which intersects the 2^N arcs of the bifurcation diagram only at the bifurcation points. Translating $v(\mu)$ vertically forms the remainder of our surface $\mathscr{V}$. Finally we extend the construction of itineraries to $\mu \in [\mu_1(\epsilon), \bar{\mu}_1(\epsilon)]$ using constant μ slices $\mathscr{V}(\mu)$ of $\mathscr{V}$ and taking the limit from the left in case a point on the orbit lies on $\mathscr{V}$. It is clear that the itineraries of specific pth stage homoclinic orbits do not change until they coalesce in pairs at the appropriate bifurcation point. Moreover, $\mathscr{V}$ can be chosen such that, as $\epsilon \to 0$, it converges on the plane $x = 0$.

We define the (double-sided) itineraries for arbitrary points q in the non-wandering set $\Omega_{\mu,\epsilon}$ of $F_{\mu,\epsilon}$ for $\mu > \bar{h}_1(\epsilon)$ just as for the homocolinic orbits to p. We continue to denote those points by their itineraries as μ decreases, until they ultimately vanish, although, as before, the meaning of the itineraries for $\mu < \bar{h}_1(\epsilon)$ is not clear: for example, two distinct periodic

orbits may have the same itineraries for $F_{\mu,\epsilon}$ when they do not for f_μ. However, for $\mu \geqslant \bar{h}_1(\epsilon)$ the itineraries are true invariants. Moreover, for $\mu > \bar{h}_1(\epsilon)$ there is a one to one correspondence between certain points $q \in \Omega_{\mu,\epsilon}$ and their *forward* itineraries $\{a_i(q)\}_{i=0}^{\infty}$ and those of the non-wandering set Ω_μ of f_μ, since both Ω_μ and $\Omega_{\mu,\epsilon}$ are hyperbolic two-shifts. In addition to this, we have the following:

PROPOSITION 5.1. *As $\epsilon \to 0$ the future itineraries of points $q = (x, y) \in \Omega_{\mu,\epsilon}$ converge on the itineraries of the points x under f_μ for all μ.*

Proof. This follows directly from the fact that, as $\epsilon \to 0$ so the coordinates of points $q \in \Omega_{\mu,\epsilon}$ approach $(x, f_\mu(x))$ and their forward orbits $\{F^n_{\mu,\epsilon}(q)\}$ approach $\{f^n_\mu(x), f^{n+1}_\mu(x)\}$. Thus, using our vertical partition $\mathscr{V} \to \{(x, y) \,|\, x = 0\}$ as $\epsilon \to 0$, we see that the itinerary of q approaches that of x for f_μ.

Remark. While there is a 1:1 correspondence between periodic orbits of $F_{\mu,\epsilon}$ and those of f_μ, we note that for any asymptotically periodic orbit of f_μ there are countably many asymptotically periodic orbits of $F_{\mu,\epsilon}$ whose *backward* itineraries $\{a_i\}_{i=-\infty}^{-1}$ differ. An obvious example is provided by the countable set of homoclinic orbits to p. Similarly, $\Omega_{\mu,\epsilon}$ contains uncountably many additional non-periodic orbits.

We now address the order of creation of the periodic orbits of $F_{\mu,\epsilon}$. Referring to the discussion of accumulating sequences of 'single pass' saddle–node bifurcations of §4.5, it should be clear that, close to a given homoclinic bifurcation point $h_1^*(\epsilon)$ there is a countable set of saddle–node bifurcations in each of which a pair of periodic orbits appears whose itineraries match those of the pair of homoclinic orbits created at $h_1^*(\epsilon)$ on an arbitrarily long block, including the central portion. To construct these itineraries (which correspond to orbits of period $k = m+n$ with m sufficiently large; cf. §4.5) we cut out a central piece of the itinerary of the bifurcating homoclinic orbit of length k and attach the initial and final '+' to form a periodic sequence. More precisely, select a homoclinic bifurcation point $\mu = h_1^*(\epsilon)$ in the primary fan and form the itinerary $\boldsymbol{a}(h(\mu))$ of the bifurcating homoclinic point $h(\mu)$. Let $a_{-p} = -$ be the first symbol of $\boldsymbol{a}$ to differ from $+$; if $a_1 = -$ is the first, let $p = 0$. Rewrite the central block of $k = p+q+1$ symbols in the form

$$\{a_0 a_1 a_2 \,..\, a_q a_{-p} a_{-(p-1)} \dots a_{-1}\} = \{a_0 - + \dots + a_{-p} a_{-(p-1)} \dots a_1\}, \tag{5.1}$$

for all $q \geqslant 1$, and iterate to form k-periodic itineraries $(b)'$ (as in §2, a prime denotes periodic repetition). For each subsequence $\{a_{-p} \dots a_{-1}\}$, we thus produce an infinite set of periodic itineraries of periods $k \geqslant p+2$.

Examples. The periodic itineraries corresponding to the four homoclinic bifurcation points $h_1(\epsilon)$, $h_{1,l}(\epsilon)$, $h_{1,lr}(\epsilon)$, $\bar{h}_1(\epsilon)$ are

$$\left.\begin{aligned}
&h_1(\epsilon)\ (p=0) + -,\ + - +,\ + - \overbrace{+ \dots +}^{k-2} && k = 2, 3, \dots,\\
&h_{1,l}(\epsilon)\ (p=2) + - - +,\ + - + -,\ + - \overbrace{+ \dots \dots + - +}^{k-4} && k = 4, 5, \dots,\\
&h_{1,r}(\epsilon)\ (p=2) + - - -,\ + - + - -,\ + - \overbrace{+ \dots + - -}^{k-4} && k = 4, 5, \dots,\\
&\bar{h}_1(\epsilon)\ (p=1) + - -,\ + - - +,\ + - \overbrace{+ \dots + -}^{k-3} && k = 3, 4, \dots.
\end{aligned}\right\} \tag{5.2}$$

PHILOSOPHICAL TRANSACTIONS OF THE ROYAL SOCIETY A MATHEMATICAL, PHYSICAL & ENGINEERING SCIENCES

Our definition of itineraries for periodic orbits of $F_{\mu,\epsilon}$ now permits us to extend the work of Gavrilov & Silnikov outlined in §4.5 and augment proposition 4.9 by the following.

PROPOSITION 5.2. *As $q \to \infty$ so pairs of periodic orbits of period $k = p+q+1$ for $F_{\mu,\epsilon}$ having itineraries of the forms $(a_0 \overbrace{- + + \ldots +}^{q} + a_{-p} \ldots a_{-1})'$ converge on the homoclinic orbits with itineraries $\ldots + + a_{-p} \ldots a_{-1} a_0 - + + \ldots$. Moreover, for $\epsilon \in (0, 1)$ fixed, the saddle–node bifurcation points in which such periodic orbits are created converge upon the corresponding homoclinic bifurcation points from the left.*

Thus the homoclinic bifurcation sequences determine the bifurcations of certain periodic orbits, in an appropriate limit. In fact the convergence of such saddle–node bifurcations of 'single pass' periodic orbits from the left holds for $0 \leqslant \epsilon < 1$, as can be seen by reference to the approximate bifurcation value $\nu_1(m)$ of (4.19). When $\epsilon \to 0$ the contracting eigenvalue $\lambda < 1$ of the saddle p likewise approaches zero, and one obtains the same asymptotic result as in (4.20). (However, we shall see later that the convergence of 'double pass' orbits from the right *does not* persist as $\epsilon \to 0$.) Not only do the saddle–node bifurcations converge: the analysis of §4.5 also shows that the attendent bifurcation curves on which flips occur and the creation of a 'single pass' shoe of period k is completed, also converge on the homoclinic bifurcation curves from the left. We summarize.

THEOREM 5.3. *For any $N < \infty$ there exists $1 \geqslant \epsilon(N) > \epsilon_0 > 0$ such that for $\epsilon_0 < \epsilon < \epsilon(N)$ the order of occurrence of period $k = p+q+1$ saddle–node bifurcations $s_k^j(\epsilon)$ (and their associated flip and homoclinic bifurcations $f_{2^j k}^j(\epsilon)$, $h_{2^j k}^j(\epsilon)$, $\ldots, h_k^j(\epsilon)$), with increasing μ is uniquely determined for $p \leqslant N$, q sufficiently large (depending on ϵ_0), and orbits having itineraries of the form $(\pm - a_{-(p+q-1)} \cdots a_{-p} \ldots a_{-1})$, $a_i = +$, $-(p+q) < i < -p$. The order is determined by $\boldsymbol{\theta}^- = \{\theta_i^-\}_{i=1}^{p+q}$, where $\theta_i^- = \prod_{j=1}^{i} a_{-j}$ and the prescription that an orbit a^m is created before an orbit a^n if and only if $\boldsymbol{\theta}^-(a^n) > \boldsymbol{\theta}^-(a^m)$.*

Remarks. We need the upper limit $\epsilon(N)$ to obtain the required order of bifurcations to pth stage homoclinic orbits, $p \leqslant N$. The lower limit ϵ_0 is required so that the homoclinic bifurcation curves in the fan are sufficiently separated for the accumulating sequences of saddle–nodes to separate as $q \to \infty$ (from theorem 4.1, their separation is, asymptotically, $O(\epsilon^p)$).

Since the first and last homoclinic bifurcations $(h_1(\epsilon), \bar{h}_1(\epsilon))$ can be uniquely continued to $\epsilon = 1$ (i.e. $\epsilon(1) = 1$), we immediately have the following corollaries to proposition 5.2 and theorem 5.3.

COROLLARY 5.4. *Consider the bifurcation boxes $[s_k^j(\epsilon), h_k^j(\epsilon)]$ associated with periodic orbits that have itineraries of the form $(+ - + + \ldots +)'$. For ϵ (depending on k) sufficiently small each such is the last of its given period k to occur as μ increases, while for ϵ sufficiently close to 1 it is the first. Moreover, for ϵ sufficiently small we have $s_{k+1}^j(\epsilon) > s_k^j(\epsilon)$, while for ϵ sufficiently close to 1 and k sufficiently large we have $s_k^j(\epsilon) > s_{k+1}^j(\epsilon)$.*

COROLLARY 5.5. *Consider the bifurcation boxes $[\bar{s}_k^j(\epsilon), \bar{h}_k^j]$ associated with periodic orbits that have itineraries of the form $(+ - + + \ldots + -)'$. For ϵ (depending on k) sufficiently small, each such is the penultimate of its given period k to occur as μ increases, while for ϵ sufficiently close to 1 it is the last. For all $\epsilon \in (0, 1)$ and k sufficiently large we have $\bar{s}_{k+1}^j(\epsilon) > \bar{s}_k^j(\epsilon)$.*

It is not hard to see that the k-periodic orbits with itineraries $(\pm - + + + .. +)'$ of corollary 5.4, which make a single circuit in the phase plane, are precisely the periodic orbits created in resonant bifurcations of order $(1/k)$ from the elliptic fixed point as μ varies from $s_1(1)$ to

$f_2(1)$ with $\epsilon = 1$ (their orbits wind once per period around the elliptic centre). We now see how these resonant bifurcation curves for which we gave asymptotic expressions for $\epsilon \approx 1$ in §4.2 (cf. figure 12) can be continued down to $\epsilon = 0$. Thus we obtain the bifurcation diagram of figure 21. We note that our 'accumulation from the left' results for $s_k^j(\epsilon) \to h_1(\epsilon)$ derived from the asymptotic behaviour of $\nu_1(m)$ of (4.19)–(4.20) for large m, fail as $\lambda\gamma = \epsilon \to 1$ and $\lambda\gamma \to 0$, so that these results do not contradict the fact that the saddle–node bifurcation curves must cross to the right of the homoclinic curve as $\epsilon \to 1$. Similarly, we note that the 'double

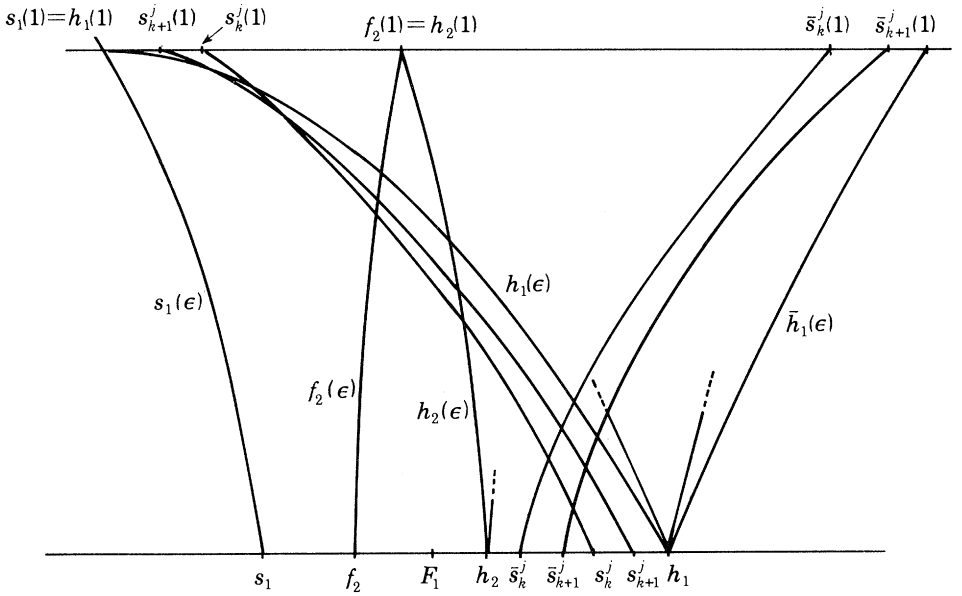

FIGURE 21. Bifurcation curves for some of the periodic and homoclinic orbits of $F_{\mu,\epsilon}$.

pass' periodic orbits with itineraries containing two consecutive strings of m_1 and $m_2 +$symbols ($m_1 \gg m_1 \gg 1$) which bifurcate to the right of homoclinic bifurcation curves such as $h_1(\epsilon)$, $h_{1,r}(\epsilon)$ for $\epsilon > 0$, no longer do so as $\epsilon \to 0$. To see this, we return to (4.23). For $\epsilon = \lambda\gamma > 0$ we have $\lambda^{m_1}\alpha\bar{x} > \gamma^{-m_2}\bar{y}$ for $m_2 \gg m_1$, and hence $\nu_1(m_1, m_2) > 0$. However, as $\epsilon \to 0$, the attracting eigenvalue $\lambda \to 0$, and for each fixed m_2/m_1 we then find $\nu_1(m_1, m_2) < 0$. Thus all these bifurcation curves pass from right to left of the homoclinic curves as $\epsilon \to 0$, so that we obtain the desired one-dimensional behaviour in the limit: i.e. h_1 is the last bifurcation point for f_μ.

We note that these corollaries imply that there are open sets of (μ, ϵ) parameter values arbitrarily close to $\epsilon = 0$ for which $F_{\mu,\epsilon}$ has at least two coexisting stable sinks (cf. Gambaudo & Tresser 1983). However, it is not obvious that one can iterate such a precess to produce the countable sets of sinks that have been proved to exist near homoclinic tangencies by Newhouse (1979) (cf. Robinson 1983)!

5.2 *Genealogies for k-periodic orbits and k-shoes*

The discussion in §4.4 shows that, while we cannot easily order all the homoclinic bifurcations for $\epsilon \in (0, 1)$ as μ increases, we can divide them into three types:

(i) *regular* bifurcations in which orbits that have itineraries with central blocks $-a_{-(p-1)} \ldots a_{-1} \pm -$ appear;

(ii) *irregular* bifurcations in which orbits that have itineraries with central blocks $- \pm a_{-(p-2)} \ldots a_{-1}a_0 -$ appear; and

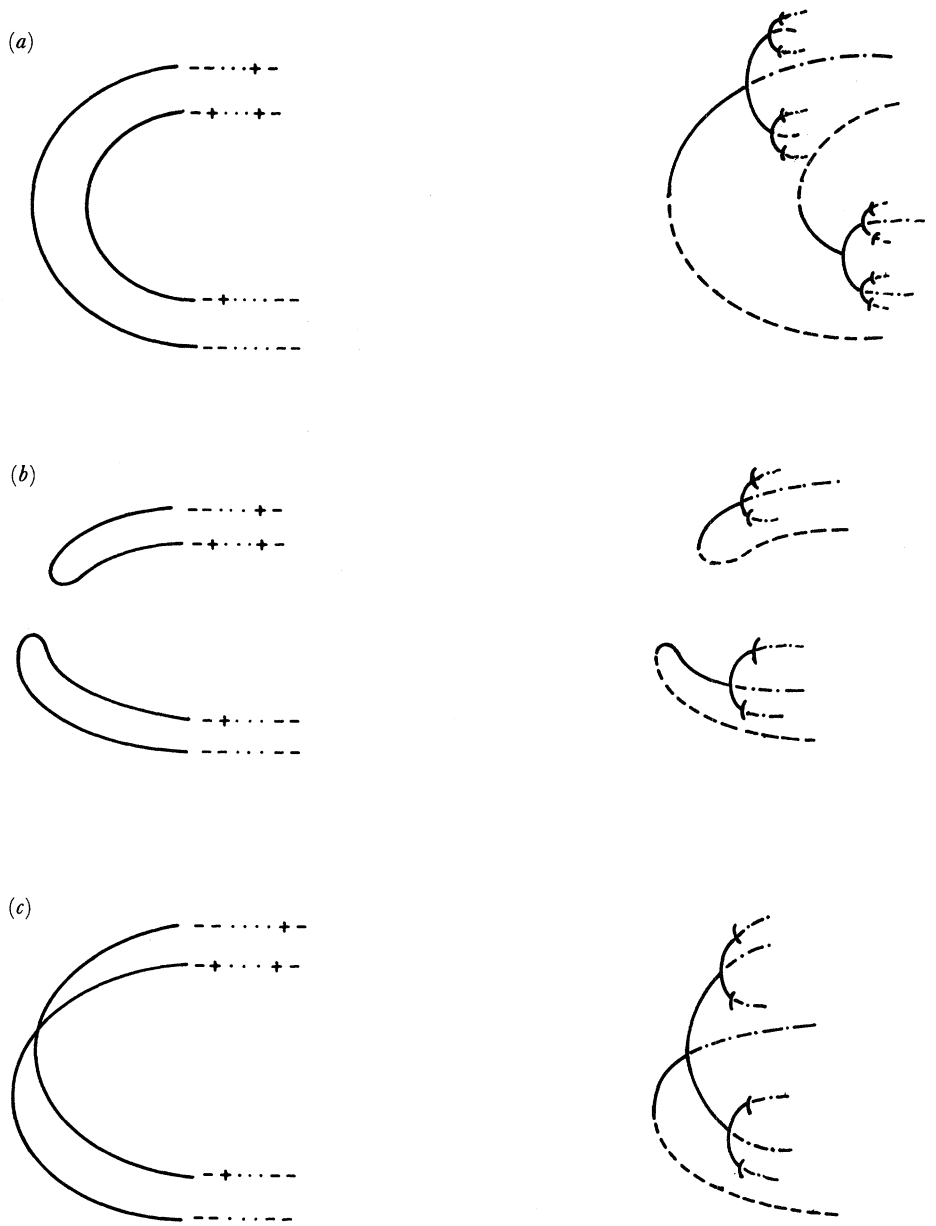

FIGURE 22. Bifurcation diagrams for homoclinic and periodic bifurcations: ——, sink; – – –, saddle with positive eigenvalues; ·–·–·–, saddle with negative eigenvalues. (*a*) Regular homoclinic bifurcations and associated saddle–nodes and flips (small ϵ). (*b*) Irregular homoclinic bifurcations and associated saddle–nodes and flips (large ϵ). (*c*) Cubic homoclinic bifurcations and associated saddle–nodes, pitchforks, and flips (intermediate ϵ).

(iii) degenerate bifurcations of cubic type in which three homoclinic orbits coalesce.

So far we have concentrated on regular bifurcations and described a unique ordering for them. As our results show, increasingly many bifurcations are of this type as $\epsilon \to 0$. The convergence results of propositions 4.9 and 5.2 imply that the bifurcation diagrams for the associated k-periodic orbits and k-horseshoes have the form indicated in figure 22*a*. In contrast, the irregular bifurcation diagrams for certain pth stage homoclinic orbits $p \geqslant 4$, change to that of figure 22*b* as ϵ increases, the periodic orbit bifurcation diagrams changing likewise. We conclude that not only does the *order* of the periodic bifurcations change as ϵ increases, as

established earlier, but the *genealogy* of pairs of k-periodic orbits also changes. Moreover, for $F_{\mu,\epsilon}$ regular and versal, the transition between the bifurcation diagrams of figure 22*a* and *b* must be via the pitchforks of figure 22*c*, and the associated bifurcation sets must exhibit cusps (cf. §3.1). It is probably possible to order subsequences of such irregular periodic bifurcations, but we have not attempted to do this in a systematic fashion.

TABLE 5. REGULAR HOMOCLINIC BIFURCATIONS OF STAGES NOT EXCEEDING 4 AND ASSOCIATED SADDLE–NODE BIFURCATIONS TO PERIODS OF 7 OR LESS

stage of orbits	central block of itinerary	associated periodic itinerary	associated saddle–nodes, s_k^j and number (q) of iterates spent near p
1	$\pm\,-$	$(+\underbrace{-+\ldots+}_{q}+)'$	s_3, (1); s_4, (2); s_5^3, (3); s_6^4, (4); s_7^9, (5)
4	$-+++\pm-$	$(+\underbrace{-+\ldots+}_{q}-+++)'$	
4	$--++\pm-$	$(+\underbrace{-+\ldots+}_{q}--++)'$	
3	$-++\pm-$	$(+\underbrace{-+\ldots+}_{q}-++)'$	
3	$--+\pm-$	$(+\underbrace{-+\ldots+}_{q}--+)'$	s_7^5, (2)
		(4, 4 omitted; irregular bifurcations)	
2	$-+\pm-$	$(+\underbrace{-++\ldots+}_{q}-+)'$	s_7^6, (3)
2	$--\pm-$	$(+\underbrace{-++\ldots+}_{q}--)'$	s_5^1, (1); s_6^2, (2); s_7^7, (3)
4	$-+--\pm-$	$(+\underbrace{-+\ldots+}_{q}-+--)'$	
4	$----\pm-$	$(+\underbrace{-+\ldots+}_{q}----)'$	s_7^1, (1)
3	$---\pm-$	$(+\underbrace{-+\ldots+}_{q}---)'$	s_7^4, (2)
3	$-+-\pm-$	$(+\underbrace{-+\ldots+}_{q}-+-)'$	s_7^3, (2)
4	$--+-\pm-$	$(+\underbrace{-+\ldots+}_{q}--+-)'$	s_7^2, (1)
4	$-++-\pm-$	$(+\underbrace{-+\ldots+}_{q}-++-)'$	
1	$-\pm-$	$(+\underbrace{-++\ldots++}_{q}-)'$	s_5^2, (2); s_6^3, (3); s_7^8, (4)

We end this section by noting that all the accumulation results for periodic orbits and bifurcations extend in the obvious way to the bifurcations occurring in fans that grow from all the points $(h_{2l_k}^j, 0)$. For example, in our discussion of orbits of periods of 7 or less in the next section we find that one of the saddle–node bifurcations to period 6 can be associated with a homoclinic bifurcation curve growing from $(h_2, 0)$. Within each horseshoe little shoes are growing!

6. CONCLUSIONS: A MODEL FOR THE MAKING OF SHOES, AND SOME NUMERICAL COMPUTATIONS FOR THE HÉNON MAP

We now attempt to summarize our results for versal families $F_{\mu,\epsilon}$, $\epsilon \in [0, 1]$. We do this by an illustration in which we trace the bifurcation boxes $[s_k^j(\epsilon), h_k^j(\epsilon)]$ for all periods $k \leqslant 7$, under assumptions on the structure of the homoclinic bifurcation set $h_1^*(\epsilon)$ for orbits of stages not

exceeding 4. Specifically, we assume that, for $\epsilon < 1$, all these homoclinic bifurcations are regular except the cubic ones in which the three orbits with central blocks $---+\,+-$, $-+-+\,+-$ and $-+-+--$ coalesce, and the subsequent irregular bifurcations of the pairs $-\pm-+--$ and $-\pm-++-$ (cf. §4.4). our numerical results for the Hénon map, described below, are consistent with this assumption. We further extend the spirit of the ordering of theorem 5.3 by associating the periodic orbits with itineraries of the form $(\pm -a_{-(p+q-1)} \dots a_{-p} \dots a_{-1})\, a_i = +,\ -(p+q) < i < -p$ with regular homoclinic bifurcations of the type $-a_{-p} \dots a_{-1} \pm -$ for *all* $q \geqslant 1$, although we can only be sure that their associated saddle–node and flip bifurcations occur close to the homoclinic bifurcations for q large.

We first write down the itineraries for the homoclinic orbits of stages of 4 or less in the correct bifurcation order, omitting the irregular pair $---+\pm-$ and $-+-+\pm-$: table 5, column 2. We then form the associated periodic itineraries according to the prescription of §5.1 (column 3). We then refer to table 1 of §2 and pick out the periodic itineraries that correspond to the ones we have just formed. Each of these can now be associated uniquely with a saddle–node bifurcation point s_k^j or a flip $f_{2^j k}$, and also with a homoclinic bifurcation curve in the fan based at $(h_1, 0)$. Thus we are able to match bifurcation boxes $[s_k^j, h_k^j]$ for all orbits of period not exceeding 7 except for the first of period 6 to appear, with itinerary $(+-+---)'$. It is not difficult, however, to see that this one is associated with the leftmost homoclinic bifurcation curve $h_2(\epsilon)$ which comes from the point $(h_2, 0)$, on which the homoclinic orbits to the saddle $q = \{\frac{1}{2}(-(1+\epsilon)+[(1+\epsilon)^2+4\mu]^{\frac{1}{2}}),\ \frac{1}{2}(-(1+\epsilon)+[(1+\epsilon)^2+4\mu]^{\frac{1}{2}})\}$ with itineraries $\dots---\pm-+---\dots$ appear. The remaining orbits unaccounted for in the sequences that accumulate on the members of the primary homoclinic fan are the period 2 and 4 orbits $(+-)'$, $(+-+-)'$ which appear on the flip bifurcation curves $f_2(\epsilon)$, $f_4(\epsilon)$, and the period 6 orbit $(+-++-+)'$ which appears on $f_{3\times 2}(\epsilon)$, where the period three sink has a period doubling bifurcation. We note that two of the three period 5 saddle–nodes, s_5^3, s_5^1, can be connected to the resonant bifurcations $\mu(1, 5)$, $\mu(2, 5)$; only s_6^4 can be connected to $\mu(1, 6)$ among the period 6 values, and s_7^9, s_7^5, s_7^1 respectively can be connected to $\mu(1, 7)$, $\mu(2, 7)$, $\mu(3, 7)$ for the period 7 saddle nodes. In making such connections, we carefully consider the number of circuits the orbit $F_{\mu,1}(q)$ of a k-periodic point q makes about the elliptic centre at $x = y = (1+\mu)^{\frac{1}{2}} - 1$. This statement is vague, but Holmes & Williams (1984) show that it can be made precise by suspending the horseshoe in a suitable flow and considering the knot types of certain periodic orbits. These knots are topological invariants and hence permit one to trace bifurcating orbits as ϵ varies. In particular a theorem in Birman & Williams (1983) implies that orbits of period $2n+1$ with itineraries of the forms $+\overbrace{---\dots--}^{2n}$ and $+-+\overbrace{---\dots-}^{2n-2}$ are torus knots of type $(n, 2n+1)$ and hence can be connected with resonant bifurcations of the form $\mu(n, 2n+1)$. Thus $+-----$ connects to $\mu(3, 7)$, and, more generally, the first saddle–node s_{2n+1}^1 of each odd period to appear in the Sarkovskii ordering for f_μ connects to the last resonant bifurcation of type $\mu(n, 2n+1)$ for $F_{\mu,1}$ from the elliptic fixed point.

To conclude this section, and the paper, we present some numerical computations of homoclinic and periodic bifurcation curves for the quadratic (Hénon) map with $f_\mu(y) = \mu - y^2$. In figure 23*a*, we show bifurcation curves for saddle–node and flip bifurcations of all orbits

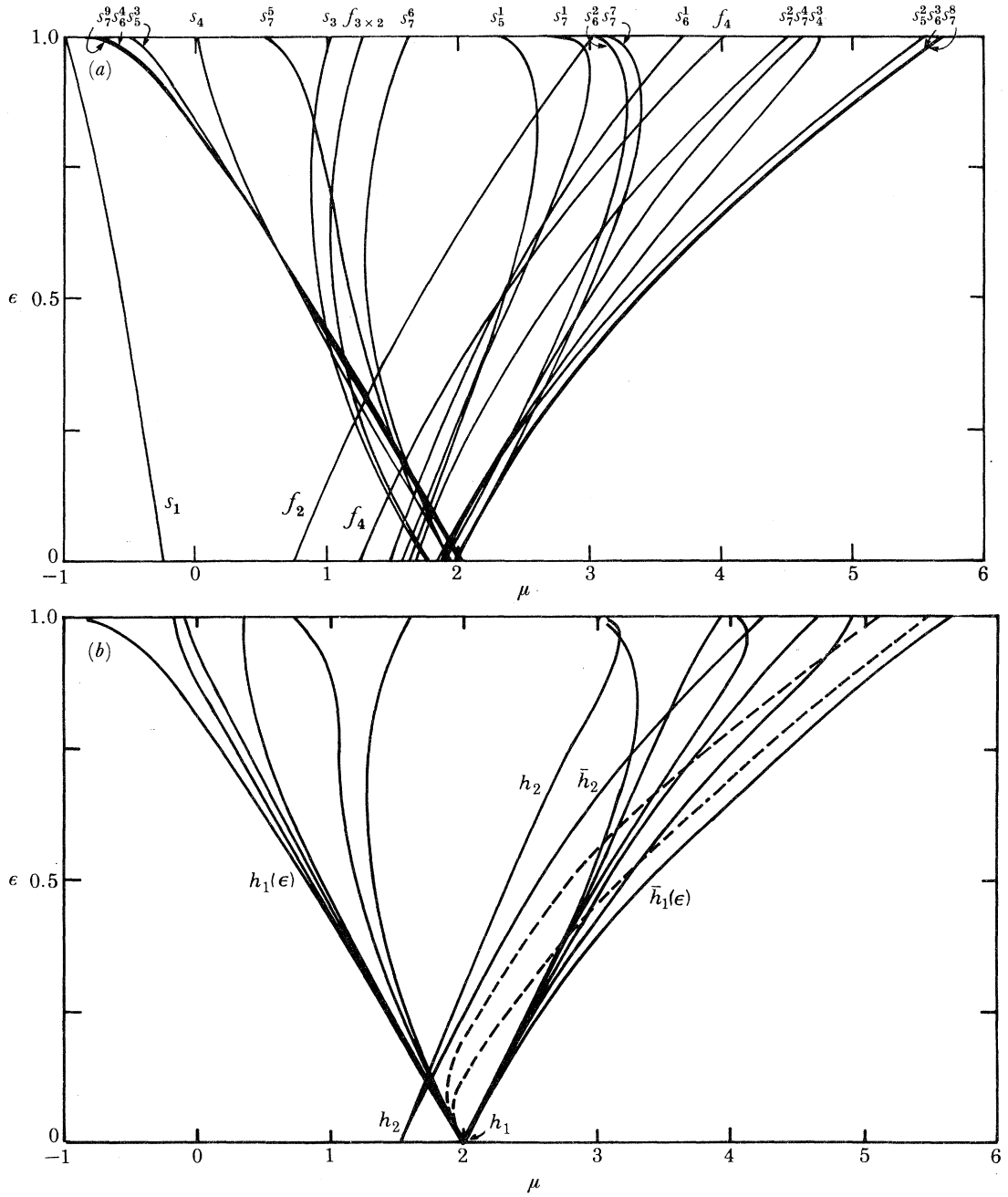

FIGURE 23. Some bifurcation curves for the Hénon map.
(*a*) Saddle–nodes and flips of periods $k \leqslant 7$. (*b*) Homoclinic bifurcation curves.

of periods $k \leqslant 7$. Similar curves for certain of these families (and some additional ones) were computed earlier by El-Hamouly & Mira (1981) and several others. We note that the ordering of the bifurcations for small ϵ and ϵ near 1 is almost as predicted by our theory, even though the blocks of successive + in the itineraries of some of these orbits are quite short. The only orbits to come 'out of sequence' are s_7^1 and s_7^2 and for these the + blocks are of length 1! In figure 23*b* we show some bifurcation curves for homoclinic orbits to both saddle points. We

have computed all but two of the 16 curves occurring in the first four stages of the fan over h_1. Note how the two fourth stage irregular curves peel away from their sector rapidly as ϵ increases and how the bounding curves $h_1(\epsilon)$ and $\bar{h}_1(\epsilon)$ appear to approach $(h_1, 0)$ with different slopes. We have only computed the bounding curves $h_2(\epsilon)$, $\bar{h}_2(\epsilon)$ for the fan over h_2, but note that they do appear to be tangent at $(h_2, 0)$, as predicted.

We remark that a 'trapping region' D exists for the map $F_{\mu,\epsilon}$ for all parameter values lying between the saddle–node bifurcation curve $s_1(\epsilon)$ and a heteroclinic bifurcation curve $h_1^*(\epsilon)$ based at $(h_1, 0)$ (cf. Hénon 1976; Feit 1978). D is bounded by the stable manifold $W^s(p)$ of the saddle point at the lower left. Thus for such *parameter* values we can define an attracting set $\mathscr{A} = \overline{\bigcap_{n\geqslant 0} F^n_{\mu,\epsilon}(D)}$. The attracting set vanishes when $W^u(q)$, the unstable manifold of the fixed point at the upper right, and $W^s(p)$ intersect: the 'first' such intersection with increasing μ defines $h_1^*(\epsilon)$. Clearly $\mathscr{A}$ contains all the unstable periodic points and their unstable manifolds, but equally certainly it is not necessarily a strange attractor, since it also contains stable periodic orbits for many parameter values (probably an open dense set) and hence cannot contain a dense orbit. The question of whether strange attractors exist for $F_{\mu,\epsilon}$ with $\epsilon \neq 0$ is still open. See Simo (1979) and Hitzl (1981) for more on the trapping region.

In closing we remark that, although we have concentrated on the parameter strip $0 \leqslant \epsilon \leqslant 1$, many of our results extend to the case $\epsilon < 0$ and moreover that, for the Hénon map one can obtain the behaviour for $\epsilon > 1$ and $\epsilon < -1$ from that occurring for $\epsilon \in (-1, 1)$, using the symmetry of the contracting and expanding maps under the transformations $(x, y) \to (\pm\epsilon y, \pm\epsilon x)$ (cf. Devaney & Nitecki 1979). Also, while we have concentrated on a study of the structure of the homoclinic bifurcation fan based at $(h_1, 0)$, and of the associated accumulating sequences of saddle nodes and flips, it should be clear that our ideas can be extended to describe the homoclinic and periodic bifurcation structures associated with other points $(h_{2^lk}, 0)$.

Appendix. Computation of the coefficient b_1 for resonant bifurcations

Employing the transformations $\bar{u} = x - \Omega$, $\bar{v} = y - \Omega$, $\Omega = 1 - (1+\mu)^{\frac{1}{2}}$, and

$$\begin{bmatrix}\bar{u}\\ \bar{v}\end{bmatrix} = \begin{bmatrix}0 & 1\\ (1-\Omega^2)^{\frac{1}{2}} & \Omega\end{bmatrix}\begin{bmatrix}u\\ v\end{bmatrix}, \quad \begin{bmatrix}u\\ v\end{bmatrix} = \begin{bmatrix}\dfrac{-\Omega}{(1-\Omega^2)^{\frac{1}{2}}} & \dfrac{1}{(1-\Omega^2)}\\ 1 & 0\end{bmatrix}\begin{bmatrix}\bar{u}\\ \bar{v}\end{bmatrix}, \tag{A 1}$$

we obtain the map $G_{0,0}(u, v)$ with the linear part in normal form (a rotation matrix):

$$\begin{bmatrix}u\\ v\end{bmatrix} \to \begin{bmatrix}\cos\theta & -\sin\theta\\ \sin\theta & \cos\theta\end{bmatrix}\begin{bmatrix}u\\ v\end{bmatrix} - \begin{bmatrix}(\sin\theta)\,u^2 + 2(\cos\theta)\,uv + (\cos^2\theta/\sin\theta)\,v^2\\ 0\end{bmatrix}, \tag{A 2}$$

where $\cos\theta = \Omega$, $\sin\theta = (1-\Omega^2)^{\frac{1}{2}}$. We next use the formula (cf. Wan 1978; Iooss 1979):

$$\alpha_{(0,0)} = \xi_{11}\,\xi_{20}\frac{(2\lambda-1)}{\lambda(1-\bar{\lambda})} + \frac{|\xi_{11}|^2}{1-\bar{\lambda}} + \frac{2|\xi_{02}|^2}{\lambda^2-\bar{\lambda}} + \xi_{21},$$

where $\lambda, \bar{\lambda} = \lambda(0,0), \bar{\lambda}(0,0) = \mathrm{e}^{\pm\mathrm{i}\theta}$ and

$$\begin{aligned}
\xi_{20} &= \tfrac{1}{8}[g^1_{uu} - g^1_{vv} + 2g^2_{uv}) + \mathrm{i}(g^2_{uu} - g^2_{vv} - 2g^1_{uv})],\\
\xi_{11} &= \tfrac{1}{4}[(g^1_{uu} + g^1_{vv}) + \mathrm{i}(g^2_{uu} + g^2_{vv})],\\
\xi_{02} &= \tfrac{1}{8}[(g^1_{uu} - g^1_{vv} - 2g^2_{uv}) + \mathrm{i}(g^2_{uu} - g^2_{vv} + 2g^1_{uv})],\\
\xi_{21} &= \tfrac{1}{16}[(3g^1_{uuu} + g^2_{uuv} + g^1_{uvv} + 3g^2_{vvv}) + \mathrm{i}(3g^2_{uuu} - g^1_{uuv} + g^2_{uvv} - 3g^1_{vvv})],
\end{aligned} \tag{A 3}$$

PHILOSOPHICAL TRANSACTIONS OF THE ROYAL SOCIETY A MATHEMATICAL, PHYSICAL & ENGINEERING SCIENCES

and g^i, g^i_{uu} etc. denote the components of the nonlinear term of (A 2) and their partial derivatives. We note that there are no third order terms in this case and hence $\xi_{21} = 0$. Finally, we can obtain the coefficient $b_1(0, 0)$ as

$$b_1(0, 0) = \mathrm{Im}\,(\alpha(0, 0)\,\bar{\lambda}(0, 0)). \tag{A 4}$$

Straightforward, if tedious, computations now give

$$\begin{aligned} \xi_{20} &= (\cos 2\theta + \mathrm{i} \sin 2\theta)/4 \sin \theta, \\ \xi_{11} &= -\tfrac{1}{2} \sin \theta, \\ \xi_{20} &= (\cos 2\theta - \mathrm{i} \sin 2\theta)/4 \sin \theta, \end{aligned} \tag{A 5}$$

and substitution of (A 5) and $\lambda, \bar{\lambda} = \cos\theta \pm \mathrm{i} \sin\theta$ into (A 3)–(A 4) yields

$$\mathrm{Re}\,(\alpha(0, 0)) = 0, \tag{A 6}$$

as required, and

$$b_1(0, 0) = \mathrm{Im}\,(\alpha(0, 0)\,\bar{\lambda}(0, 0)) = -(2 + \cos 2\theta)/8 \sin\theta(1 - \cos\theta). \tag{A 7}$$

Since in our matrix representation of (A 2) we take $\theta \in (0, \pi)$, we have $\sin\theta > 0$ and all the other terms in (A 7) are likewise positive. Thus we have $b_1(0, 0) < 0$ for all $\mu \in (-1, 3)$.

This work was partly supported by N.S.F. grant CME 80-17570 and the Center for Applied Mathematics, Cornell University.

References

Allwright, D. J. 1978 Hypergraphic functions and bifurcations in recurrence relations. *Siam Jl appl. Math.* **34**, 687–691.

Arnol'd, V. I. 1976 Loss of stability of self oscillations close to resonances and versal deformations of equivariant vector fields. *Funct. Anal. Appl.* **11** (2), 1–10.

Arnol'd, V. I. 1983 *Geometric methods in the theory of ordinary differential equations.* New York: Springer Verlag.

Arneodo, A., Coullet, P., Tresser, C., Libchaber, A., Maurer, J. & d'Humières, A. 1983 On the observation of the uncompleted cascade in a Rayleigh Bénard experiment. *Physica* **6D**, 385–392.

Aronson, D. G., Chory, M. A., Hall, G. R. & McGeehee, R. P. 1982 Bifurcations from an invariant circle for two parameter families of maps of the plane: a computer assisted study. *Commun. Math. Phys.* **83**, 303–354.

Birman, J. S. & Williams, R. F. 1983 Knotted periodic orbits in dynamical systems II: knot holders for fibred knots. *Contemp. Math.* **20**, 1–60.

Block, L., Guckenheimer, J., Misiurewicz, M. & Young, L.-S. 1980 Periodic points and topological entropy for one dimensional maps. *Springer Lecture Notes in Maths* **819**, 18–34.

Bogdanov, R. I. 1975 Versal deformations of a singular point in the plane in the case of zero eigenvalues. *Funct. Anal. Appl.* **9**, 144–145.

Bowen, R. 1978 *On axiom A diffeomorphisms.* C.B.M.S. Regional Conference Series in Mathematics, no. 35. *Am. math. Soc.*

Bowen, R. & Franks, J. 1976 The periodic points of maps of the disk and the interval. *Topology* **15**, 337–342.

Brown, J. R. 1976 *Ergodic theory and topological dynamics.* New York: Academic Press.

Carr, J. 1981 *Applications of centre manifold theory.* New York: Springer Verlag, Applied Mathematical Sciences **35**.

Chillingworth, D. R. J. 1976 *Differential topology with a view to applications.* London: Pitman.

Collet, P. & Eckmann, J.-P. 1980*a* *Iterated maps on the interval as dynamical systems.* Boston: Birkhauser.

Collet, P. & Eckmann, J.-P. 1980*b* On the abundance of aperiodic behaviour for maps on the interval. *Communs math. Phys.* **73**, 115–160.

Collet, P., Eckmann, J.-P. & Lanford, O. E. 1980 Universal properties of maps on an interval. *Communs math. Phys.* **76**, 211–254.

Cvitanović, P. & Myrheim, J. 1983 Complex universality. Nordita preprint.

Derrida, B., Gervois, A. & Pomeau, Y. 1979 Universal metric properties of bifurcations of endomorphisms. *J. Phys.* A **12**, 269–296.

Devaney, R. 1982 Homoclinic bifurcations and the area conserving Hénon mapping. Boston University preprint.

Devaney, R. & Nitecki, Z. 1979 Shift automorphisms in the Hénon map. *Communs math. Phys.* **67**, 137–146.

Douady, A. 1982 Systèmes dynamiques holomorphes. *Séminaire Bourbaki* **35**, (1982/3), no. 599.
Douady, A. & Hubbard, J. H. 1982 Itération des polynomes quadratiques complexes. *C.r. hebd. Séanc. Acad. Sci., Paris* **294**, 123–126.
El-Hamouly, H. & Mira, C. 1981 Lien entre les propriétés d'un endomorphisme de dimension un et celles d'un diffeomorphisme de dimension deux. *C.r. hebd. Séanc. Acad. Sci., Paris* **293**, 525–528.
Feigenbaum, M. J. 1978 Quantitative universality for a class of nonlinear transformations. *J. statist. Phys.* **19**, 25–52.
Feit, S. D. 1978 *Communs math. Phys.* **61**, 249–260. Characteristic exponents and strange attractors.
Gambaudo, J. M. 1982 Perturbation d'une bifurcation de Hopf d'equation differentielle par une excitation periodique. Ph.D. thesis, Université de Nice.
Gambaudo, J. M. & Tresser, C. 1983 Simple models for bifurcations creating horseshoes. *J. statist. Phys.* **32**, 455–476.
Gavrilov, N. K. & Silnikov, L. P. 1972 On three-dimensional dynamical systems close to systems with a structurally unstable-homoclinic curve. I. *U.S.S.R. Sbornik*, **88**, 467–485.
Gravilov, N. K. & Silnikov, L. P. 1973 On three-dimensional dynamical systems close to systems with a structurally unstable homoclinic curve II. *U.S.S.R. Sbornik* **90**, 139–156.
Grebogi, C., Ott, E. & Yorke, J. A. 1982 Crises, sudden changes in chaotic attractors, and transient chaos. Laboratory for Plasma and Fusion Energy Studies, University of Maryland preprint.
Greenspan, B. D. & Holmes, P. J. 1983 Homoclinic orbits, subharmonics and global bifurcations in forced oscillators. In *Nonlinear dynamics and turbulence* (ed. G. Barenblatt, G. Iooss & D. D. Joseph), pp. 172–214. London: Pitman.
Greenspan, B. D. & Holmes, P. J. 1983 Repeated resonance and homoclinic bifurcation in a periodically forced oscillator. (Submitted.)
Guckenheimer, J. 1977 On the bifurcation of maps of the interval. *Invent. Math.* **39**, 165–178.
Guckenheimer, J. 1979 Sensitive dependence to initial conditions for one dimensional maps. *Communs math. Phys.* **70**, 133–160.
Guckenheimer, J. 1980 Bifurcations of dynamical systems. In *Dynamical systems*. CIME Lectures, Bressanone, Italy, Progress in Maths. **8**, Boston: Birkhauser.
Guckenheimer, J. & Holmes, P. J. 1983 *Nonlinear oscillations, dynamical systems and bifurcations of vector fields*. New York: Springer Verlag.
Guckenheimer, J., Oster, G. & Ipatchki, I. 1977 The dynamics of density dependent population models. *J. math. Biol.* **4**, 101–147.
Gumowski, I. & Mira, C. 1980 *Recurrences and discrete dynamical systems*. Springer Lecture Notes in Maths **809**.
Hénon, M. 1976 A two-dimensional mapping with a strange attractor. *Communs math. Phys.* **50**, 69–78.
Hirsch, M. W. 1976 *Differential topology*. New York, Heidelberg, Berlin: Springer Verlag.
Hitzl, D. L. 1981 Numerical determination of the capture/escape boundary for the Hénon attractor. *Physica* **2D**, 370–378.
Holmes, P. J. 1979 A nonlinaer oscillator with a strange attractor. *Phil. Trans. R. Soc. Lond.* A **292**, 419–448.
Holmes, P. J. & Marsden, J. E. 1983 On exponentially small Melnikov functions. (In preparation.)
Holmes, P. & Whitley, D. 1983*a* On the attracting set for Duffing's equation; I: analytical methods for small force and damping. (In the press.)
Holmes, P. & Whitley, D. 1983*b* On the attracting set for Duffing's equation; II: a geometrical model for moderate force and damping. *Physica* **7D**, 111–123.
Holmes, P. & Williams, R. F. 1984 Knotted periodic orbits in suspensions of Smale's horseshoe: torus knots and bifurcation sequences.
Iooss, G. 1979 *Bifurcation of maps and applications*. Mathematical Studies **36**, Amsterdam: North Holland.
Jakobson, M. V. 1978 Topological and metric properties of one dimensional endomorphisms. *Soviet Math. Dokl.* **19**, 1452–1456.
Jakobson, M. V. 1981 Absolutely continuous invariant measures for one parameter families of one dimensional maps. *Communs math. Phys.* **81**, 39–88.
Jonker, L. 1979 Periodic orbits and kneading invariants. *Proc. Lond. math. Soc.* **39**, 428–450.
Jonker, L. & Rand, D. 1981 Bifurcations in one dimension. I. The non-wandering set. *Invent. Math.* **62**, 347–365; II. a versal model for bifurcations. *Invent. Math.* **63**, 1–15.
Lanford, O. E. 1982 A computer assisted proof of the Feigenbaum conjectures. *Bull. Am. math. Soc.* **6**, 427–434.
Li, T.-Y. & Yorke, J. A. 1975 Period three implies chaos. *Am. Math. Monthly* **82**, 985–992.
Milnor, J. 1977 The theory of kneading and a piecewise linear model for kneading. (Unpublished.)
Milnor, J. & Thurston, W. 1977 On iterated maps of the interval. I. The kneading matrix, Princeton preprint.
Misiurewicz, M. 1981*a* The structure of mappings of an interval with zero entropy. *Publ. I.H.E.S.* **53**, 17–52.
Misiurewicz, M. 1981*b* Absolutely continuous measures for certain maps of the interval. *Publ. I.H.E.S.* **53**, 17–52.
Moon, F. & Holmes, P. 1979 A magnetoelastic strange attractor. *J. Sound Vib.* **65**, 275–296.
Moser, J. 1973 *Stable and random motions in dynamical systems*. Princeton University Press.
Narasimhan, C. C. 1979 The periodic behaviour of Morse–Smale diffeomorphisms on compact surfaces. *Trans. Am. math. Soc.* **248**, 145–169.

PHILOSOPHICAL TRANSACTIONS OF THE ROYAL SOCIETY A MATHEMATICAL, PHYSICAL & ENGINEERING SCIENCES

Nitecki, Z. 1981 Topological dynamics on the interval. In *Ergodic theory and dynamical systems*, vol. II (ed. A. Katok). Proceedings, Special Year, Maryland. Boston: Birkhauser.
Newhouse, S. E. 1974 Diffeomorphisms with infinitely many sinks. *Topology* **13**, 9–18.
Newhouse, S. E. 1979 The abundance of wild hyperbolic sets and non-smooth stable sets for diffeomorphisms. *Publ. I.H.E.S.* **50**, 101–151.
Newhouse, S. E. 1980 Lecture on dynamical systems. In *Dynamical systems*. C.I.M.E. Lectures, Bressanone, Italy. *Prog. Math.* **8**, Boston: Birkhauser.
Robinson, C. 1983 Bifurcation to infinitely many sinks. *Communs math. Phys.* **90**, 433–459.
Ruelle, D. 1977 Applications convervant une mesure absolument continue par rapport a dx sur [0, 1]. *Communs math. Phys.* **55**, 47–51.
Sarkovskii, A. N. 1964 Coexistence of cycles of a continuous map of a line into itself. *Ukranian Math. J.* **16**, 61–71.
Simo, C. 1979 On the Hénon–Pomeau attractor. *J. statist. Phys.* **21** (4), 465–494.
Singer, D. 1978 Stable orbits and bifurcations of maps of the interval. *SIAM Jl appl. Maths.* **35**, 260–267.
Smale, S. 1963 Diffeomorphisms with many periodic points. In *Differential and combinatorial topology* (ed. S. S. Cairns), pp. 63–80. Princeton University Press.
Smale, S. 1967 Differentiable dynamical systems. *Bull. Am. math. Soc.* **73**, 774–817.
Smale, S. & Williams, R. F. 1976 The qualitative analysis of a difference equation of population growth. *J. math. Biol.* **3**, 1–4.
Stefan, P. 1977 A theorem of Sarkovskii on the existence of periodic orbits of continuous endomorphisms of the real line. *Communs math. Phys.* **54**, 237–248.
van Strien, S. 1982 On the bifurcations creating horseshoes. Springer Lecture Notes in Maths. **898**, 316–351.
Takens, F. 1973 *Introduction to global analysis. Communs math. Inst.* Rijksuniversiteit Utrecht, **2**.
Takens, F. 1974 Forced oscillations and bifurcations. *Communs math. Inst.* Rijksuniversiteit Utrecht, **3**, 1–59.
Tresser, C., Coullet, P. & Arneodo, A. 1979 Topological horseshoes and numerically observed chaotic behaviour in the Hénon map. University of Nice preprint.
Ueda, Y. 1980 Explosion of strange attractors exhibited by Duffing's equation. *Ann. N.Y. Acad. Sci.* **357**, 422–434.
Ulam, S. M. & von Neumann, J. 1947 On combinations of stochastic and deterministic processes. *Bull. Am. math. Soc.* **53**, 1120.
Wan, Y. H. 1978 Computations of the stability condition for the Hopf bifurcation of diffeomorphisms on $\mathbb{R}^2$, *SIAM Jl appl. Math.* **34**, 167–175.
Whitley, D. C. 1983 A C^1 Kupka–Smale diffeomorphism of S^2 with no sources or sinks. (Submitted.)
Yorke, J. A. & Alligood, K. T. 1983 Cascades of period-doubling bifurcations: a prerequisite for horseshoes. *Bull. Am. math. Soc.* (new series) **9**, 319–322.
Zeeman, E. C. 1977 *Catastrophe theory: selected papers.* New York: Addison-Wesley.

PHILOSOPHICAL TRANSACTIONS OF THE ROYAL SOCIETY A MATHEMATICAL, PHYSICAL & ENGINEERING SCIENCES